Politecnico di Torino

Master's Degree Course in
ARCHITECTURE FOR HERITAGE
February 2025

Integrating HBIM and GIS for Flood Risk Assessment and Heritage Conservation

A Case Study of Valentino Castle in Turin

Supervisor
Prof. Lorenzo Teppati Lose'
Co-supervisor
Prof. Elisabetta Colucci

Candidate
Peizhi Su

Content

Abstract:

Extreme weather events, such as stormwater and flooding, have become increasingly frequent over the past few decades. They pose significant challenges to human life, infrastructure, and urban environments. Italy is known for its rich cultural heritage; however, many of them are quite vulnerable to extreme weather events due to their geographical location and the nature of cultural heritage itself.

Valentino Castle (Castello del Valentino) is a significant World Heritage Site. Located along the Po River and closely connected to the river's groundwater system, this castle is facing escalating flood risks due to the increasing frequency of extreme weather events.

In recent decades, Historic Building Information Modeling (HBIM) has become an important tool for the preservation, restoration, and archiving of historic buildings. In addition, an emerging trend is to integrate HBIM with other disciplines to provide multifaceted insights for heritage conservation.

This study is dedicated to integrating HBIM and Geographic Information System (GIS) to gain a comprehensive understanding of the impacts of various flood scenarios on Valentino Castle. The process involves detailed and targeted modelling and information management of Valentino Castle by an HBIM system. Subsequently, a GIS system is used to conduct complex analysis, simulation, and visualisation of various flood and stormwater scenarios. The findings derived from this analysis will not only offer valuable guidance but also provide recommendations for flood prevention and enhancement programmes specifically designed to protect cultural heritage sites.

It should be noted that Valentino Castle serves as a case study to evaluate and validate the proposed approach, which is intended to be adapted and generalised to other cultural heritage sites. Through this HBIM-GIS framework, the study contributes to the protection and conservation of valuable cultural heritage in the face of flood risks.

Keywords: HBIM-GIS Framework, Integrated application, flood impact analysis, 3D visualisation

Chapter 1 Introduction

1.1 Overview of Climate Change, Extreme Weather, and Flooding in Italy

Floods are among the most devastating natural disasters, profoundly impacting human populations and cultural heritage worldwide. The risk of flooding is expected to increase due to climate change and other factors. Floods result in significant losses of life, extensive infrastructure damage, and displacement of communities, disturbing local economies and causing long-term financial hardships [1], [2].

According to the report *Il clima in Italia nel 2023*, Italy has experienced significant climatic changes, characterized by rising temperatures and shifting precipitation patterns. From 1981, the average temperature has increased at a rate of (+0.40 ± 0.04) °C per decade, with the maximum temperature increasing by (+0.42 ± 0.05) °C per decade and the minimum temperature by (+0.38 ± 0.04) °C per decade. Heatwaves and warm nights have become more frequent, with record-breaking events in 2023, particularly in July and October. Despite the absence of statistically significant trends in annual and seasonal precipitation during the period from 1961-2023, the precipitation in 2023 decreased by 4% compared to the climate average. In the latter half of 2023, persistent droughts affected regions such as Sardinia and Sicily, while localised extreme rainfall events caused severe flooding, especially in central Italy [3].

The frequency of extreme weather events, such as floods, wildfires, and heatwaves, continues to increase, significantly affecting Italy. In 2024 alone, 351 extreme weather events were recorded, exceeding 300 for the third consecutive year and representing a 485% increase compared to 2015. Prolonged drought (+54.5%), river flooding (+24%) and intense rainfall (+12%) were the main causes of damage. Northern Italy experienced 198 such events, with Emilia-Romagna being the hardest hit (52 events), followed by Lombardy (49) and Sicily (43). Although not among the highest, Piedmont also experienced 22 events. Among provinces, Bologna (17 events) recorded the highest number, while Rome and Ravenna followed with 13 each, and Turin recorded 12 events. In major cities, Rome suffered the most (8 events), followed by Genoa (7) and Milan (6) [4].

From 2010 to October 31, 2023, the *Osservatorio Città Clima* recorded 684 instances of flooding caused by intense rainfall, 166 river overflows, and 86 landslides also triggered by heavy rains, accounting for 49.1% of the total documented extreme weather events. During this period, both flooding caused by intense rainfall and river overflows events exhibited an overall increasing trend year by year. (Figure 2). Sicily (86 floods), Lazio (72), and Lombardy (66)

were the most affected regions. River overflows were most frequent in Lombardy (30 cases), Emilia-Romagna (25), and Sicily (18). Large cities like Rome (49 floods), Bari (21), and Milan (20 river overflows) have become particularly vulnerable [5, pp. 3–8].

Cultural heritage sites are especially at risk, as floodwaters erode foundations, submerge structures, and degrade materials, leading to irreversible damage and the loss of cultural identity [6]. The areas previously considered safe under conventional risk assessment frameworks may now be exposed to risks due to climate change. According to the Rapporto Spiagge 2024, which analyses meteorological and hydrological events in coastal municipalities from 2010 to 2024, intense rainfall caused damage to historical heritage in nine documented instances (Figure 1)[7, p. 10]. For example, the May 2023 floods in Emilia-Romagna devastated historic towns and buildings, with 23 rivers overflowing and over 280 landslides affecting 44 municipalities, including the historic centre of Castel Bolognese[5, pp. 7–9]. To mitigate these risks, various measures can be implemented, including the construction of dams and levees, land-use planning, early warning system, and community awareness programs [8], [9].

Gli eventi meteo-idro nei comuni costieri per categoria (2010-2024)
Fonte: Legambiente - Osservatorio Città Clima

Nota: alcuni eventi in precedenza attribuiti a "Danni alle infrastrutture da piogge intense" sono stati riclassificati.

Categoria	Valore
Allagamenti da piogge intense	295
Danni da trombe d'aria e raffiche di vento	226
Danni da mareggiate	83
Danni alle infrastrutture da piogge intense	81
Esondazioni fluviali	47
Danni da grandinate	23
Frane da piogge intense	21
Danni da siccità prolungata	19
Temperature record in città	12
Danni al patrimonio storico da piogge intense	9

Figure 1 Weather-Hydro Events in Coastal Municipalities by Category. Source: Legambiente - Osservatorio Città Clima. Rapporto Spiagge 2024 Gli impatti di erosione ed eventi meteo estremi nelle aree costiere italiane
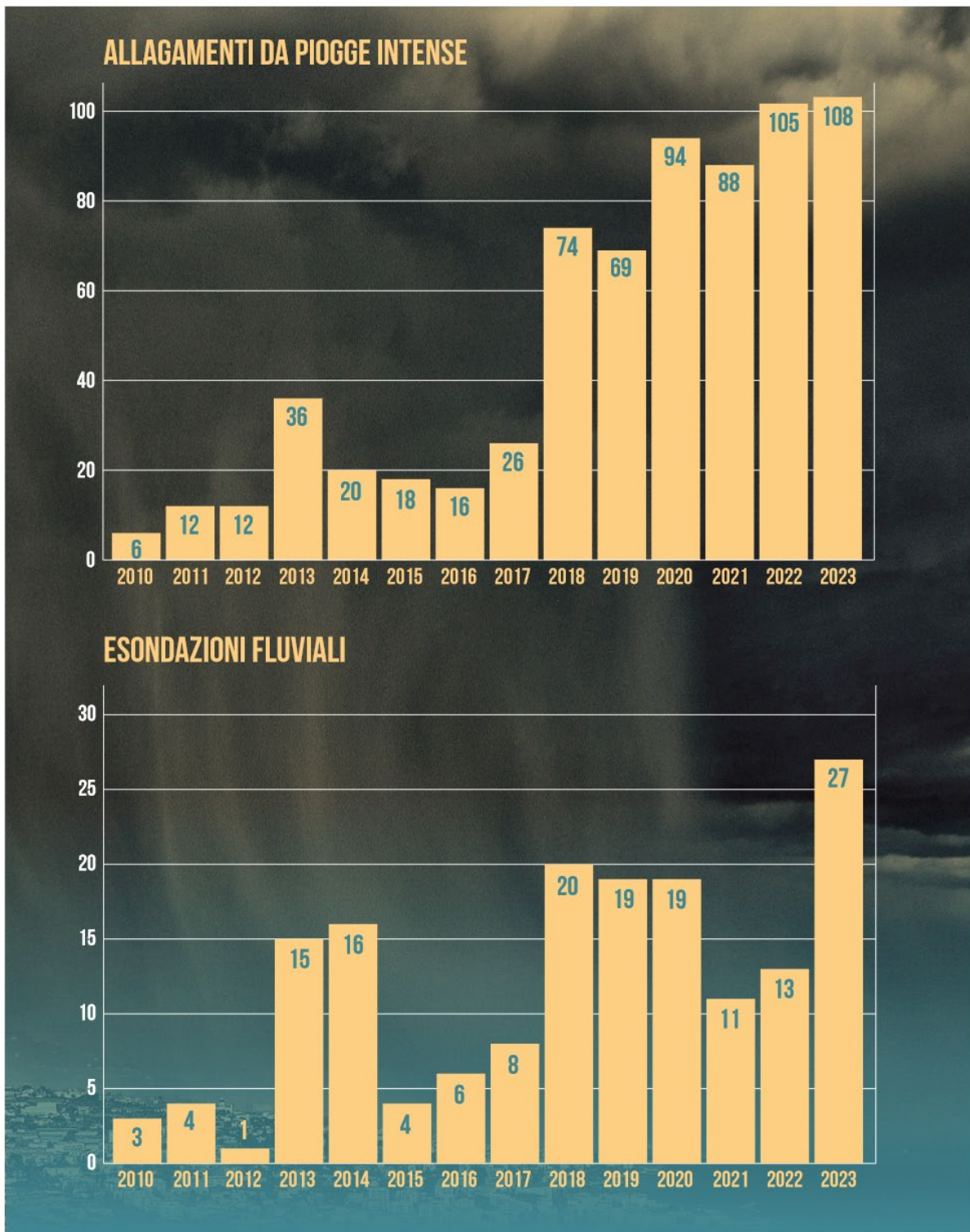
Figure 2 Floods Caused by Intense Rainfall and River Overflows.

Source:[5]

1.2 The Flood Risk of Valentino Castle in Turin

In hydrology, the probability of a flood refers to the likelihood of a specific size of flooding occurring within a given time frame. This probability is typically described using statistical

methods, which analyse historical flood data through the application of probability theory. The results are often expressed in terms of a "return period," which represents the estimated recurrence interval of a flood of a certain size or greater. For instance, "XXX-year flood" refers to an event that has a 1 in XXX chance of occurring in any given year. a "100-year flood", for example, represents a flood with a 1% probability (1/100) of being equalled or exceeded in any year [10]. Flood risk is the probability of flooding combined with the potential adverse consequences associated with a flood event. It is determined by the likelihood of flooding and the vulnerability of the exposed assets and populations. Vulnerability combines susceptibility, exposure and the value of elements to assess their resilience. Exposure refers to the presence of assets or people in flood prone areas, while susceptibility indicates an area's predisposition to flood damage [11], [12].

Nowadays, human society universally faces various challenges brought by climate change. According to *ANALISI DEL RISCHIO I cambiamenti climatici in sei città italiane TORINO* [13], the impacts of climate change are becoming increasingly evident, with a notable rise in extreme weather events, particularly heatwaves and floods , causing widespread damage to cities, populations, and economies.

In the city of Turin, a significant portion of the territory is highly urbanized. The urbanized land is 8 472 hectares, accounting for 65.1% of the surface area [14]. Most of these urban areas are covered by impervious materials, which inhibit infiltration and accelerate surface runoff. In the natural hydrological cycle, this acceleration contributes to an increased risk of flooding, even in areas not typically associated with floodplain.

Also, Turin is located within Po River Basin, which is characterized by a complex and dense river system that includes the Po River, Dora Riparia River, Sangone River, Stura di Lanzo River, and Chisola River. Over the last 50 years, the Po River Basin has suffered several floods, with the most severe event being the 200-year flood in 2000, and the second most severe flood occurring in 1994. Figure 3 illustrates the extent of inundation in 2000. In the vicinity of Valentino Castle, areas such as Murazzi and Borgo Medievale were flooded multiple times, (see Figure 4).

Figure 3 The extent of the 2000 inundation in areas near Valentino Castle.

Description

The dataset represents the ground effects associated with the floods that occurred along the river and stream courses of Chisone, Pellice, Sangone, Dora Riparia, Dora Baltea, Stura di Lanzo, Malone, Orco, Soana, and Po, linked to the flood event of October 13-16, 2000. It includes: the delineation of the floodplain, the main erosive and depositional processes, estimates of hydrometric levels, remnant fluvial forms, and major damages. Landslides triggered by river activity or with deposits directly interfering with the riverbed are also reported.

The left figure illustrates the extent of flooding around Valentino Castle during the 2000 flood event. Although Valentino Castle itself was not submerged, both the Murazzi area and the Borgo Medievale were inundated, with water depths of 3.5 m and 0.3 m, respectively.

Scale: 1:10,000.

Source: Arpa Piemonte

Legend

▲ Altezze in metri

→ Direzione di deflusso (correnti ad alta energia)

— Sponda

⋯ Sponda erosa

Area con deposito non classificato

Area inondata/allagata

Canale attivo (al momento dell'osservazione)

Canale in alveo inattivo

Buildings

Figure 4 The Po River flood of 2000 in Murazzi, Turin. Source: LA STAMPA

To assess and manage the flood risk, The European Directive 2007/60/CE, incorporate into Italian law through Legilative Decree 49/2010, initiates a new phase of national policy. The Flood Risk Management Plan (Piano di gestione del rischio di alluvioni, PGRA), introduced by the Decree for each river basin district, assesses the flood risk within Po River Basin and defines the intervention at the district or city level. This approach is coordinated among all administrations and managing bodies, including stakeholders and general public [15], [16], [17].

In the updated Flood Risk Management Plan (II cycle) for the Po River Basin [16, p. 55，310], Flood risk assessments have been conducted for cultural heritage within the basin across three levels of risk (with return periods of 20, 200, and 500 years).However the result only provide general information regarding the areas, types, and quantities of the cultural heritage at risk. There is no detailed analysis of significant architectural heritage, nor are there interventions proposal to mitigate flood risks for the important cultural heritage.

According to Flood Risk Management Plan (II cycle) for the city of Turin [15] (Figure 5), approximately 35 square kilometres of Turin are at risk of overflow from the water systems mentioned above, with 60% classified as low flood risk zones, 29% as medium risk zones, and 11% as high-risk zones. The area where the Valentino castle is situated falls within the flood

risk zone. However, due to the small scale of the map, it is difficult to determine the specific flood risk impact on Valentino castle.

The map contains the following labels and legend:

Piano di Gestione del rischio di alluvioni
Secondo ciclo – dicembre 2019
Mappe di pericolosità e rischio

Scenari di pericolosità

- P1 (scarsa probabilità)
- P2 (media probabilità)
- P3 (elevata probabilità)
- APSFR
- Autorità di bacino distrettuale
- Limiti regionali

Unità di Gestione (Unit of Management - UoM)

ITN008 Po
ITI026 Fissero-Tartaro-Canalbianco
ITI021 Reno
ITI01319 Marecchia-Conca
ITR081 Bacini Romagnoli

● Valentino Castle (Castello del Valentino)

APSFR Città di Torino - Po, Dora Riparia, Stura di Lanzo, Sangone, Chisola   TAV. 14   1 : 100000   0 08 16 24 32 4 Km

Figure 5 APSFR Città di Torino

source: https://pianoalluvioni.adbpo.it/piano-gestione-rischio-alluvioni-2021/

11

In the latest Flood Risk Management Plan (II cycle) for the Po River Basin [18], significant emphasis is placed on public participation. Public participation refers to the mechanism for the active participation of the public in all stages of the plan, from preparation to implementation. This process aims to improve decision-making, increase environmental awareness, and ensure that more people accept and share the measures taken. Public participation is developed through three levels of involvement: information provision, consultation and active participation. Although professional terms, schematics and WebGIS tools are widely used, they may not be very effective for non-professional audiences. Therefore, more intuitive visual representations, such as 3D visualization, are essential to improve public participation and communication efficiency.

1.3 The Feasibility of Integrating HBIM and GIS for Flood Risk Management in Heritage Preservation

1.3.1 Building Information Modelling (BIM)

Building Information Modelling (BIM) is widely used in the AEC (Architecture, engineering and construction) industry, especially in collaboration between different departments. It plays an important role in the whole lifecycle of project management of new construction. In recent decades, BIM has gradually begun to play a wider role in the management of heritage projects. In 2009, the concept of Historic Building Information Modelling (HBIM) was first introduced by M. Murphy[18, pp. 311–327]. It is a specialized form of Building Information Modelling (BIM) tailored to the documentation and preservation of historical buildings. HBIM typically employs detailed 3D digital models created based on data obtained through 3D metric surveys, documentation, and relevant methods. Furthermore, it combines these geometric models with extensive information on materials, construction techniques, historical significance, and so on., providing a solid framework for managing and preserving cultural heritage [19].

1.3.2 Geographic Information System (GIS)

A geographic information system (GIS) is a configuration of computer hardware and software specifically designed for the acquisition, maintenance, and use of cartographic data.[20] GIS system excel in modelling the outdoor and large-scale geographic features. GIS could integrate various types of data layers using spatial location, including imagery, features, and basemaps that are linked to tables of attribute data. This integration allows for sophisticated spatial analyses to identify problems, monitor changes, understand the trends, perform forecasting and manage and response to emergencies. For instance, P. Carbajales-Dale et al. used GIS to improve public health emergency responses in rural areas of South Carolina, US, during the

COVID-19 crisis. They developed a GIS-based multi-criteria decision analysis model that policymakers and public health experts could use in similar emergency scenarios in the future. [21] Yikang Rui *et al.* developed a GIS-based emergency response system for sudden water pollution accidents, leveraging the capacity of spatial analysis and 3D visualization in GIS. This system can provide early warning and emergency response services for water pollution incidents[22]. Furthermore, GIS enhances the visualisation and interpretation of spatial data, enabling the creation of detailed and dynamic maps that represent complex geographical information. Thus, the results of GIS analysis and the generated map can be easily shared across various platforms, allowing stakeholders from different sectors to access and utilise the information for informed decision-making. The widespread accessibility and interoperability improve collaboration and communication among stakeholders [23].

1.3.3 The Current State of BIM-GIS Integration in Heritage Conservation

Applications of BIM-GIS Integration in Heritage Conservation

The application of BIM-GIS integration in heritage conservation is primarily reflected in three aspects:

(1) Multi-scale documentation

The integration of Historic Building Information Modelling (HBIM) and Geographic Information Systems (GIS) has emerged as a transformative approach to documenting and managing cultural heritage at various scales. This approach enables the development of a comprehensive database encompassing not only structural data of historical assets but also information about the current condition of heritage sites and their surrounding environmental context.

The integration between HBIM and GIS facilitates multi-scale analysis, ranging from territorial and urban environments to detailed architectural elements. For example, Sammartano et al. conducted a study focusing on the application of a multi-scale 3D geographic database for seismic vulnerability assessment, which integrates remote sensing data, urban maps, and building damage information. This method ensures comprehensive documentation, which is essential for conservation and risk mitigation[24]. Matrone et al. developed an interoperable HBIM-GIS database to support the maintenance and preservation of the Sacri Monti UNESCO heritage sites. Their platform integrates spatial and semantic data at various levels of detail (LoD), demonstrating scalability to other cultural heritages[25].

(2) Multi-disciplinary Collaboration and Real-Time Information Sharing

Restoration works, which require well-coordination among multidisciplinary teams, can benefit greatly from such an integration. By offering a shared platform, the integrated HBIM-GIS framework facilitates collaborative decision-making among government agencies and stakeholders. At the same time, it increases public participation and improves accessibility to heritage-related information. This holistic approach emphasises the significance of a multidisciplinary approach in conserving and managing historical buildings[25], [26].

(3) Multi-Scale Analysis

The integrated HBIM-GIS approach can be applied to various analyses, such as seismic damage assessment. By employing a geographical multi-scale framework, this approach enhances the understanding of systemic damage and vulnerability from an urban viewpoint, overcoming the limitations of conventional single-building analysis method. Through the introduction of a geospatial data science methodology, it can develop a multi-scale 3D urban geodatabase that combines urban cartography, emergency mapping, and 3D resources. This geodatabase includes detailed geometric, semantic, and structural data regarding architectural elements and their seismic damage [25], [28].

Overall, the integration of BIM and GIS has represented a significant advancement in the preservation and management of heritage sites, providing a robust framework for informed decision-making and public engagement.

Current State of BIM-GIS Integration from a Technical Perspective

All the BIM-GIS integration applications mentioned above utilise the interoperability between BIM and GIS standards. There are three levels of BIM-GIS integration: data level, process level, and application level (Figure 6).

At the data level, integration often involves introducing new standards, revising existing standards, or converting and translating data formats between BIM and GIS systems. For example, standards such as InfraGML and IndoorGML have been developed to facilitate interoperability[27], while CityGML and IFC have been extended or transformed to bridge their semantic and geometric differences. Semi-automatic methods, such as the Extract-Transform-Load (ETL) process, play a key role in achieving this integration. ETL tools like Feature Manipulation Engine (FME) and ArcGIS Data Interoperability allow bidirectional data conversion, maintaining relative consistency in semantics and geometry. However, challenges such as information loss, high costs, and the complexity of mapping between standards persist.

Process-level integration seeks to maintain the original structure and format of data from both domains. Semantic web technologies and services-based methods are commonly used here. Semantic web technologies employ ontologies and frameworks such as the Resource Description Framework (RDF) to enable data integration without altering original schemas. While highly flexible and scalable, these methods require significant initial effort. Services-based methods, on the other hand, rely on OGC Web Feature Services (e.g., WFS-T) to dynamically integrate BIM and GIS over the web. Although effective for maintaining interoperability, these solutions often lack extensibility and are tailored to specific tasks.

Application-level integration focuses on solving specific cases without modifying source or object data. For instance, ArcGIS support the direct import of BIM files (e.g., .ifc, .rvt), allowing seamless integration for spatial analysis and visualization. Additionally, intermediate formats such as Green Building XML (gbXML) are used to connect BIM and GIS systems, enabling data visualization in tools like Google Earth. While efficient and low-cost, application-level integration is generally limited to predefined use cases and lacks generalizability [28].

BIM-GIS Integration

- Data level
  - New Standards and Models
    - InfraGML
    - IndoorGML
    - Unified Building Model (UBM)--based on UML
    - QUASY (Quartierdaten-Managementsystem)
  - Conversion, Translation and Extension of Existing Standards
    - .IFC ←→ .CityGML
      - BIM Sever--GeoBIM —— IFC→CityGML —— extend the CityGML as GeoBIM extension to support IFC semantics and geometries. It was demonstrated in an XML Schema file (XSD) and as a UML class diagram
      - IFCExplorer
      - ETL（Extract-Transform-Load）
        - Oracle Spatial with Spatial ETL
        - ArcGIS Data Interoperability
        - FME
- Process level (not change the data format and structure from both sides)
  - Semantic Web Technologies —— Reference Ontology
    - IFC for GIS (IFG) data model and buildingSMART Data Dictionary (formerly the International Framework for Dictionaries or IFD
    - Resource Description Framework (RDF)
    - distributed models
  - Services-Based Methods —— OGC map services
    - Web Feature Server (WFS)
    - Transactional Web Feature Service (WFS-T for BIM)
    - Onuma System.
- Application level
  - Green Building XML (gbXML) —— KML and COLLADA —— Google Earth
  - MS Access
  - ArcGIS .ifc / .rvt directly import → fewer .ifc Format Data loss / .rvt more compatibility

Figure 6 Three Level of BIM-GIS Interoperability

In this study, two approaches are adopted: the methods highlighted in orange in Figure 6, which represent widely adopted techniques, and those highlighted in green, which are based on commercial platforms. Additionally, a method utilizing FZKViewer 6.5.1[29] was tested to convert and export CityGML models. However, upon importing the models into QGIS, significant data loss was observed, and the geometry conversion proved to be highly unsuccessful.

Industry Foundation Classes (IFC) and City Geography Markup Language (CityGML) are the two most widely adopted standards within BIM and GIS domains, respectively. Both of them are extensively used for exchanging semantic 3D information and geographical data, serving as critical standards for interoperability in the BIM and GIS fields [30].

IFC and CityGML Structure

The Industry Foundation Classes (IFC) standard provides a standardized digital description for the architecture, engineering, and construction (AEC) industry. It is neutral, vendor-independent, and freely accessible to all users. The most common exchange format for IFC is the STEP Physical File Format (ISO 10303-21:2002), which is based on a schema defined using the EXPRESS language (ISO 10303-11:2004). By providing machine-readable information, IFC facilitates workflow automation.

The IFC model integrates geometric representations with semantic definitions, employing a class-based system where real-world objects are represented as entities along with their associated attributes and relationships. Entities in the IFC model are broadly categorized as rooted or non-rooted. Rooted entities, belonging to the IfcRoot category, possess identity attributes such as name and description, while non-rooted entities exist only when associated with rooted entities.

The IfcRoot category is divided into three key subclasses: IfcObjectDefinition, IfcRelationship, and IfcPropertyDefinition. These subclasses represent material and conceptual objects, relationships between entities, and extensible object properties, respectively. Among them, IfcObjectDefinition is further subdivided into IfcObject, which addresses the physical presence of individual objects, and IfcTypeObject, which manages type information.

Both of them divided into IfcProduct, IfcProcess, IfcControl, IfcResource, IfcActor, and IfcGroup—enable detailed classifications of tangible objects, processes, and resources within a project. IfcProduct represents entities by providing information on description, representation and spatial arrangements of the elements. It is divided into: IfcAnnotation, IfcElement, IfcGrid,

IfcPort, IfcProxy, IfcSpatialElement, IfcStructuralActivity e IfcStructuralItem. IfcElement serves as a superclass for building components such as walls, columns, and windows, while IfcSpatialElement organizes spatial entities like sites, buildings, and floors. Additionally, IfcProxy provides placeholders for entities that do not fit predefined semantic types. This hierarchical structure ensures comprehensive representation and relationship management of both physical and conceptual elements, supporting detailed and scalable BIM applications. (Figure 7) [31],[32].
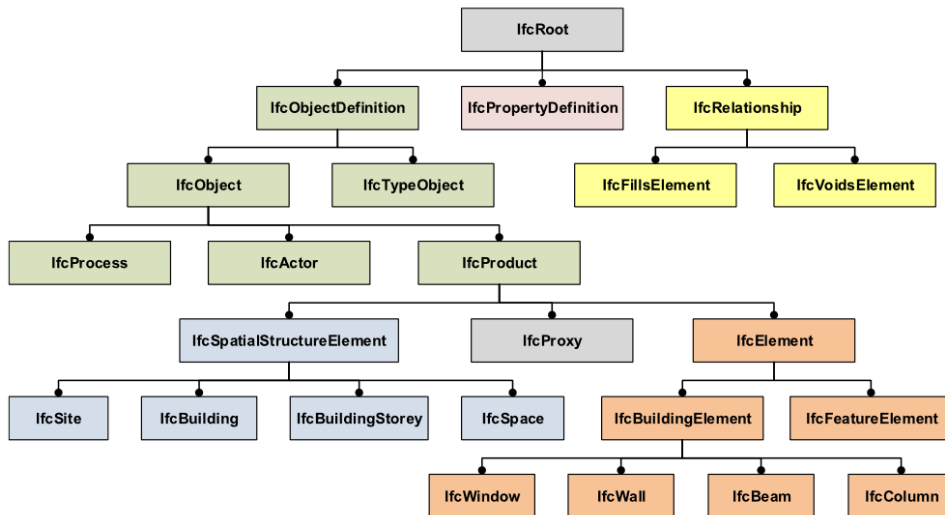
Figure 7 Part of the IFC data model showing the most important entities in the upper layers of the inheritance hierarchy. Source:[31]

CityGML is an open data model and XML-based, which uses the XML Schema Definition (XSD) to define the relationships between entities, designed for the representation and exchange of 3D geospatial data related to cities, including features like buildings, terrain, and vegetation and so on.

In 2003, different standard Levels of Detail (LoD) for 3D objects as part of the "Geodata Infrastructure" were defined by the Special Interest Group 3D (SIG 3D) in North Rhine-Westphalia, Germany [33]. These standards were later adopted by the Open Geospatial Consortium (OGC) to evaluate the quality of 3D city model datasets, thereby facilitating dataset comparability and integration. This framework was incorporated into the City Geography Markup Language (CityGML) with the release of CityGML 1.0 in 2008, which quickly gained worldwide acceptance. Subsequently, CityGML 2.0 was introduced in 2012. In 2020, the OGC released the CityGML 3.0 Conceptual Model Standard; however, the CityGML 3.0 GML Encoding Standard has not been published officially.

In CityGML 2.0, The most basic level, LoD0, is essentially a 2.5D Digital Terrain Model (DTM) over which aerial images or maps can be draped. At this level, buildings can be represented by their footprint or roof edge polygons. LoD1 features a block model of prismatic buildings with flat roofs. In contrast, LoD2 includes differentiated roof structures and thematically distinct boundary surfaces. LoD3 offers architectural models with detailed wall and roof structures, potentially including doors and windows. LoD4 extends LoD3 by adding interior details such as rooms, interior doors, stairs, and furniture (Table 1). High-resolution textures can be applied across all LoDs for enhanced appearance. LoDs are also characterised by differing accuracies and minimal dimensions of objects. The accuracy requirements given in this standard are debatable and are to be considered as discussion proposals [34].

	LoD0	LoD1	LoD2	LoD3	LoD4
Model scale description	regional, landscape	city, region	city, city districts, projects	city districts, architectural models (exterior), landmark	architectural models (interior), landmark
Class of accuracy	lowest	low	middle	high	very high
Absolute 3D point accuracy (position / height)	lower than LOD1	5/5m	2/2m	0.5/0.5m	0.2/0.2m
Generalisation	maximal generalisation	object blocks as generalised features > 6*6m/3m	objects as generalised features > 4*4m/2m	object as real features > 2*2m/1m	constructive elements and openings are represented
Building installations	no	no	yes	representative exterior features	real object form
Roof structure/representation	yes	flat	differentiated roof structures	real object form	real object form
Roof overhanging parts	yes	no	yes, if known	yes	yes
City Furniture	no	important objects	prototypes, generalised objects	real object form	real object form
Solitary Vegetation Object	no	important objects	prototypes, higher 6m	prototypes, higher 2m	prototypes, real object form
Plant Cover	no	>50*50m	>5*5m	< LOD2	<LOD2
…to be continued for the other feature themes					

Table 1 LOD 0-4 of CityGML 2.0 with their proposed accuracy requirements

The concept of Level of Detail (LoD) has been redefined in CityGML 3.0 (Figure 8) to address the practical limitations of CityGML 2.0. Compared to its predecessor, CityGML 3.0 has

removed LoD4 and allows all LoDs (LoD0–LoD3) to represent both interior and exterior features. In CityGML 3.0, LoD is no longer tied to the semantic decomposition of urban objects but is instead solely related to spatial representation. This adjustment enables, for example, the inclusion of thematic surfaces (such as walls and floors) in LoD0 and LoD1 representations, while doors and windows can be represented at all levels of detail.

CityGML 3.0 also introduced a new "Space Concept," which provides greater flexibility for ensuring consistency between geometry and semantics. This is achieved by mapping all CityGML features to the semantic concepts of "space" and "space boundary.
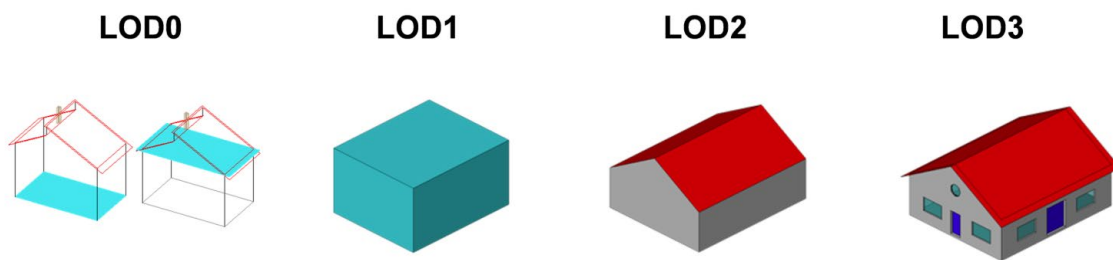
Figure 8 Representation of the same real-world building in the Levels of Detail 0-3.

source:[35]

From IFC to CityGML

The conversion from IFC to CityGML is a widely used approach for data integration. In this process, text-based IFC files are parsed into object models. Subsequently, the geometric and semantic information within the IFC object models is separately processed and converted into CityGML models. This procedure, referred to as geometric conversion and semantic mapping, constitutes the primary task of BIM-to-GIS integration.

Geometric and Spatial Reference System Conversion

The Industry Foundation Classes (IFC) framework uses a local Cartesian coordinate system (X, Y, Z) for geometric positioning, while Geographic Information Systems (GIS) rely on a global geographic coordinate system. Transforming between these systems, known as geo-referencing, is essential for BIM-GIS integration but is frequently impeded by the lack of geo-referencing information in IFC models.

The IFC standard supports various geometric representation methods to meet diverse modelling needs, primarily including (1) Swept Solids: This method defines geometric shapes through the combination of parametric cross-sections and paths. It is suitable for modelling regular building elements such as columns, beams, walls, and pipes, offering high efficiency in both storage and computation. (2) Constructive Solid Geometry (CSG): By applying

Boolean operations (e.g., union, subtraction, and intersection) to basic geometric primitives such as cubes, spheres, and cylinders, this method enables the creation of parametric and regular shapes. (3) Boundary Representation (B-Rep): This approach defines three-dimensional shapes using boundaries such as vertices, edges, and faces, making it ideal for representing complex geometries.

In contrast, CityGML primarily adopts surface representation, with Mult Surface serving as the core of its geometric framework. Each surface is typically a polygon, or a series of polygons defined by vertices, edges, and face orientations. For example, CityGML represents a wall's geometry through the visible interior and exterior wall surfaces, whereas IFC describes a closed cube using six distinct faces. These differences in geometric representation make solid-to-surface conversion an essential task during geometric transformations.

Semantic Mapping

The process of semantic mapping involves mapping IFC classes to CityGML entities, attributes, and relationships. IFC, based on the EXPRESS data modeling language, defines over 800 classes, but only 60-70 of these are relevant to geospatial information. Further research indicates that only 17 classes can be mapped to CityGML[36]. These mappings can be implemented through the following approaches: (1) One-to-One Mapping, for example, the IfcDoor class can be directly mapped to the Door entity in CityGML. (2) One-to-Many Mapping: A single IFC class can be mapped to multiple CityGML classes based on the orientation of surface normal vectors. For instance, IfcSlab can be mapped to OuterFloorSurface, WallSurface, or OuterCeilingSurface depending on the direction of its normal vectors. (3) Indirect Mapping: When direct mapping is not feasible, geometric operations can be used in combination with one-to-one or one-to-many mappings to achieve the transformation. As mentioned before CityGML 3.0 introduced a new "Space Concept", This concept may facilitate the direct mapping of Industry Foundation Classes (IFC) volumetric objects, such as IfcWall and IfcSlab, to CityGML volumetric objects. It represents a significant shift from CityGML 2.0, where surfaces such as InteriorWallSurface and ExteriorWallSurface had to be separately identified and extracted. Additionally, due to the relatively lightweight nature of the CityGML data model, some semantic information from IFC may be lost during the mapping process. To address this limitation, extensions such as Application Domain Extensions (ADE) allow new attributes or objects to be added to CityGML. However, incorporating these extensions increases the complexity of the resulting model [37].

1.3.4 Leveraging Integrated HBIM-GIS Approaches to Enhance Flood Risk Management in Heritage Preservation

In current practices, flood damage assessments typically concentrate on evaluating the structural integrity of individual buildings during floods [38], [39] or assessing the condition and extent of urban or archaeology areas affected by flood water[40], [41]. However, for heritage buildings, this approach requires expansion. It's necessary to not only assess structural stability but also to devise comprehensive flood strategies, which include protective measures, plans for restoration and stabilization, and public communication. A detailed understanding of how floods affect heritage buildings at the level of individual building elements is essential for informed decision-making and adaptive strategies.

Here "Building element" refers to a distinct physical part of a building that serves as a specific function in the structure. Building elements could be structural (e.g., walls, columns, roofs) or non-structural (e.g., windows, doors, partitions), and they contribute to the overall functionality, performance, aesthetic, and integrity of the building. In the context of cultural heritage, elements also consist of decorations, ornamental plasterworks, carved stone, sculptures, etc. Evaluating the impact of floods at this granular level involves how floodwater impacts these elements, including material degradation, loss of cultural value and so on. This approach enables the development of targeted strategies for preservation and restoration.

Preserving cultural heritage not only protect the heritage structures themselves but also maintains the context of cultural heritage, including the surrounding environment and intangible aspects[42], [43]. HBIM could create detailed 3D models of historic buildings, incorporating comprehensive historical, architectural, and material information. GIS could integrate extensive spatial data, including topography, precipitation, infiltration rate, land use, etc., which establishes a solid framework for understanding and analysing flood disasters. Its spatial analysis capabilities and hydrology tools are also useful in identifying flood-prone areas, evaluating vulnerability and predicting potential impacts.

As established in Section 1.3.3, the integration of HBIM and GIS is both meaningful and feasible from practical application and technical perspectives. Combining these technologies allows for a comprehensive understanding of the unique environments in which buildings are situated and facilitates multi-scale simulation and analysis. This integrated approach improves the understanding of the flood impacts on heritage and ensures flood management strategies are tailored to each heritage site. Additionally, it provides insight into flood response strategies

and guidance for post-flood restoration. This ensures better preservation and protection of heritage sites, allowing cultural heritage to adapt to climate change.

Chapter 2 History of the Valentino Castle (Castello del Valentino)

2.1 Brief History of Valentino Castle (Castello del Valentino)

The history of Valentino Castle (Castello del Valentino), a distinguished castle located on the banks of the Po River, exemplifies the profound architectural and socio-cultural evolution in European history.

The term "Vallantino," used since the 13th century, identified a region characterized by its unique topography, marked by a natural depression intersected by a stream. Specifically, for the location of the current Valentino Castle, it referred to an area outside the city limits of Turin, situated along the left bank of the Po River. This location was distinguished by a stream that now flows underground.
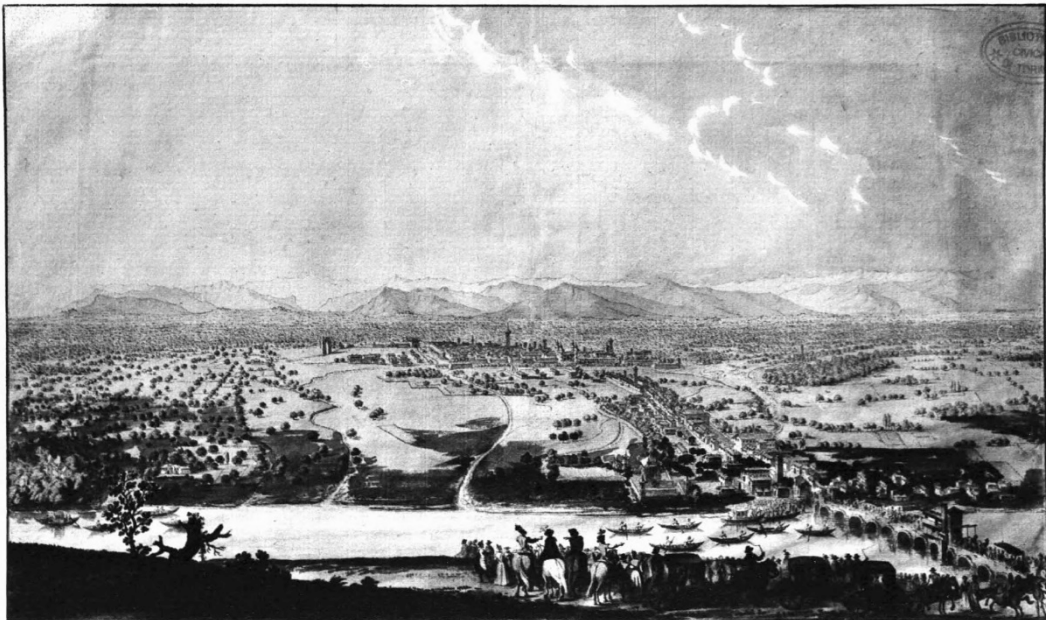
Figure 9 Randoni's watercolor drawing reproducing an ancient painting already preserved in the royal palaces, almost certainly representing a stop on the hill of Iaria Cristina during the celebrations (1620) for her arrival in Turin. (Collection Viscon ti Veno sta, castle of S. Martino Alfieri).

Source:Il Castello del Valentino, Turin: SET - Società Editrice Torino, 1949, p. 51 [44]

Development of Valentino Castle in the 16th Century

The structure we now recognize as Valentino Castle initially began as a riverside villa. In 1543, the Valentino fief, including a palace built on an ancient foundation on the Po's left bank, was acquired by Renato Birago, Grand Chancellor of France, from Melchiorre Borgarelli, an official of the French government. The Grand Chancellor and his wife, Valenza Balbiana,

resided there until 1564, using the villa as a representation of the French government. In that year, Duke Emmanuel Philibert of Savoy purchased the Valentino estate, encompassing the palace and its agricultural lands. This acquisition was part of a broader strategy to prepare Turin as the new capital of the Savoy state and to create a military isolation zone beyond the city walls, separating the city from rural areas. Consequently, the Duke also acquired adjacent territories, including Altessano from Birago and the estates of Stupinigi (1563) and Regio Parco (1565).

However, Duke Emmanuel Philibert sold the Valentino property in 1565, only to reacquire it in 1577. After the death of his wife in 1574, the Duke used Valentino privately until his death in 1580, often residing there from May to June. During this period, the villa was also occupied by Don Amedeo of Savoy, the Duke's natural son with a noblewoman from Turin. Don Amedeo not only resided at the estate but also oversaw its upkeep and initiated several building enhancements.

From 1576 to 1578, the palace underwent what can be described as its first ceremonial renovation. Don Amedeo of Savoy commissioned the development of the interior's decorative elements, assigning the painting work to Alessandro Ardente and the sculpting to Pietro Antonio Vanello, a marble sculptor from Lugano. The villa's structure largely remained the same, featuring a single wing parallel to the Po River. This wing, rising four stories high from the river side, included the main entrance. A watchtower was situated to the south of the wing, while the north side housed ceremonial halls, such as the decorated hall (presently the Hall of Columns) and below it, the Pallamaglio Hall, located within a protruding section.

Upon the passing of Emmanuel Philibert, his successor, Carlo Emanuele I, initially transferred the estate to his brother-in-law Filippo d'Este, prioritizing his interests in Lucento and Regio Parco. However, in 1586, he reacquired it. Subsequently, his wife, Duchess Caterina of Austria, incorporated the villa into her appanage, initiating a tradition of entrusting the riverside residence to the future spouse of the heir apparent.

Duchess Caterina instigated several projects on the estate, focusing not on the embellishment of the residence but on enhancing the gardens, access routes, city connections, and the estate's agricultural and functional dependencies.

In 1597, upon Duchess Caterina's death, Carlo Emanuele I regained ownership. Continuing the established tradition, in 1619, he gifted the complex to his daughter-in-law, Cristina of France, wife of heir apparent Vittorio Amedeo.

The 17th Century Transformations

The transformation of the building commenced in 1620 after Carlo Emanuele I donated it to Princess Cristina of France. Architect Carlo di Castellamonte, and subsequently his son Amedeo, were instrumental in evolving the palace into a "maison de plaisance," inspired by the French "pavillon-système" model.

An initial concept by Carlo di Castellamonte proposed a wing, double the existing size, parallel to the Po River, flanked by two towers and topped with a pavilion roof. Though this design wasn't realized, it influenced subsequent developments.

The reimagined design centered the Cour d'Honneur, loggia, staircase, and a new double-height Hall of Honor (above the existing Hall of Columns) at the heart of the complex, promoting symmetrical expansions around this nucleus. This reconfiguration involved constructing square interconnected halls adjacent to the main structure, extending the wing parallel to the river, integrating the south tower into a larger build, and erecting a new northern tower. A two-sloped "*lose*" roof was also added.

Around 1633, the construction of porticoed galleries commenced, further enhancing the estate.

In 1639, the building's renovations were interrupted due to a civil war instigated by Madama Reale and Princes Tommaso and Maurizio of Savoy after Vittorio Amedeo I's death. Renovations resumed in 1644, focusing on the construction of two porticoed galleries to the west, the front towers, and a circular exedra around the Cour d'Honneur. Simultaneously, the southern apartment's decorative work began, led by craftsmen like Isidoro Bianchi and his son Pompeo, and Alessandro Casella, who specialized in gilding stuccos and vaults. By 1646, the focus shifted to the northern apartment's interior, where Casella continued his stucco work, complemented by the Bianchi family and Giovanni Paolo and Antonio Recchi.

Between 1659 and 1660, enhancements to the facade facing the city included the addition of striped masonry columns on a high base flanking the loggia, four statues representing the seasons, fake windows to soften the roof's steep slope, and a central pediment plaque, later replaced in the early 19th century.

Figure 10 Anonymous painting depicting the Valentino Castle according to the Theatrum Statuum Regiae Celsitudinis Sabaudiae Ducis, Blaeu, Amsterdam, 1682.

Source: Museo Civico, Turin.

18th and 19th Century Changes

After Christine of France's death in 1663, Valentino ceased as a ducal residence, supplanted by the Venaria Reale, and was repurposed for public festivities. Consequently, it underwent only maintenance work until the end of the 17th century.

In 1729 with the establishment of the Botanical Garden of the Royal University of Studies in the northeastern square garden. It wasn't until 1800 that the building found a more permanent function. The French government, then ruling Piedmont, designated the castle as the "National House," hosting the School of Veterinary Medicine until the Restoration era, when control reverted to the Crown.

After the reacquisition, Valentino palace faced significant static instability issues in its galleries, porticos, and hemicycle. Thus, the General Intendancy of the Royal House mandated their demolition in 1822, followed by a reconstruction in 1823 at the same location, maintaining the original style but allowing for different, visually similar materials.

Simultaneously, the palace's function shifted to a Barracks for the Genius Pontieri Company of the Royal Corps of Artillery, a role it maintained until 1850 when the Crown's properties were transferred to State ownership. From the early 19th century, the Valentino area also hosted several industrial product exhibitions, including the notable sixth exhibition in 1858.

Figure 11 Lithograph of the "Gab.o di Dis.o e Litog. Dell'Uff. Spec.le dei Brevetti d'Invenzione Capuccio e Latini", in Album descrittivo dei principali oggetti esposti nel Real Castello del Valentino in occasione della Sesta Esposizione Nazionale dei prodotti d'industria nell'anno 1858, Torino, Stamperia dell'Unione Tipografico Editrice, 1858, unnumbered tables. ASCT, Collezione Simeom, C 1911, by concession of the Archivio Storico della Città di Torino.

Source:https://castellodelvalentino.polito.it/?page_id=995#jp-carousel-3439

Late 19th to 20th Century Evolutions

In 1857, the government enacted legislation for "Expansion and Restorations to the Valentino Castle for the exhibition of national products." This period marked a transition in the building's identity, as it began to be referred to as a "Castle" rather than a palace. During this time, the main entrance was moved from the Po-facing facade to the city-facing side.

The castle underwent extensive restoration, including the construction of new two-story, porticoed exhibition wings for industrial prototypes and machinery, replacing the existing galleries.

Post-exhibition, the building served as the Regia Scuola di Applicazione per Ingegneri di Torino, established under the Casati Law of 1859. This role prompted further modifications, such as the 1862 demolition of the hemicycle and the construction of terraced structures in its stead, along with a new sleeve parallel to the Po between 1868 and 1880. These developments culminated in the construction of comb-like sleeves near the entrance from 1897 to 1899.

Further transformations took place in the 20th century when the Politecnico di Torino, established in 1906, acquired the castle. These included the construction of a mechanical workshop (1912-1913) and new classrooms (1946-1948) to adapt the building to its educational role.

The early 20th century restoration efforts at Valentino Castle focused on structural consolidation and the refurbishment of the decorative elements, including, in some instances, their replacement.

Subsequent restoration projects commenced in 1961, coinciding with the National Exhibition of Labor. This phase included overhauling the roof structure, replacing beams, and installing new floors, notably in the Hall of Columns. In 1975, further work was carried out on the central loggia, including the restoration of stucco decorations on the exterior facade and repainting the south wing of the ceremonial section of the Castle. Elm trees to the south of the Castle were also removed to accommodate two temporary prefabricated classrooms.

Late 20th Century Restorations

From the mid-1980s, further restoration began, focusing on the comprehensive revival of the structure, enhancing its appeal, and improving its accessibility for visitors.

In 1997, Valentino Castle was recognized as a UNESCO World Heritage Site, as part of the Savoy Residences Circuit.

2.2 Water System and Basement of Valentino Castle(Castello del Valentino)

The history of Valentino Castle is closely linked to its location near the Po River. Originally named "Vallantinum," the area was characterized by a natural valley with a watercourse, known as the "bealera del Valentino," which still flows underground today.

Chapter3 Methodology

Typically, flood depths exceeding 1 metre above floor level have the potential to cause structural damage to buildings, particularly when the buildings are in a poor state of repair. However, it is uncommon for the structure integrity of a historic building to be compromised under such conditions. [6, p. 16] In this thesis, hydrostatic and hydrodynamic flooding actions are not considered. The primary focus is on low flow velocity floods, emphasizing the impact of flood depth. The study concentrates on identifying vulnerable elements of Valentino Castle under various flood scenarios, assuming that the overall structural stability is maintained. The proposed workflow is purely theoretical and experimental; therefore, the results of the analysis are not guaranteed to be fully accurate and should not be cited as definitive conclusions.

The objective of this study is to propose an integrated HBIM-GIS framework for flood risk management at the elements (such as doors, walls, movable-assets, etc.) level of heritage buildings. This is achieved through targeted HBIM modeling and leveraging the interoperability between BIM and GIS systems. The specific challenges addressed in this process are as follows:

Heritage assets possess unique architectural and historical significance. Unlike contemporary buildings, they often feature complex designs and irregular elements such as intricate decorations, sculptures and vaults. Thus, modelling these features can be time-consuming and typically results in a heavy HBIM file that complicates data reading, editing and interoperability.

Moreover, for flood impacts analysis, the elevation of the objects is a crucial factor. Floodwater or rainwater tends to accumulate in lower terrain areas, inundating certain building elements at lower elevations. Consequently, basements and openings lower stories are at higher risk during flooding. To access the impacts on built heritage caused by floodwater, it is essential to consider hazard-sensitive information of the building, such as the building's material properties, historic fabric, possible damage types and precautions for remedial works, etc.

The raw point cloud data was acquired using various 3D metric survey methods, detailed in chapter 4.1. Analysing flood impacts requires converting the asemantic point cloud data into an HBIM model with comprehensive information. Integrating various geological data and the HBIM model in a GIS system allows for analysis, visualization and identification of

vulnerabilities when flooded. Given that Valentino Castle is a built heritage, it is fundamental to ensure the geo-referencing accuracy of the existing building in a 3D GIS environment.

High accuracy of the topographical data is essential for analysing stormwater and riverine flooding impacts on Valentino Castle. The 1:5000 DTM (digital terrain model) provided by Geoportale Piemonte lacks the necessary precision. Obtaining a more accurate DTM is crucial for reliable analysis.

Comprehensively addressing aforementioned challenges, creating a multi-scale 3D GIS model is a crucial step for flood impacts analysis. This model should integrate essential HBIM and Geospatial data for downstream analysis. To handle interoperability issues between BIM and GIS, adopting standards that facilitate effective communication is necessary.

In this workflow, the commercial GIS platform ArcGIS Pro 3.3 and open-source GIS platform QGIS were employed, and the CityGML 3.0 standard was adopted to guide the modelling of city and building features at different Levels of Detail (LoD). Due to the requirement for high-resolution results in the flood impact analysis on Valentino Castle, LoD 3 should be achieved in the creation of a multi-scale 3D GIS project. However, in the scan-to-BIM process, the LoD 3 Specification in CityGML 3.0 is not sufficiently detailed to guide the BIM modelling process. In BIM filed, the concept of the level of development (LOD) is applied in the case of new construction. The LOD framework was established by the American Institute of Architects (AIA) and the Associated General Contractors of America (AGC). It refer to a standardized framework for defining the amount of detail and accuracy that should be included in a building information model (BIM) at different stages of a project.

LOD 100—conceptual design: At this stage, the model represents the basic shape and size of elements without detailed information. It's used to convey the overall design intent.

LOD 200—schematic design: The model becomes more refined, incorporating approximate quantities, sizes, shapes, and locations of elements. It helps in analysing spatial relationships and early design concepts.

LOD 300—detailed design: In this phase, the model includes geometric information, specific sizes, shapes, and detailed object elements. It's used for producing construction documents and coordinating different disciplines.

LOD 350—construction documentation: The model includes detailed assemblies and fabrication or construction-level information. It's used for generating construction documents and shop drawings.

LOD 400—fabrication and assembly: This level involves the creation of detailed models with specific assemblies and connections, suitable for fabrication and assembly purposes.

LOD 500—as-built or facility management: The model at this stage includes information about the installed and operational elements of the building, reflecting real-world conditions for maintenance and facility management.[45, pp. 14–15](In this thesis, LoD refers to the Levels of Detail as defined by the CityGML standard, while LOD refers to the Level of Development in BIM.)

A model element can contain two types of information: the element's geometry and associated numeric and/or textual attributes [45, p. 192] defined in UNI11337 :2017 as the livello Geometrico (level of geometry, LOG) and livello informative (level of level of Information, LOI), respectively. LOG and LOI together compose the Level of Definizione, which is a concept similar to the Level of development [46]. ISO 19650-1:2018 emphasize defining the use or purpose before specifying the required information to avoid information waste and introduced the level of information need (LOIN) .[47] The new UNI EN 17412-1:2021 standard provides details on specifying LOIN Need and further develops it. the focus of LOIN is no longer on the characteristics of the object but on the information that the object must contain to meet the professional's needs at that precise moment in the design process. It describes the granularity of the information exchange in terms of geometric, alphanumeric, and documentation information [48].

The traditional LOD concept (establish by AIA) applied to new construction case is based on a linear progression of geometric and alphanumeric information throughout the design and construction process. This linear approach ensures that as the project advances, the BIM model evolves in geometric and information aspect. It is not suitable to apply to the restoration-preservation management process because it risks delaying the understanding of the geometry, the current state, and the behaviour of the structures. This delay can lead to significantly increased costs due to unforeseen issues. Additionally, insufficient information limits the ability to develop design solutions that are consistent with the current state and preservation objectives [49], [50]. The evolution of the LOD concept introduced the Level of Geometry (LOG) and the

Level of Information (LOI) to collectively explain the LOD framework. Further advancements led to the development of the Level of Information Need (LOIN), which emphasizes the project's purpose and related information requirements. These developments enable flexible combinations of different LOG and LOI levels. For example, a low LOG can be paired with a high LOI to meet the requirements of cultural heritage documentation, while a high LOG combined with a lower LOI can satisfy visualization needs. This approach provides a more flexible and comprehensive framework, enhancing the effectiveness of BIM in various fields, particularly in the management and conservation of historic buildings.

The reference [51] propose a framework for the Levels of Geometry (LOG) applicable to Heritage Building Information Models (HBIM), defining detailed specifications for the Levels of Geometry (LOG 100–500) within the heritage domain:

- LOG 100: Conceptual Model, Historical Reports, Archives

LOG 100 represents the foundational level where historical information about a building is collected. It includes historical building contracts, historical drawings, and other forms of historical documentation such as pictures, photos, and documents. The primary aim at this level is to gather and understand the historical context and past records of the building. The conceptual model provided the basis for developing the HBIM and provided important historical information for subsequent phases.

- LOG 200: Appropriate Geometry, 3D Survey, Data Acquisition

At LOG 200, the focus shifts to on-site data acquisition and geometric surveying. This level involves comprehensive 3D surveying using techniques such as laser scanning and photogrammetry. Generate 2D and 3D reconstructions (floor plans and cross-sections) and 3D mesh based on the collected point cloud data. LOG 200 ensures that the geometric description of the building is captured accurately, providing a detailed foundation for creating precise models. This stage is crucial for ensuring the accuracy and reliability of the HBIM model, supporting detailed analysis and restoration planning.

- LOG 300: Precise Geometry, Scan-to-BIM Model Object

LOG 300 involves the generation of accurate 3D models from the point cloud data acquired in LOG 200. This stage focuses on object modelling and precise drawing extraction, resulting in

detailed HBIM models suitable for various analyses, including energy analysis and finite element modelling (FEM). The precision of the models at this level supports advanced applications and simulations, making LOG 300 critical for in-depth architectural and structural assessments.

- LOG 400: BIM Uses – Conservation Plan

LOG 400 is dedicated to the conservation plan and involves using the HBIM model for comprehensive BIM-based analyses. It includes material and decay mapping, diagnostics (such as infrared thermography and non-destructive testing), BIM-to-FEA, energy analysis and on-site construction management. At this level, the HBIM models are refined with precise geometric accuracy and combine extensive information to support various conservation and restoration tasks. The models are utilised to conduct intricate analyses and simulations, thereby ensuring the preservation and maintenance of the building's structural integrity and historical value.

- LOG 500: Conservation Site

LOG 500 represents the construction stage, focusing on on-site conservation interventions. The geometric model at this level combines as-found, as-designed, and as-built layers to provide a comprehensive representation of the building. LOG 500 addresses the geometric and typological functions of various data, analyses, and models aimed at preserving architectural heritage. This level supports the practical implementation of conservation plans, involving multiple professionals such as restorers and structural engineers, who rely on flexible and accurate HBIM models to guide their work.

Valentino Castle is an existing building where an LOD 500 model could potentially be achieved. However, considering the Level of Information Need (LOIN) and to avoid information waste, the primary geometry of the building, without highly detailed specifics, is sufficient for flood impact analysis. Therefore, the geometric modeling is based on LOG 300 within the HBIM framework, with some simplifications made to decorative elements to enhance efficiency. It also allows for relatively high-quality 3D visualization of the results, thereby enhancing communication among stakeholders. In terms of alphanumeric information, the model includes additional data relevant to flood impact assessment, such as materials, building decay, potential damage types and precautions for remedial works. The specific modelling process will be

elaborated in Section 4.2. An integrated workflow is applied in this research to assess and manage the impact on Valentino Castle, as shown in Figure 12.
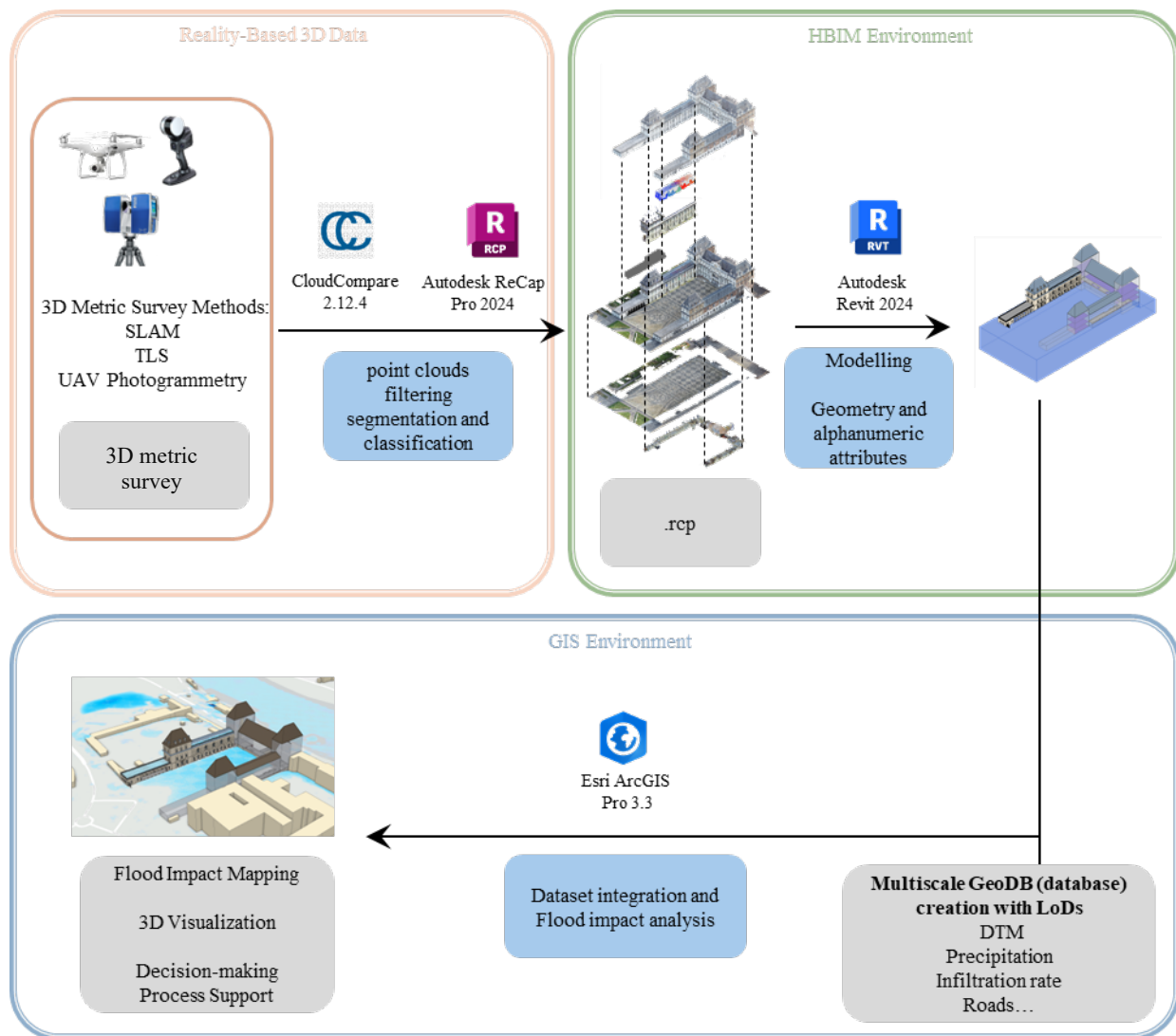
Figure 12 The Integrated Workflow for Flood Impact Assessment

The integrated workflow begins from a series of georeferenced point cloud data to achieve the ultimate goal of flood impact assessment on built heritage. The entire workflow encompasses three working environments: reality-based 3D data, HBIM And GIS. Initially the point cloud is processed and then used as a reference for HBIM modelling. The HBIM process converts the asemantic point cloud into a semantic model with necessary alphanumeric information for flood impact assessment. Finally, HBIM data and relevant geospatial data are integrated into a 3D GIS project for downstream analysis and visualization of results. The subsequent chapters of this thesis provide a detailed introduction to each stage of the workflow.

Chapter 4 Multi-scale 3D GIS Project

4.1 Data Acquisition and Process

Geomatics

"Geomatics is defined as a systemic, multidisciplinary, integrated approach to selecting the instruments and the appropriate techniques for collecting, storing, integrating, modeling, analysing, retrieving at will, transforming, displaying, and distributing spatially georeferenced data from different sources with well-defined accuracy characteristics and continuity in a digital format"[52].

In the field of cultural heritage conservation, geomatics were employed to monitor and acquire information through several widely adopted techniques, such as remote sensing, laser scanning, drones, and GIS. These non-destructive techniques enable to collect information about cultural heritage and its surroundings effectively and accurately. Then the acquired data could be processed and digitally reconstructed, incorporating multi-semantic information. This method facilitates plenty of analysis, helping to identify the potential risks, support informed decision-making, develop tailored risk management plans and long-term monitoring.

Remote Sensing (satellite image) for Large-scale Monitoring

Remote Sensing uses sensors on satellites to collect electromagnetic waves reflected or emitted from the Earth's surface, and these data are usually presented in the form of images, such as satellite images from Landsat and Sentinel. These images not only record spatial information but also various spectral bands, such as visible light, infrared, and so on.

Remote sensing enables the detection and monitoring of environmental and anthropogenic changes across extensive spatial and temporal scales. It not only enables the identification of buried features at archaeological sites but also provides important data support for the long-term conservation. This makes it particularly suitable for the monitoring, protection, and management of archaeological sites.

Techniques Commonly Employed in Cultural Heritage Survey

Cultural heritage surveys play a vital role in documenting, preserving and conserving the tangible and intangible aspects of cultural heritage. The following section briefly discusses the common techniques, corresponding data processing methods and instruments employed in geospatial surveys related to cultural heritage. Survey techniques could generally be categorized into image-based survey techniques, range-based techniques and sensor fusion methods based on the core principles used in 3D data acquisition:

Image-Based Survey Techniques

Photogrammetry

"Photogrammetric surveys are those where overlapping image sets are used together with survey control to produce a 3-D representation of the subject from which the required output is generated. Products may be orthophotographs, scaled drawings digitised from them, digital surface/terrain models (DSM/DTM) or other vector products derived from them (such as point cloud,3d models, contour lines)"[53, p. 27].

Photogrammetry uses two central perspectives of the same object with non-coincident projection centres to derive the spatial position of points (figure 13).
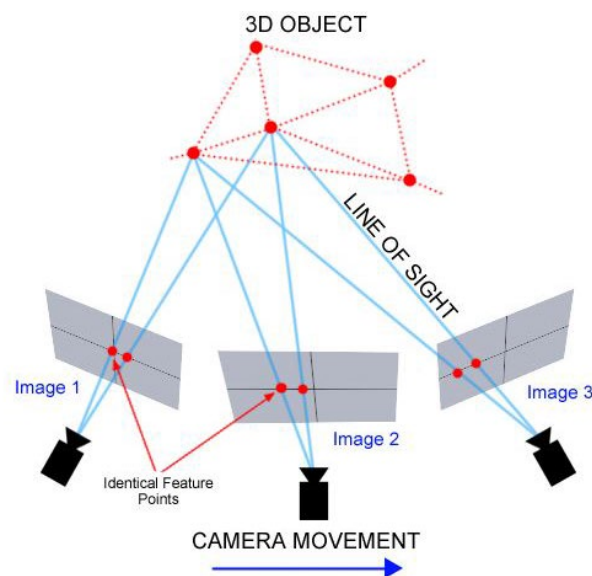
Figure 13 two central perspectives of the same object with non-coincident projection centres to derive object points in 3D space.

Source: https://thehaskinssociety.wildapricot.org/photogrammetry

In photogrammetry, the quality of the output is dependent on the quality of the input. Poor photography will inevitably lead to inaccurate results. So, the survey object must be sufficiently illuminated naturally or artificially, and the camera needs to be adjusted to obtain a high-quality image with the correct exposure. And there should be a sufficient proportion of overlap between the captured images, which varies depending on the specific method used in survey.

Image acquisition can be done either statically or dynamically and performed terrestrially or aerially.

Recently, structure from motion (SfM) combined with multi-view stereo (MVS) algorithms could process a series of overlapping input images, which are uncalibrated and lack camera location and orientation, to generate 3D information. In this process, SfM is employed to estimate the camera positions and orientations, even for uncalibrated images. Then, MVS derives a dense point cloud based on this information. This approach represents a rapid and cost-effective solution for both aerial and terrestrial applications. For instance, photogrammetry with UAVs (Unmanned Aerial Vehicles) is suitable for mapping large architectural complexes, archaeological sites, landscapes and areas difficult to access or with safety hazards. Its main advantage is lower cost while still providing enough accuracy that is adequate for some applications compared to laser scanning.

Most photogrammetric processing work needs to use dedicated photogrammetric software utilising overlapping imagery, such as, Agisoft Metashape, Pix4D, RealityCapture, and MicMac. The outcome could be a textured 3D point cloud model, orthophotos, 3D mesh models or digital elevation models (DEMs), depending on the project requirements [54].

Range-Based Survey Techniques

LiDAR（Light Detection and Ranging）

"Lidar stands for 'light detection and ranging', which describes a method of determining three-dimensional (3D) data points by using a laser. It is a remote-sensing technique, using either ground-based (terrestrial laser scanning; TLS) or airborne (airborne laser scanning; ALS) systems; it can be used from static or moving platforms, including aircraft and vehicle-mounted sensors. It is also referred to as airborne laser swath mapping (ALSM), and in some military contexts it is known as laser detection and ranging (LaDAR)"[55].

In cultural heritage field, ALS is often used in archaeological survey, especially for wide-area survey and inaccessible environments. While TLS is employed in archaeology and architecture, focusing on the high-precision and detailed recording of sites and buildings.

Terrestrial Laser Scanning (TLS)

"*Terrestrial laser scanning is defined as the use of a ground-based device that employs a laser to measure 3D coordinates automatically on the surface of an object in a systematic order and at a high measurement rate*" [55].

The factors that affect the accuracy of coordinate points include: (1) Distance measurement accuracy. (2) Roughness of the surveyed surface: Rough surface scatters the laser beam, reducing the strength and quality of return signals, which affects the accuracy of measurement. (3) Reflectivity of the surveyed surface: Low reflectivity surface weakens return signals, leading to data loss or increased noise. (4) Precision of the angular displacements of the laser beam. (5) Inclination of the laser beam with respect to the surface: Steeper angles can result in less precise data.

Although laser scanning could be conducted in dark or poorly illuminated conditions, it should not be undertaken during inclement weather (e.g. rain, snow, fog, mist, strong winds). Since during inclement weather, the particles or droplets in the air scatter or reflect the laser beam, this introduces noise to the point clouds and affects the data quality.

In the scanning process, moving obstructions, such as cars and pedestrians will introduce noise or create voids in the datasets by blocking the laser beam or obscuring the scanning area. So, it is necessary to restrict public access to the scan area when possible or scanning during low-traffic period. Occlusions are inevitable due to the fixed-position scanning. Thus, multiple scans from different positions or alternative measurement technologies should be used to fill the data voids.

The raw product of a laser scan survey is a point cloud. It is a collection of data points defined in a 3D coordinate system, representing the surface of a real-world object. (Products generated from photogrammetry can also be in the form of point clouds). Generally, point cloud data is represented using XYZ coordinates, stored in proprietary or non-proprietary formats. Point cloud facilitates the rapid visualization of real-world objects. Beyond basic XYZ coordinates,

point clouds can include additional attributes such as intensity. Most laser scanning systems also use an imaging sensor to acquire colour imagery, then assign RGB values to each point. These attributes can provide more detailed information about the scanned surface.

After the data collection process, the scans should be registered under the same coordinate system to form a merged dataset of the whole project. Scan registration can be performed using control targets, a 'cloud-to-cloud' approach or a combination of both. This process can be carried out automatically or manually using business software, such as FARO Scene, Leica Cyclone, or open-source software, like CloudCompare. Then the point clouds undergo cleaning, filtering, segmentation, classification and other processing steps to improve the quality. These steps ensure the reliability and usability of the point clouds for further applications, such as serving as a reference for BIM modelling.

Terrestrial Laser Scanning could achieve millimetre-level precision. However, it has relatively high monetary and time costs compared to photogrammetry. TLS could capture high-resolution details, which enables the recording of minor damages and provides a robust basis for future restoration work. At the same time, it facilitates long-term monitoring and periodic comparisons. The combination of laser scanning technology and advanced 3D modeling methods, such as BIM, provides an innovative approach for cultural heritage conservation and documentation.

Mix Method

Mix methods leverage both image-based and range-based techniques to acquire data efficiently and accurately.

MMS (Mobile Mapping System)

Mobile Mapping Systems (MMS) integrate photogrammetric and laser scanning techniques. It also combines additional devices such as Global Navigation Satellite System (GNSS), inertial measurement units (IMU), and accelerometers. MMS allows to estimate sensor positions and orientations in real-time and collect georeferenced 3D point clouds with high efficiency. These point clouds are generally less dense than those created by laser scanners or photogrammetry.

Mobile Mapping System (MMS) is usually installed on a mobile platform such as vehicles, UAVs, or backpack systems. It is suitable for large-scale surveying in outdoor environments

with GNSS signals, such as mapping street scenes, urban areas, and other large-scale landscapes. The system can obtain measurement data at centimetre-level accuracy.

Simultaneous Localization and Mapping (SLAM) provides an approach for environments where GNSS is unavailable. SLAM system commonly uses the Iterative Closest Point (ICP) technique and inertial platform data to monitor the linear and angular movements of the instrument during data processing. SLAM system often integrates with Lidar and digital cameras. This enables the system to record 3D data in real-time in the coordinate system defined by the instrument. Additionally, SLAM systems could combine point cloud data with colours acquired by integrated digital cameras. It is particularly suitable for use in indoor spaces, basements, or other complex environments where GNSS signals are unavailable.

Instruments and Techniques Used in Data Acquisition

In the field of cultural heritage (CH) conservation and management, various surveying techniques are often combined to measure the built heritages due to the constraints related to site location, safety conditions and operational time[56], [57], [58] .The raw point cloud data used in this work originates from the Laboratory of Geomatics for CH, of the Department of Architecture and Design (DAD) . Except the point clouds of the north wing office (②)and the chapel (④), all other data are registered. The survey methods for these data are outlined in Table 2. The exterior shell of the castle and the surroundings (①⑤) were captured using DJI® Phantom 4, an Unmanned Aerial Vehicle (UAV) and photogrammetry method and the courtyard (③) was acquired through Terrestrial Laser Scanning (TLS). The basement section was acquired through Mobile Mapping Systems (MMS) with Simultaneous Localization and Mapping (SLAM) algorithm, a relatively quick method suitable for complex environments(Figure 14)[59].

Figure 14 Processed and Validated Point Cloud Data Utilized in the Workflow

Position	Instrument	Main Specification	Source	Other
⑥Basement	STONEX® X120GO SLAM	**LiDAR:** Hesai XT16 Range:0.5-120m Relative Accuracy:6mm Scanning Point Frequency: 320 000 pts/s Field of View (FOV): 360°×270° **Camera** N°of Camera 3 (5 megapixels each) FOV: 200°×100°	https://www.stonex.it/project/x120go-slam-laser-scanner/	Ensures high-precision 3D point cloud data without GPS/GNSS
①& ⑤Exterior Shell of the Castle and The Surroundings	DJI® Phantom 4	Sensor: 1-inch CMOS sensor Effective Pixels: 20 megapixels Pixel size: 2.34527 micron Lens: Field of View (FOV) 84°, 8.8 mm -24 mm (35 mm format equivalent), f/2.8 - f/11 Max Flight Height: 6000 meters above sea level Accuracy: centimetre-level (with Real-Time Kinematic (RTK) module)	https://www.dji-store.it/prodotto/dji-phantom-4-rtk-se-combo/	The results shown in the figure 14 are classified and cropped point clouds.

Position	Instrument	Main Specification	Source	Other
③The Courtyard of the Castle	FARO® Focus3D X 330	Measurement Speed: 122,000 / 244,000 / 488,000 / 976,000 pts/sec FOV: 300° vertical / 360° horizontal Range: 0.6 - 130 meters Accuracy: ±2 mm Resolution: Up to70 megapixels	https://downloads.faro.com/index.php/s/wG7fpekQexTiZtW	The point cloud data was utilized for modelling doors and windows.

Table 2 Main Technical Specification of the acquisition instruments

Based on the different acquisition methods and data characteristics, the point cloud data underwent filtering, classification, segmentation, and fusion processes. The primary principle of these processes is to facilitate geometric modelling while ensuring a certain level of accuracy (LOA).

Filtering

During the data acquisition process, some unwanted features, such as adjacent buildings, people, vegetation, obstructions, data through windows, etc. are unintentionally acquired. Point cloud data is often very large and includes many redundant or duplicate points, especially after a high-resolution scan or multiple scans. Moreover, there are many factors that cause noise during laser scanning: (1) surface with high reflectivity transparent materials, such as glass, mirrors, or water surfaces, can produce erroneous return signals, resulting in noise. (2) Plants, dust, mist, or suspended particles in the environment can interfere with the laser signal, causing invalid or erroneous points to be recorded. (3) When the laser beam falls on the edge of an object, such as a wall corner or the edge of a thin object, the laser may reflect in multiple directions, causing a chaotic return signal. Thus, it is necessary to clean and filter the point cloud to improve the quality of the point cloud.

Cloud Compare was utilized to clean all the raw point cloud data by cropping out erroneous and unnecessary parts. Then statistical outlier filter (SOR) was employed to remove noise and outliers from the data. SOR identifies and remove points with unusual distances to their neighbours by calculating the average distance and standard deviation for each point's nearest neighbours. (Figure 15)
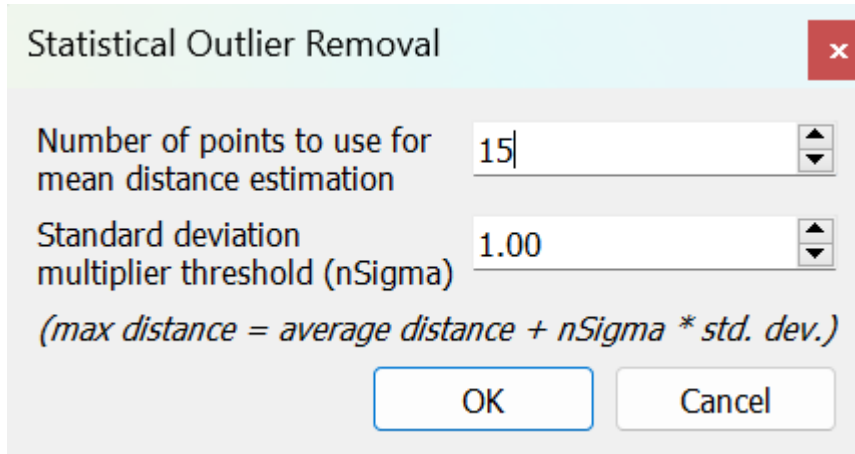
Figure 15 Statistical Outlier Removal in Cloud Compare

 These methods ensured only the points accurately representing the object's surface were retained. And this process not only reduced the file size to improve the overall efficiency of the software but also ensure the accuracy and reliability of following steps.

Classification and Segmentation

Although there is a significant amount of research on classifying point clouds through automatic or semi-automatic methods [60], [61] including machine learning and deep learning algorithms which require extensive training samples and are time-consuming[62] [63].the complexity of historical buildings makes it challenging for these methods to achieve satisfactory results. However, for simple classification, such as distinguishing the ground surface, these methods can be effective.

Ground Surface

In this thesis, only a simple yet necessary classification was conducted using ReCap, according to the modelling requirements. The cleaned UAV point cloud files of the overall castle were imported into Autodesk ReCap, which utilized its automatic ground classification function to identify and classify the ground surface. The automatic classification successfully extracted most of the ground surface-related point clouds, although some were misclassified and later manually corrected.

Doors and Windows

To enhance the Level of Accuracy (LOA) in modeling windows and doors, the Terrestrial Laser Scanning (TLS) point cloud was adopted due to the insufficient density and accuracy of the UAV (Unmanned Aerial Vehicle) point cloud of the overall castle. The positions of the selected scanning data are illustrated in Figure 16. By using data from multiple scanning locations, blind spots inherent to single fixed-point scanning were effectively eliminated. This multi-positional approach ensures comprehensive coverage and captures intricate details that might otherwise be missed. Additionally, by selecting suitable scanning angles, the accuracy of the point cloud data was significantly improved, leading to a more accurate and reliable representation in the final model.
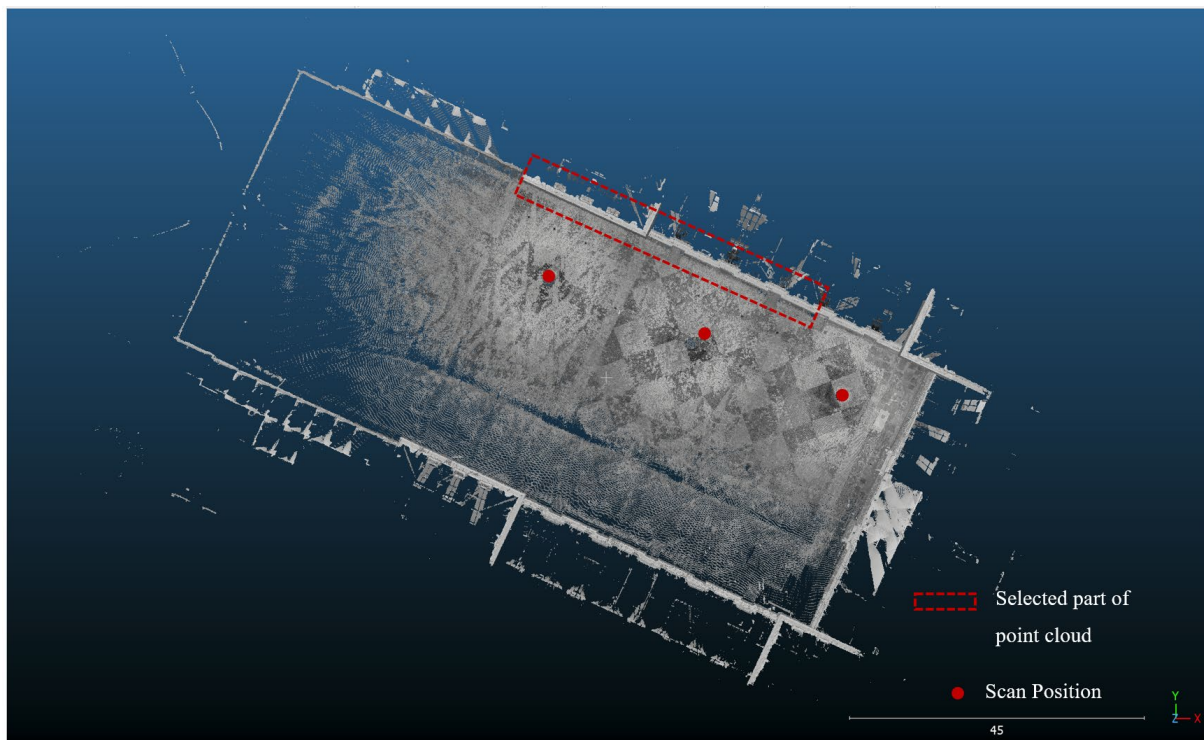
Figure 16 Scan Position in the courtyard

Data Fusion (Alignment)

All the point cloud datasets were imported into Autodesk ReCap to update the origin by shifting the same distance to comply with Revit's display range limit of within 10 miles (16 kilometers) from the model's internal origin, as shown in Figure 17. The point cloud datasets were then saved as seven Reality Capture Project (RCP) files, as depicted in Figure 14. Subsequently, a point in the courtyard was selected, and its coordinates were extracted and set as the project base point in Revit, as shown in Figure 18. Finally, the RCP files were imported into Revit using the shared coordinate system. Since the registered point cloud datasets are under the same

coordinate system (WGS1984 UTM 32N) and use the same UCS origin, they aligned well in Revit.

For the point clouds that were not registered — the north wing office (②)and the chapel(④) in Figure 14 — they were registered in Cloud Compare through the 'cloud-to-cloud' method. It utilized the suitably dense overlapping areas between the unregistered point clouds and registered point clouds (the façade point cloud acquired by TSL) to enable sufficient matching points to be derived. Subsequently, these unregistered point clouds were accurately aligned and successfully registered.

By controlling the visibility of different point cloud and cropping box range in Revit, the modelling operations were facilitated. (Although some Revit plugins, such as Faro As-Built, offer functionality for managing the visibility of different classifications or layers within a single RCP file, limitations in the programming interface often lead to undesirable outcomes in practical applications.)
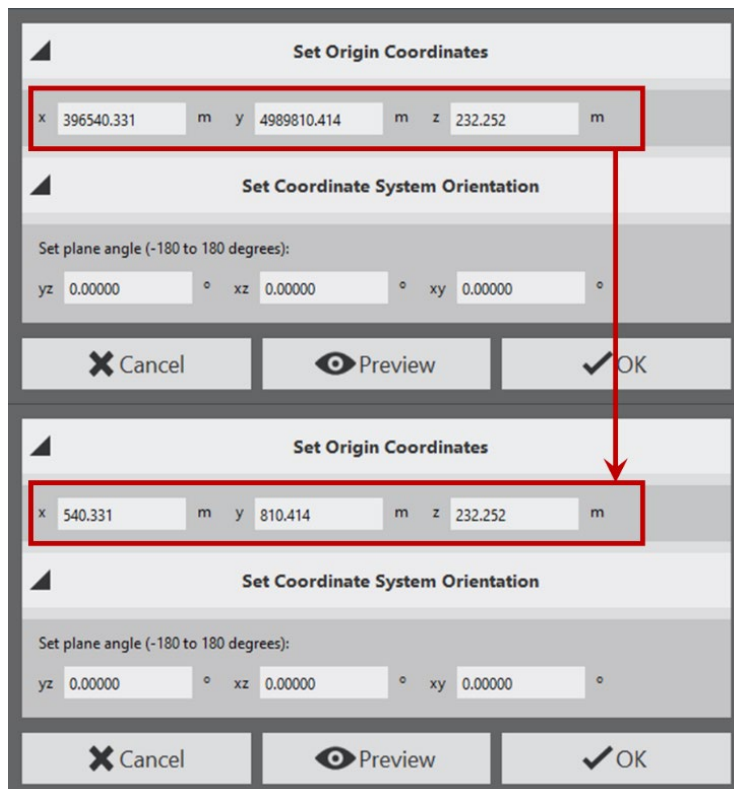
Figure 17 Cut off Big Cartographic Coordinates
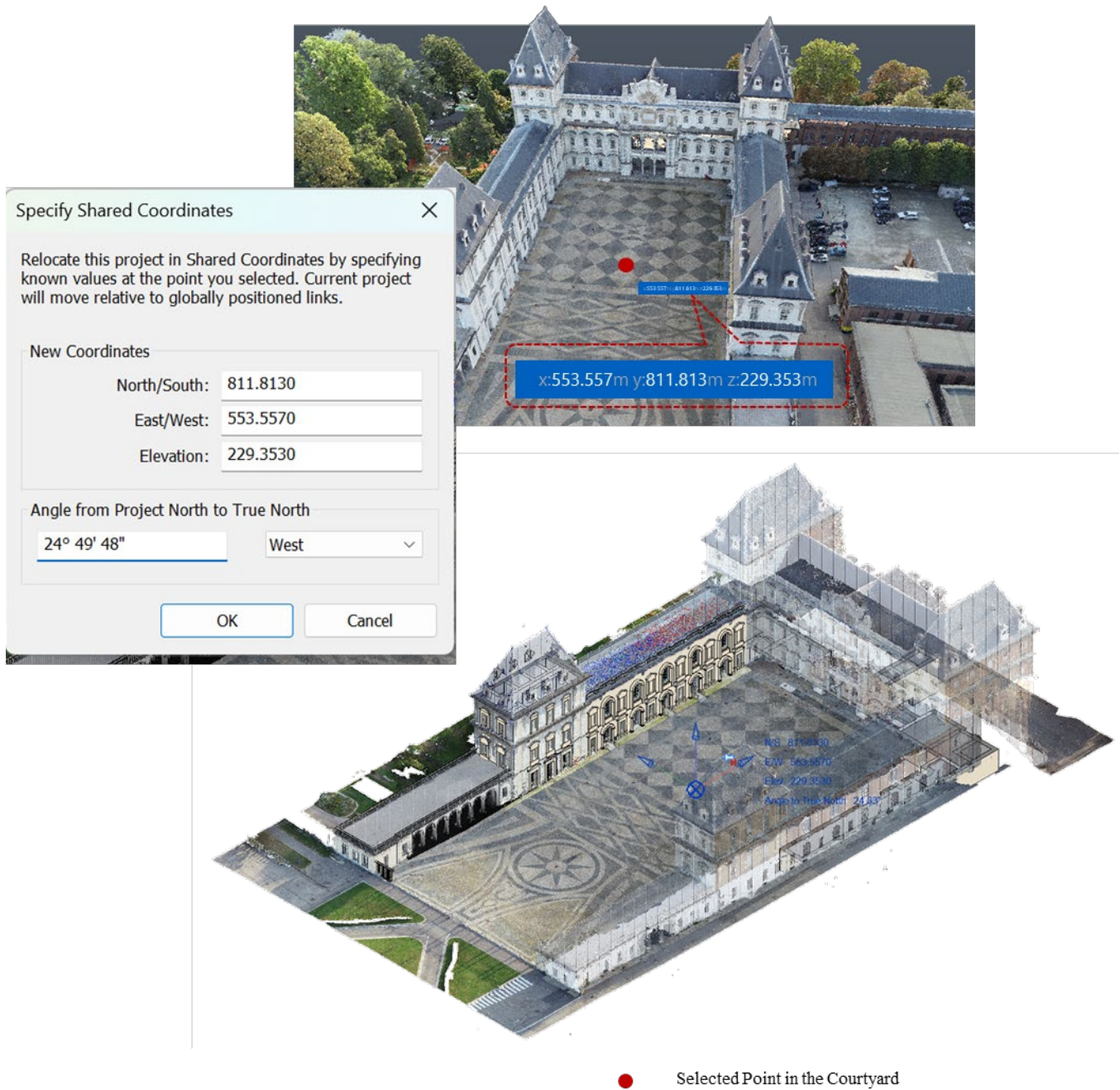
Figure 18 Set the Project Base Point

4.2 Modelling Strategies

The transformation from optimized point clouds to a semantic HBIM model represents the most crucial phase in the entire workflow. This phase establishes the foundation for all downstream analysis and have significant influence in the accuracy and reliability of subsequent results. The purpose of HBIM modelling in this study is to achieve identifiable building elements (such as windows, walls, and movable furniture) in the ACE fields, to enable flood damage assessment at the element level. At the same time, the model should meet the requirements for information exchange and interoperability.

The first step is to semantically classify and identify building elements, their relationships and hierarchies. This process ensures the accurate representation of the semantic information of elements, facilitates the organization of object libraries and family types, and ensures efficient management of materials and information while maintaining interoperability. The classification system employed in this study is based on Italian regulations (UNI 10838:1999 and UNI 8290:1981), The UNI 8290 standard provides a detailed classification and articulation of the technological units and technical elements that comprise the technological system. This decomposition defines three levels, which are organized into three sets:

1. Classes of technological units (Classi di unità tecnologiche): These refer to the categorization of functions that are technologically compatible and necessary for achieving predefined performance standards.

2. Technological units (Unità tecnologiche): A group of compatible functions that are combined when needed to achieve predetermined technical performance.

3. Classes of technical elements (Classi elementi tecnici): These are elements capable of performing, either fully or partially, the functions of one or more technological units.

The classification outlined in the [64]standard aids in the understanding and management of various technical elements in building systems, offering a structured approach to evaluating and organizing these elements in terms of their technological functions and contributions to overall building performance.

As previously noted, highly detailed models are not necessary for flood risk management at the element level in heritage buildings. Accurately recording the basic geometry, position and elevation of these element is sufficient. Thus, this study developed a geometric simplification method (particularly aimed at complex decorative elements) to effectively reduce the modeling workload. However, geometric simplification must adhere to certain standards and guidelines

to prevent excessive geometric errors or the loss of critical information. Here we introduce the concept Grade of Accuracy (GOA) to address some constraint in the modelling accuracy.

It is crucial to start with a clear understanding of the model's purpose, the required scale, and the measurement methods. Different applications have varying accuracy requirements for BIM models. Traditional surveying specifications provide precise criteria for selecting scales, which can also be applied to generating HBIM models. Therefore, the GOA concept inherits the principles of surveying detail and tolerance linked to various common scales of representation, from which the level of detail was automatically and conventionally fixed and adopted, as in the cartographic tender specification.

At different scales, the definitions of graphic error (G.E.) and tolerance (T) vary. G.E. represents the smallest detail at a given scale, while T is usually 2 to 3 times the G.E. value. For example, at a 1:50 scale, the G.E. value is 1 cm, with a permissible tolerance range of 2 to 3 cm. For a 1:20 scale, the G.E. is 4 mm, and T is 8 to 12 mm, as illustrated in Table 3.

ADOPTED SCALE	GRAPHIC ERROR G. E.=0,2 mm	TOLERANCE T = 2 ÷ 3	GOA
1:10	2 mm	4 ÷ 6 mm	GOA 10
1:20	4 mm	8 ÷ 12 mm	GOA 20
1:50	10 mm	20 ÷ 30 mm	GOA 50
1:100	20 mm	40 ÷ 60 mm	GOA 100
1:200	40 mm	80 ÷ 120 mm	GOA 200
1:500	100 mm	200 ÷ 300 mm	GOA 500
1:1000	200 mm	400 ÷ 600 mm	GOA 1000

Table 3 The grade of model accuracy correspondent to the different scales.

Source:[49]

In this study, a reliable HBIM model is needed for flood impact analysis. The final deliverables require analysis results at scales ranging from 1:200 to 1:1000. GOA200, applicable to the 1:200 scale range, is used to guide the modeling and verification processes.

Historic buildings encompass many more irregular elements than modern constructions, and representation of complex 3D geometries typically results in heavy files, complicating their use and interoperability. BIM software limitation also pose challenges for using native parametric objects to model irregular geometries, such as vaults and lunettes, without compromising model functionality. Therefore, modelling these non-standard elements is a

time-consuming and laborious process that also depends on the operator's level of knowledge and skill in modelling.[44] To enhance the efficiency of modelling, numerous studies have explored semi-automatic or automatic as-built BIM reconstruction from point cloud data. (961 papers from 2019–2024 and 345 papers from 2014–2018 were found on the SCOPUS database using the keywords *BIM* and *Automation*.) In general, it is difficult to achieve high accuracy, high applicability, and high levels of automation at the same time. High levels of automation are often limited to environments with straight geometrical features, adhering to the Manhattan world assumption, which refers to the spatial organization of a scene based on a three-dimensional Cartesian coordinate system. This structure known as the Manhattan grid, defines three dominant and perpendicular axes ($\vec{i}, \vec{j}$, and $\vec{k}$). Many building elements, such as walls, streets, corridors, are typically align with these axes. This alignment simplifies computational modelling of scenes and interpretation of environments by leveraging orthogonal geometries commonly found in urban areas [65]. Conversely, semi-automated approaches are more user-friendly and partially automate repetitive tasks, while complex tasks still require manual input. Theses method reduce human errors, improve efficiency over manual modelling, and are cost-effective[66].

In this study, the Revit plugin Faro As-built was tested to enhance the modelling process, with the modeling principles based on LOG 300 and tolerances conforming to GOA 200 standards for non-simplified elements. However, the geometry of certain decorative elements was simplified to some extent. For these simplified elements, the methods of simplification, modeling procedures, and associated metadata were documented as text descriptions within the shared parameters. Once verified, the model was imported into GIS for preliminary analysis, and refinements were made based on the analysis to meet specific project requirements.

Historic buildings face flood-related damage not only from floodwater but also from inappropriate remedial works undertaken by contractors unfamiliar with historic fabric. The use of inappropriate techniques and materials or poorly controlled restoration process can cause particularly damaging to historic structures. To mitigate such damage, effective cooperation and communication among various stakeholders are necessary. Thus, the HBIM developed for this study integrates both geometric representations and essential information on materials, historical fabric, potential damage types, and precautions for remedial works. This comprehensive approach enhances the identification of potential risks, facilitating easier monitoring, analysis, and planning for preventive measures. Additionally, it promotes

improved coordination among stakeholders by providing a unified platform that consolidates critical data, ensuring better informed decision making throughout the project's lifecycle.

Given the conditions of flooding, the possible damage or decay types is typically based on the material composition and construction methods of the building elements, while precautions for remedial work are determined by both these construction methods and the specific type of decay. Therefore, each element in a specific position is subject to unique risks, decay types, and corresponding precautions. Utilizing shared parameters in Revit to represent this information for flood-prone building elements could provide a simple and effective approach to flood risk management.

Historic building materials include both organic and inorganic types, comprising elements such as stone, solid brick-and-mortar walls, timber frames, timber boarding and panelling, earthen walls and floors, lime-plaster walls and ceilings, as well as various decorative finishes.

Organic materials such as timbers, are prone to swelling and distortion when exposed to moisture and can suffer from fungal and insect infestations if left damp for extended periods. Rapid drying at high temperatures can cause timber to shrink，split or twist, especially when confined within panel structures. In contrast inorganic porous materials are generally less vulnerable to biological damage. However, they can suffer significant deterioration when inherent salt and water (often in the form of frost crystals) are released due to improper drying method or exposure to extreme cold conditions. Table 4 presents the potential flood damage and precautions for remedial work for historical buildings.

Table 4 Potential Flood Damage and Precautions for Remedial Works [6, pp. 18–37], [67], [68]

Elements	Materials or Construction Inference	Possible Types of Flood-Related Damage	Precautions for Remedial Works
Masonry	Stone, solid brick-and-mortar walls, lime mortar	Saturation by floodwater can cause salt crystallization and efflorescence; spalling and exfoliation due to salt trapped under impermeable coatings; damage to bricks or stone during freeze-thaw cycles; weakening of lime mortar joints.	Allow historic masonry to dry and breathe; use permeable lime-wash coatings; protect soft saturated bricks from frost and rain with ventilated shelter; replace impermeable cement mortar with lime-based mortar; rinse masonry flooded by seawater with clean, salt-free water; leave mortar joints open and fill with clean dry sand, re-point with porous lime-based mortar to help wick salts away from the paving.
Structural Timber	Timber, used in historic buildings, generally with high resistance to decay	Susceptible to rot if moisture content exceeds 25%; risk of fungal and insect infestation when trapped moisture raises content above 28%; risk of dry rot spores germinating.	Allow timber to dry thoroughly after flooding; ensure adequate ventilation for wall cavities, sill plates, and hidden voids; Consider key-hole injection-drying techniques for drying hidden areas. Flaking paint is typically an indication of wet wood rather than rot. Consult a conservation specialist for advice on drying and preserving historic timber.
Timber Panelling and Woodwork	Timber frames, timber boarding and panelling	Swelling and distortion from moisture; fungal and insect infestation if left damp; buckling of floorboards and warping of panelling; loosening and weakening of structural joints.	Drill small holes to drain water; use injection drying or dismantle panels if necessary; dry in well-ventilated space, use spacers, and apply uniform weights to prevent warping; remove buckled boards for slow drying to avoid distortion. Consult experts for monitoring and treating potential fungal infestations.
Render and Plaster	Lime-based and gypsum-based plasters, plasterboards	Softening, swelling, and de-bonding of lime plaster; deterioration of gypsum plaster; separation of plasterboards due to paper liner damage; cracks, bulging, or sagging from water saturation.	Use lime-based plaster for restoration to maintain breathability; re-anchor de-bonded lime plaster using resins; avoid gypsum plasters as they deteriorate in water; check for structural integrity before removing plaster. Consult conservation officers for guidance on handling historic plaster materials.

Metalwork	Iron, steel, copper, bronze, brass	Rusting and oxidation of iron and steel, particularly in damp or maritime environments; expansion of rusted metal components, leading to cracking and spalling in surrounding masonry; staining from oxidized metals.	Dry metal components quickly after flooding; inspect rusted components for signs of structural weakness; remove any surface stains; consult a structural engineer for cracks or deformations in lintels and other embedded metal elements. Use protective lacquer or wax coatings for historic metalwork.
Ironmongery	Locks, hinges, door and window hardware	Rusting and seizing of locks and hinges; general deterioration due to prolonged moisture exposure.	Dry thoroughly before applying powdered graphite for lubrication; temporarily lacquer or wax historic metalwork to protect from future flood damage.
Wallcoverings	Paper, textile, pressed metal, leather	Mold growth on wall-coverings due to dampness; staining, flaking, and degradation of historic materials.	Remove and discard non-historic wallcoverings; consult a specialist conservator for cleaning and disinfecting historic wallcoverings; ensure slow drying to avoid mould growth.
Paint Finishes	Lime-wash, distemper	Water can cause the staining, flaking, blooming and dissolution of binders in historic varnishes and paints.	Use appropriate safety precautions when handling lead-based paints; Avoid paint any previously painted interior surface with impermeable modern paints; Use appropriate safety precautions when handling lead-based paints; Historic paintwork should be treated by a specialist conservator.
Wall Paintings	Traditional paints on plaster or timber	Damage due to salt crystallization, paint flaking, and mould growth; deterioration from heat or rapid drying methods.	Avoid using dehumidifiers or heaters that have historic wall paintings on plaster or timber; use cold-air fans for slow substate micro-drying methods under supervision; prevent salt crystallization and mould growth; Specialist advice should be sought from conservators.
Building Services	Modern plumbing, electrical, and HVAC systems	Floodwater can damage plumbing and electrical systems, leading to high costs for repair or replacement; flood can damage wiring, appliances, and HVAC components.	Have all retained services tested and recommissioned by appropriate engineers; repair work should respect the historical context and be minimally invasive.
Personal Possessions	Furniture, paper, photographs, fabrics	Water damage and mould growth on organic materials; possible irreparable damage to valuable historic items.	Consult specialist conservators for cleaning and restoring valuable items; ensure items are thoroughly dried before storing to prevent mold growth.
Other(Monitoring and Long-Term Maintenance)	Foundation walls, mortar joints, timber structures	Cracks in foundation walls due to soil hydration and expansion; potential structural instability over time if foundation erosion occurs; risk of fungal infestation and rot in under-floor timbers.	Monitor structural integrity over time, especially foundation walls; inspect under-floor timbers periodically for signs of fungal infestation; use fibre-optic boroscopes for hard-to-reach areas. Engage structural engineers for persistent cracks and signs of foundation erosion.

In addition, identifying areas within the structure that are vulnerable to floodwater is crucial for understanding key aspects of the modelings process. Typically, floodwater can enter a building through various points, including masonry and mortar joints, cracks in exterior walls, vents and air bricks, around windows and doors, door thresholds, manholes, and gaps around pipes that pass-through walls and floors. Other potential points of entry include back flow from drainage systems, entrances to cellars and basements (such as coal holes and pipe ducts), as well as from beneath the floor or foundations. Consequently, the lower levels of the building are most prone to flooding, impacting elements such as external and internal walls, basements or cellars, floors, floor cavities, building services, various appliances and fittings and movable assets. The modelling strategies thus focus on three main aspects:

1) Topography: Ensuring topographic accuracy to enhance the reliability of the final results.

2) Modelling of Vulnerable Entry Points (such as windows, doors, etc.): This step prepares for simulating various flood scenarios and identifying potential points of water entry in ArcGIS.

3) Modelling of Flood-Susceptible Building Elements (such as floor, walls etc.): The goal is to assess whether specific elements are at risk, quantify potential damage, get information about possible types of decay and precautions for remedial work. Additionally, the results can be applied to insurance assessments for more accurate risk valuation and coverage planning.

The following section details the modelling process for the building elements of basement and north wing of Valentino Castle, including the application of semi-automated modelling techniques (As-Built). Please note that the following construction inferences about Valentino Castle are based on limited available data and may not accurately reflect the actual conditions. This section is intended solely to demonstrate the HBIM modelling workflow for flood risk management and should not be considered a definitive basis for restoration. Comprehensive on-site surveys and experimental analysis are necessary for informing decisions prior to any restoration work.

Ground Surface
Point Cloud Data

As-Built----Surface Analysis
Function
calculate the distance from the
point cloud to the slab

a Horizontal Slab

Profile Lines

Topographic Surface

Toposolid Volume
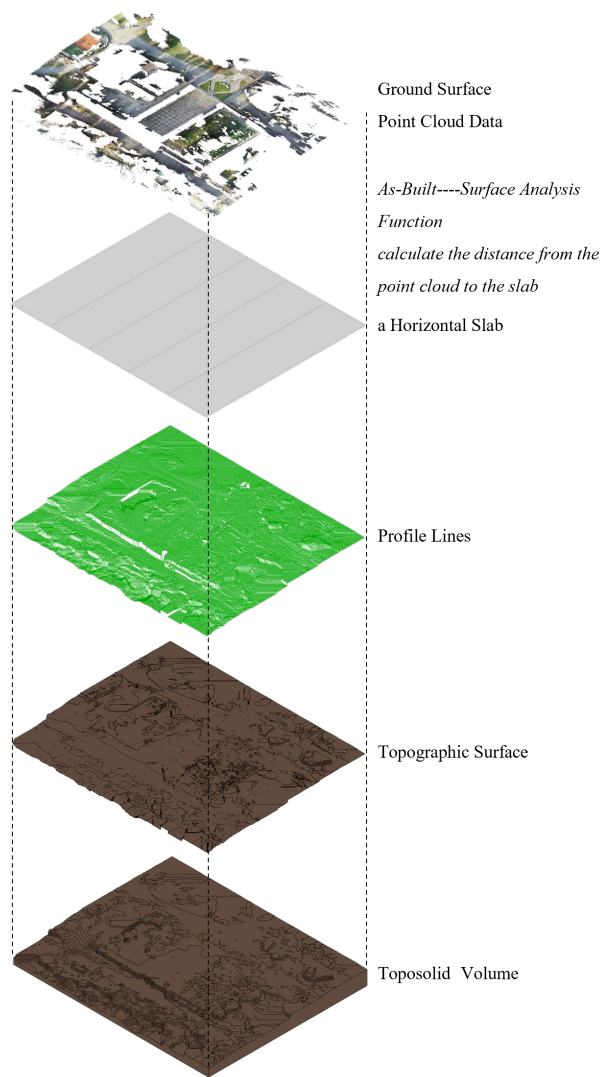
Figure 19 the Topography Modelings Process

Topography

Ensuring topographic accuracy is critical for reliable results. First, the ground surface point cloud data, obtained from the point cloud classification and segmentation step, was isolated and displayed. A horizontal slab was then placed within the area where the topography needed to be established. The As-Built Surface Analysis function was employed to calculate the distance from the point cloud to the slab, using a mean grid size of 500mm to balance accuracy and processing efficiency. Following this calculation, profile lines were generated and exported, with any obvious errors manually removed. Using the refined profile lines, a topographic surface was established and subsequently converted into toposolid volume, as shown in Figure 19.

Another method involves using the point cloud of the ground surface. After being cleaned, filtered, and classified to isolate ground points, the CloudCompare Rasterize tool was employed to generate a georeferenced DTM. It is appropriate for use in GIS environments (figure 20).
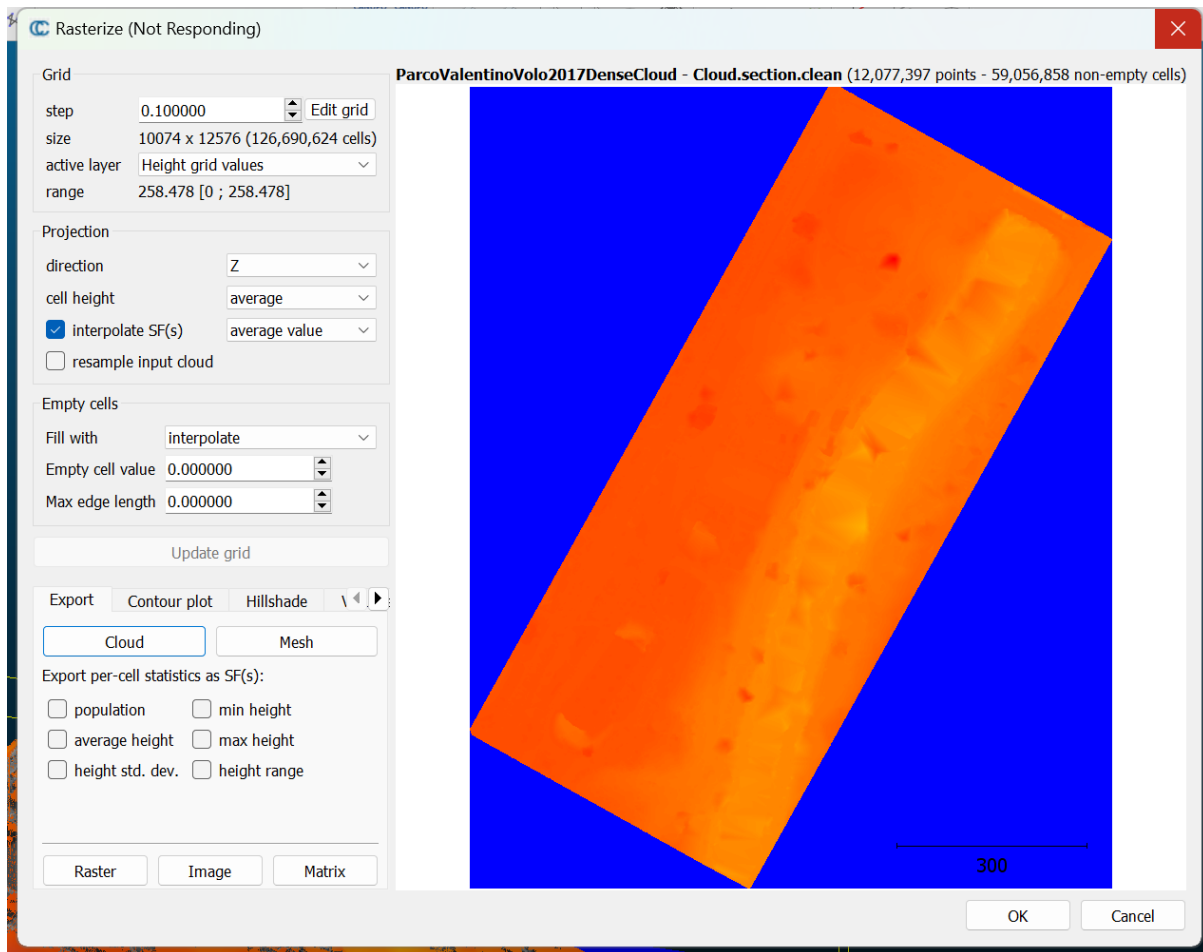
Figure 20 DTM generation in CloudCompare

Vulnerable Entry Points and Flood-Susceptible Building Elements

Since there is some overlap between Vulnerable Entry Points and Flood-Susceptible Building Elements, the following sections are organised according to building categories in Revit.

-Walls

Walls, as planar architectural elements, exhibit significant continuous planar features in point cloud data, which facilitates automatic recognition. The Faro As-Built plugin is an efficient tool for modelling such element, utilizing a series of algorithm to fit continuous clusters of point cloud data into planar shapes, thereby identifying building walls. The plan fitting algorithm automatically recognize adjacent, coplanar, or geometrically continuous regions within the point cloud as a single element. Subsequently, wall models are generated to match these detected planes. These model elements can be adjusted according to the precise location and dimensions derived from point cloud data to ensure alignment with the actual building

structure. Final manual calibration and adjustment, incorporating additional details such as material specifications, potential decay types and precautions for remedial works, further enhance the model's alignment with real-world conditions. Figure 21 illustrates the wall modelling process using As-Built.

For the basement walls, only the interior surfaces could be scanned and represented as a point cloud. Consequently, the thickness of the basement walls was inferred based on the thickness and alignment of the ground floor walls, as depicted in Figure 21, step 3.

Figure 21 Underground Wall Modeling Workflow Using Faro As-Built
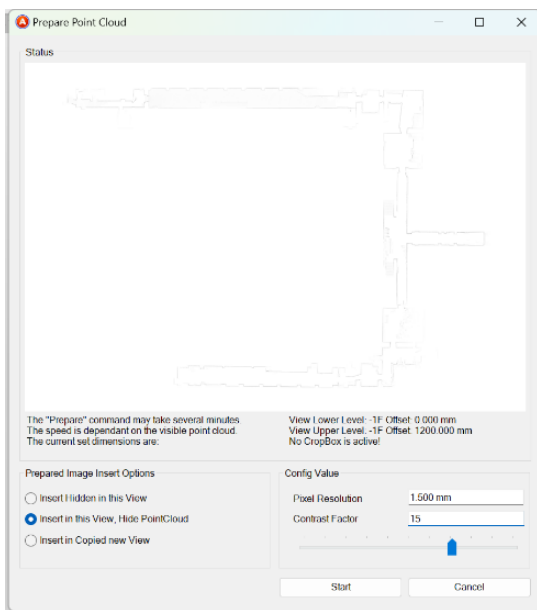
Step 1: Prepare Point Cloud
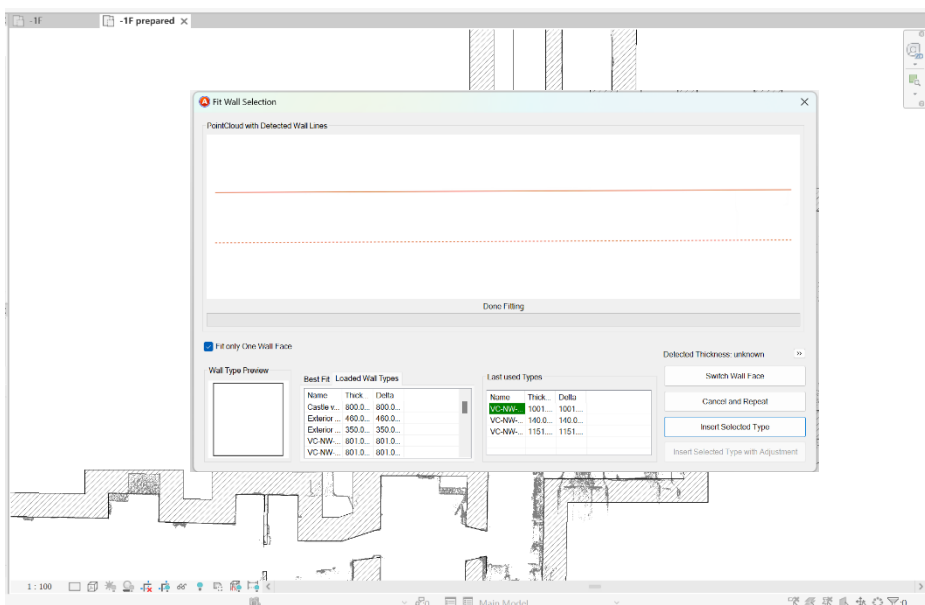
Step 2: Fit continuous clusters of point cloud data into planar shapes and wall models are generated to match these detected planes
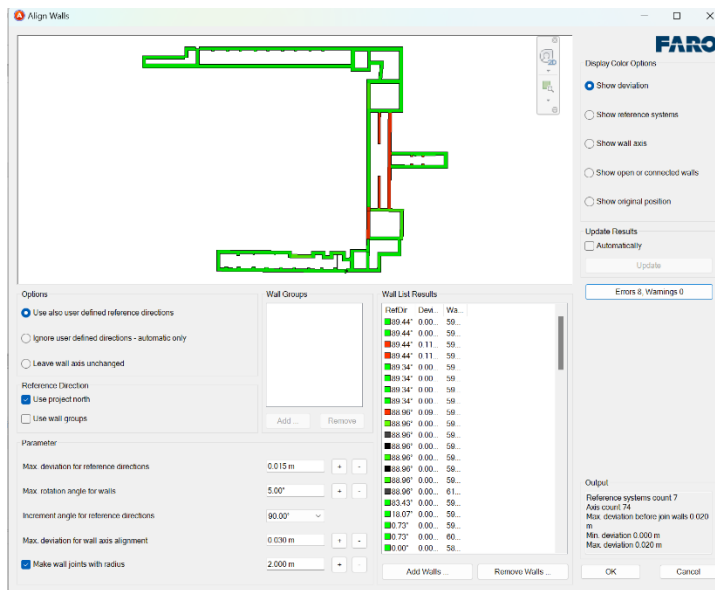
Step 3: Manual calibration and adjustment

However, As-Built is not particularly effective for modelling complex decorative elements. Additionally, for elements level flood risk assessment, such high level of decorative detail is unnecessary. The decorative elements are primarily concentrated around doors and windows, with additional false windows positioned between actual windows. A comparison of sections with and without plaster in Valentino Castle, as shown in Figure 22, suggests that the structure likely employs the construction techniques illustrated in Figure 23. By examining these contrasting areas, it is possible to infer the underlying construction methods and materials used. And the construction layers of these decorative walls are the same as those of general plastered walls. The main decorative features are created by constructing large recessed and protruding shapes with bricks, followed by the application of plasters to form mouldings. Consequently, simplified in place wall family was used to represent these decorative elements effectively.

Figure 22 Photos of Valentino Castle
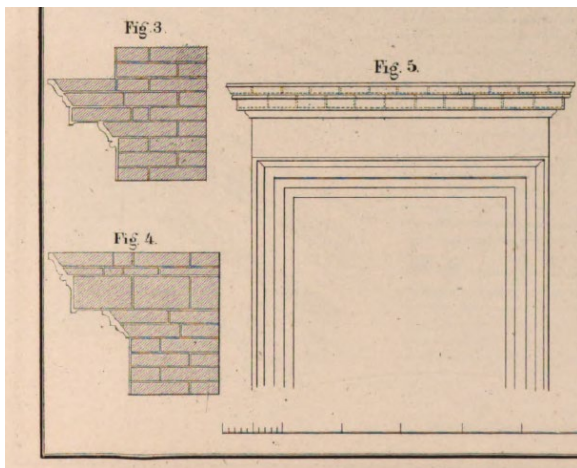
Figure 23 Construction Techniques for the Decorations [69, p. Taf.52]

- Vaults and Lunettes

Vaults are architectural elements frequently found in historic buildings, serving both as separators of interior space into multiple levels and as load-bearing structures, much like floors in contemporary buildings. However, various types of vaults cannot not be directly modeled as a floor system family in Revit. Several approaches exist for modelling vaults, each with its own advantages and limitations. One method involves creating in-place families to cut through a thick floor slab, which is modelled by the system family, but this results in inaccurate volume calculations and section detail displays. Similarly, using adaptive loadable families also leads to inaccuracies in volume calculations and section displays. While importing objects from an OBJ. file created in Rhino to achieve high accuracy, it faces similar issues with incorrect volume calculations and section displays. Dynamo offers parametric adjustments but likewise results in inaccuracies in volume and sectional representation.[69, pp. 92-94(Taf. 45–46)] First

two methods ensure interoperability whereas latter two methods offer higher accuracy for complex vault geometries. To accurately display section details, manual drawing using a call-out was required. (Figure 24.) The vaults in Valentino Castle are primarily barrel or groin vaults with relatively simple geometries; therefore, the first two modeling methods were employed for their representation.
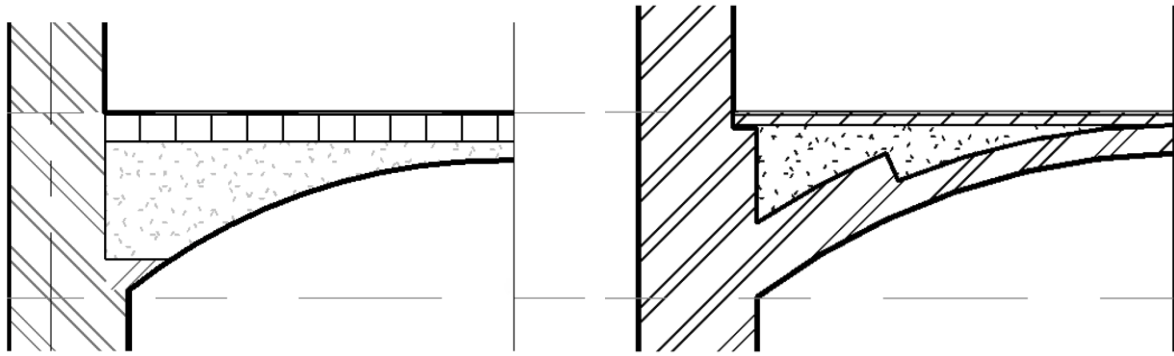
Figure 24 Manually Draw the Details of the Vaults
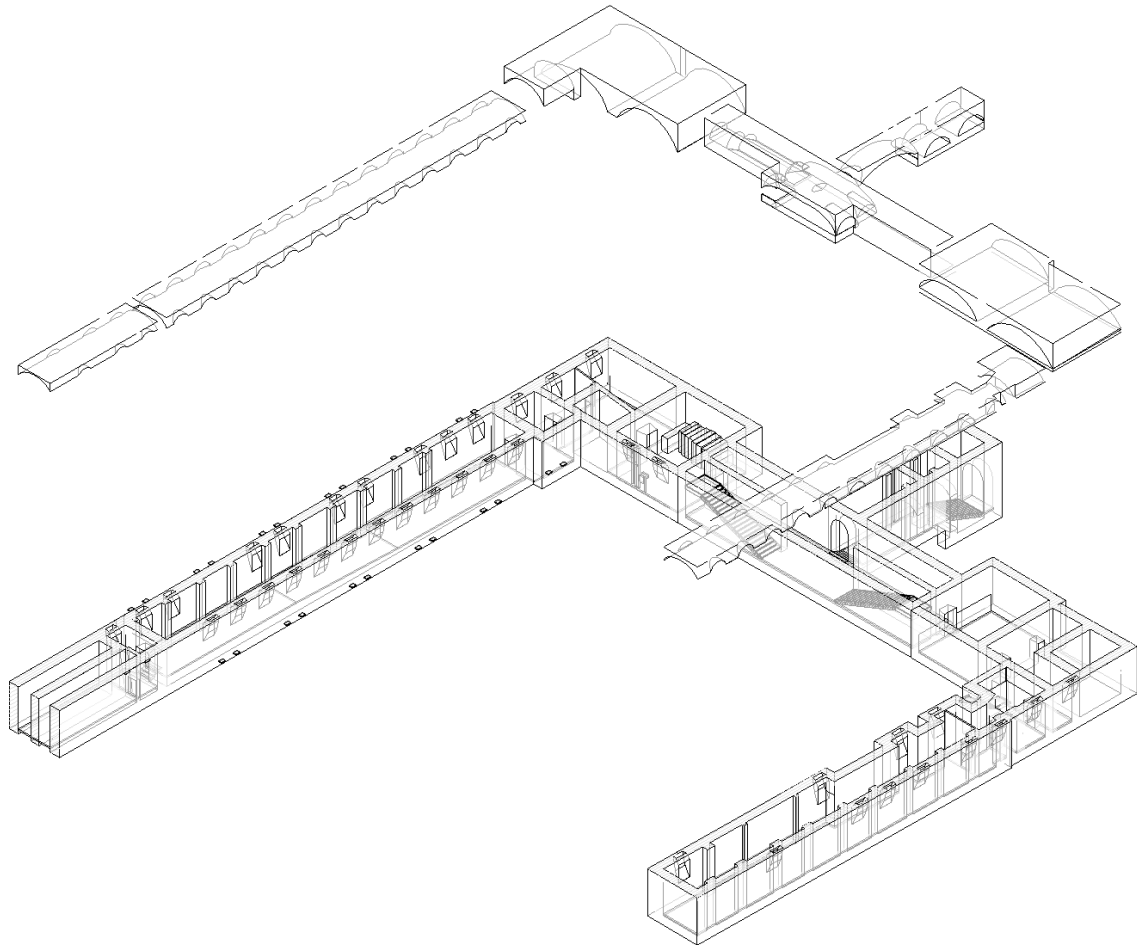
Figure 25 Underground Vault System

Lunettes, although a form of window, are structurally and functionally interconnected with vaults. Lunettes are commonly used for basement ventilation and lighting, with their exterior openings positioned slightly above ground level. Those openings, which slope through the walls from the basement to the ground floor, create vulnerabilities that allow floodwater to enter the basement easily (Figure 27, 28). Based on the point cloud and technical references, the construction of lunettes resembles the configuration shown in Figure 26.

Due to their positioning, lunettes are frequently obstructed, leading to incomplete point cloud data. Thus, a relatively complete point cloud section was selected as a reference for modelling. The basic outline of the window opening was created using a generic adaptive family template (loadable family), which was then converted to hollow, loaded and adjusted in size and position, and used to cut through the wall.
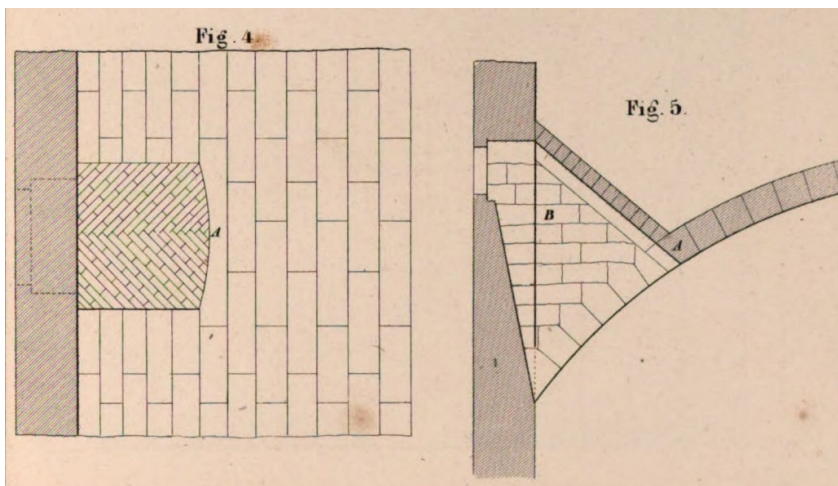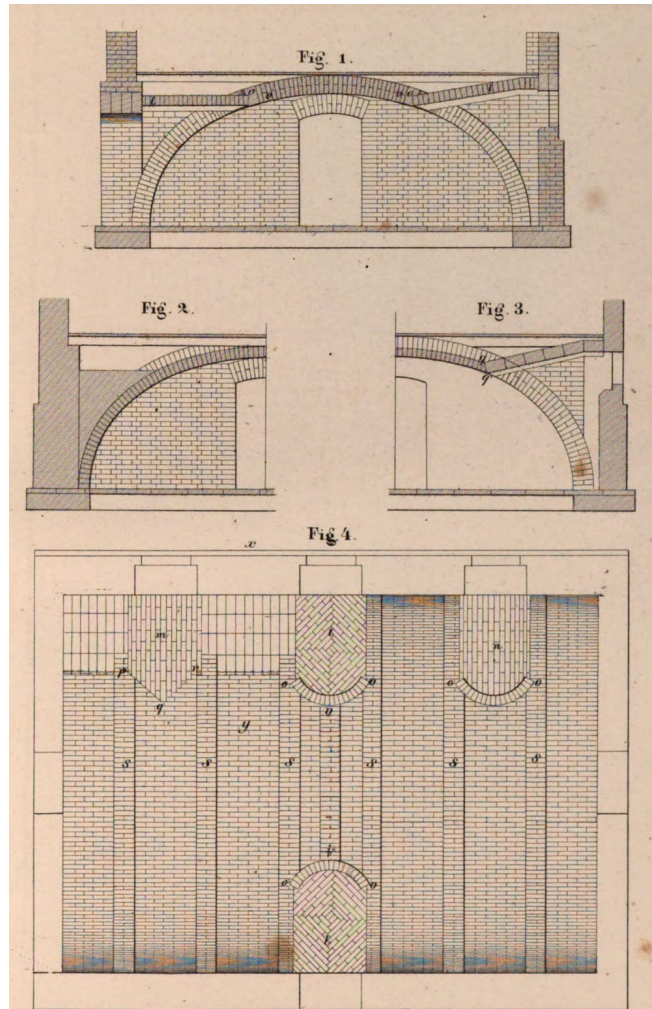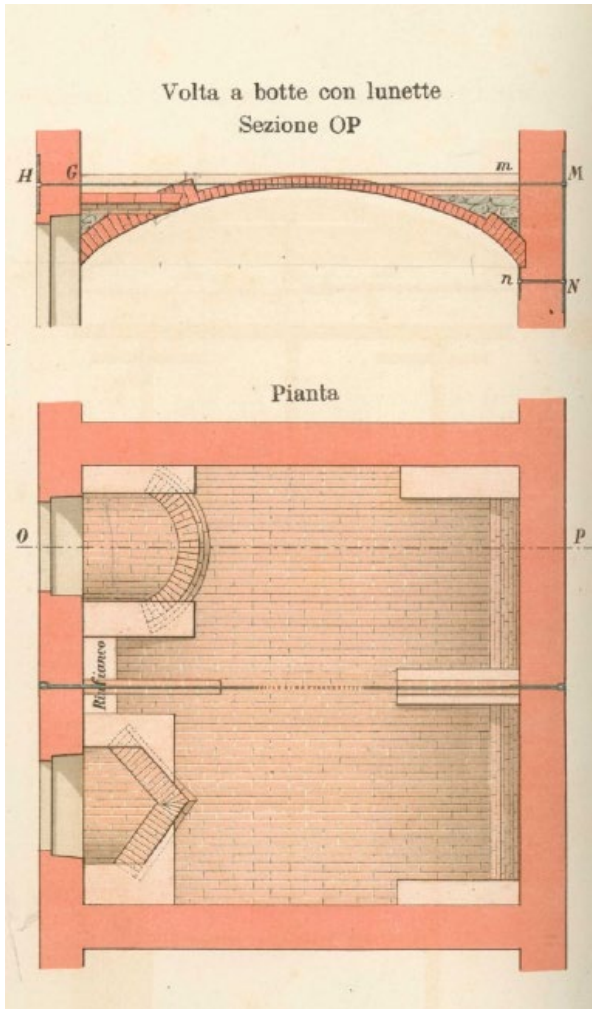
Figure 26 References for the Lunette

[69, p. Taf.45，46], [70, p. Tav.XX]
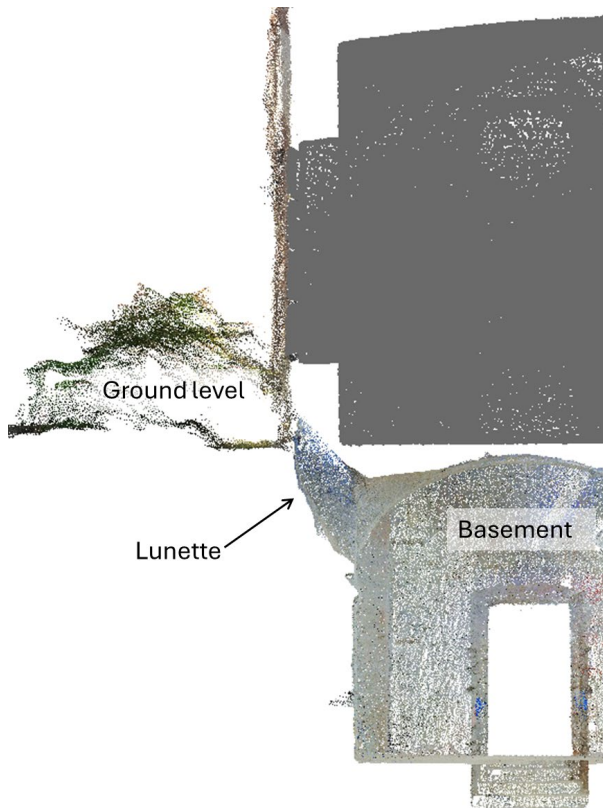
Figure 28 Point Cloud Section of Lunette
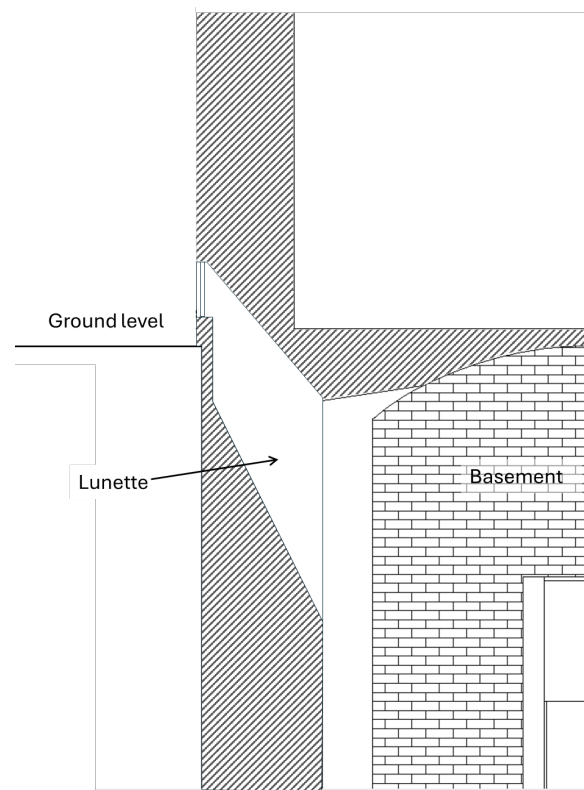
Figure 27 Details of Vaults with Lunette

- Staircases

The staircase serves as a vertical connector between different floors within the building. Due to the inherent layout of staircase and occlusion in staircase, portions of the staircase point cloud are missing. To address this, supplementary manual measurements are necessary. From the point cloud section of the staircases, the threads appear rectangular in shape (Figure 30). Based on technical references[69, p. 114(Taf.61)], this configuration suggests a monolithic staircase type, which is typically assembled on-site. Accordingly, in Revit, an assembled stair was selected as the family, with "monolithic stair" specified in the family type name. In historical buildings, however, the layout of the treads may vary from pre-set system families. Therefore, the treads were manually adjusted to align with the point cloud data. Metadata and modelling methods were documented in the shared parameter for reference.

Figure 30 Point Cloud Section of Staircase
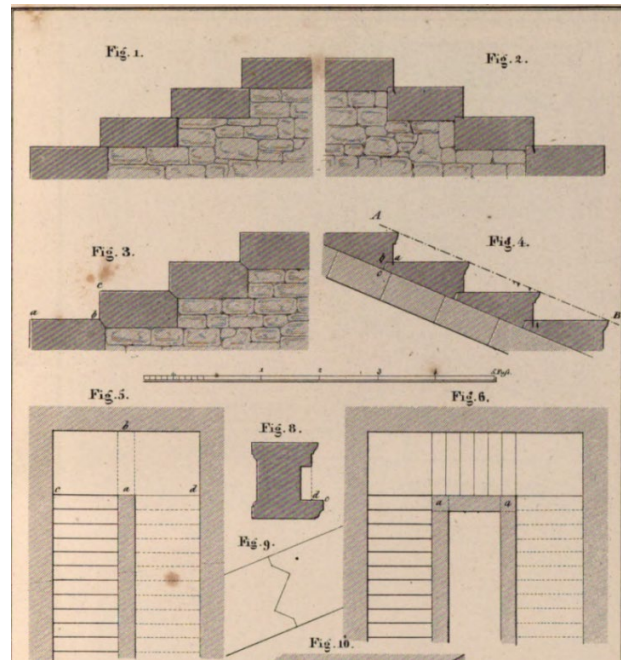
Figure 29 References of Staircases[69, p. Taf.61]
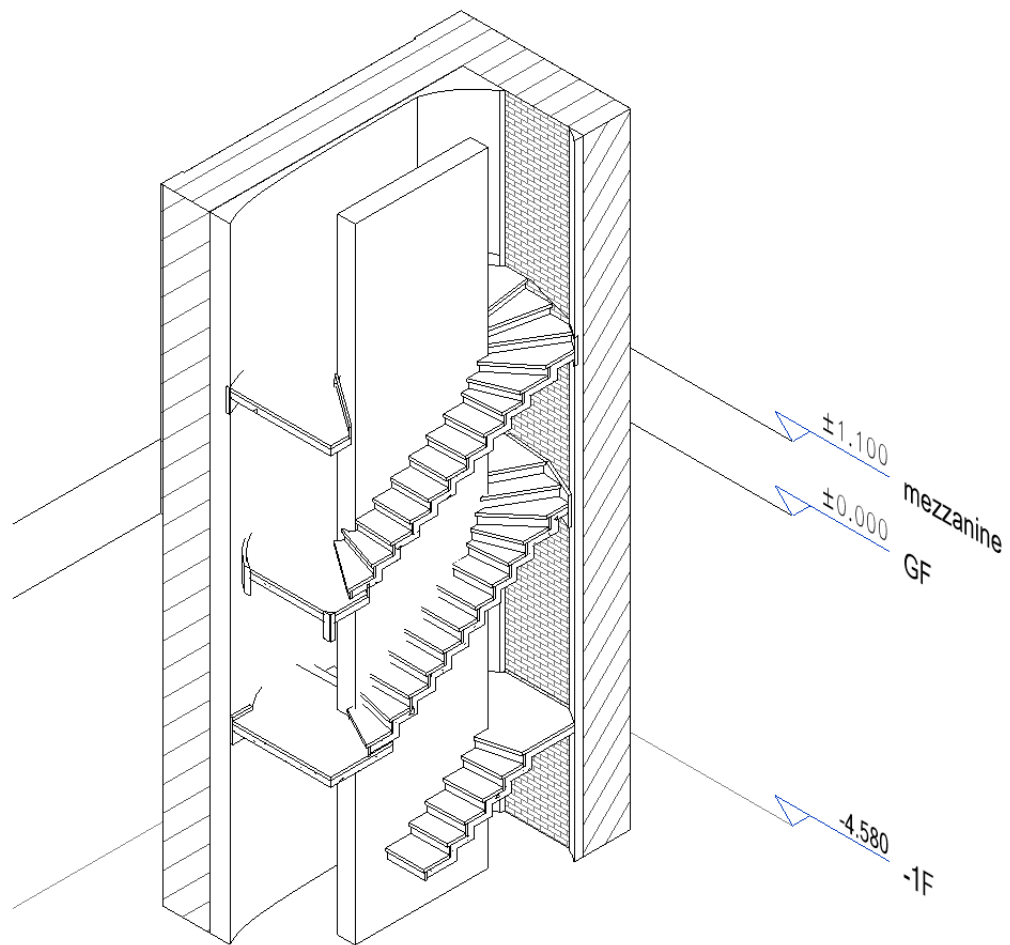
Figure 31 Axonometric Section of Staircase

-Doors and Windows

Door and window modeling utilized a loadable family, with orthogonal point cloud images exported from As-built serving as the basis for accurate modeling . Then, load the family into the model and precisely place it in the wall openings designated for windows and doors to ensure structural and functional integrity within the building model (Figure 32).

*Figure 32 Examples of Door Types and Orthogonal Point Cloud Images (Top),
Different Doors families (bottom)*

-
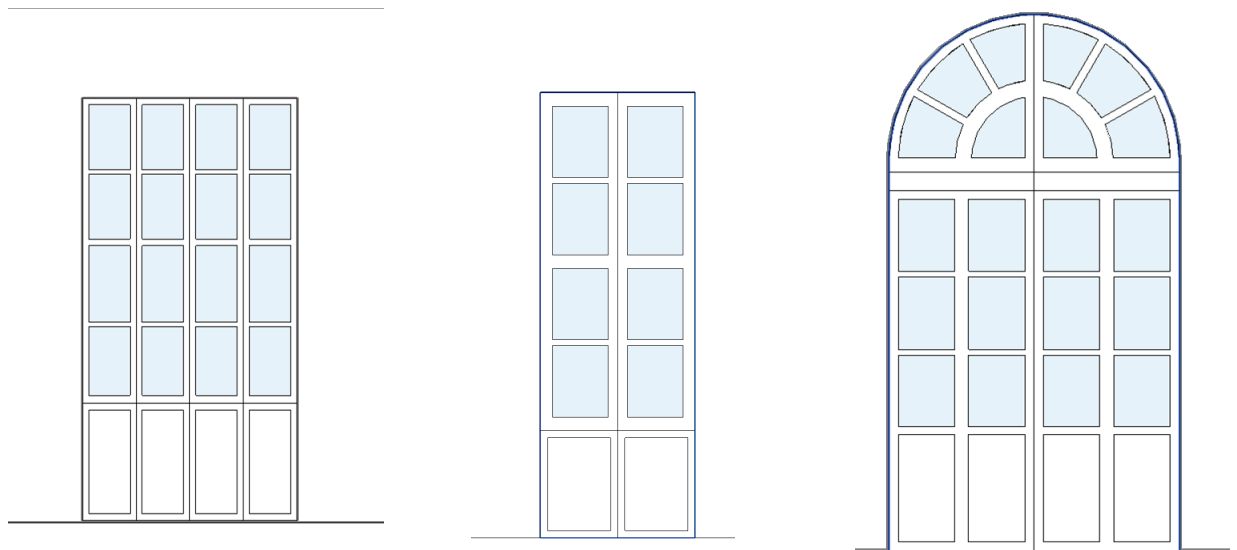
Basement Floors

In the initial modeling phase, the floor elevation was adjusted using the "Modify Shape of an Element" function, with point cloud of the basement floor surface serving as a guide. For more precise analysis, procedures similar to those used in establishing the topography were employed to accurately define basement elevations, facilitating further analysis result.

Due to the lack of historical drawings, the basement floor's construction layers were inferred from information provided in reference (Figure 33)[71, p. PARTE1 TAV XXVI]. Based on these references, relevant information—including materials, potential decay types, and

recommended precautions—was added to shared parameters to support a comprehensive analysis.
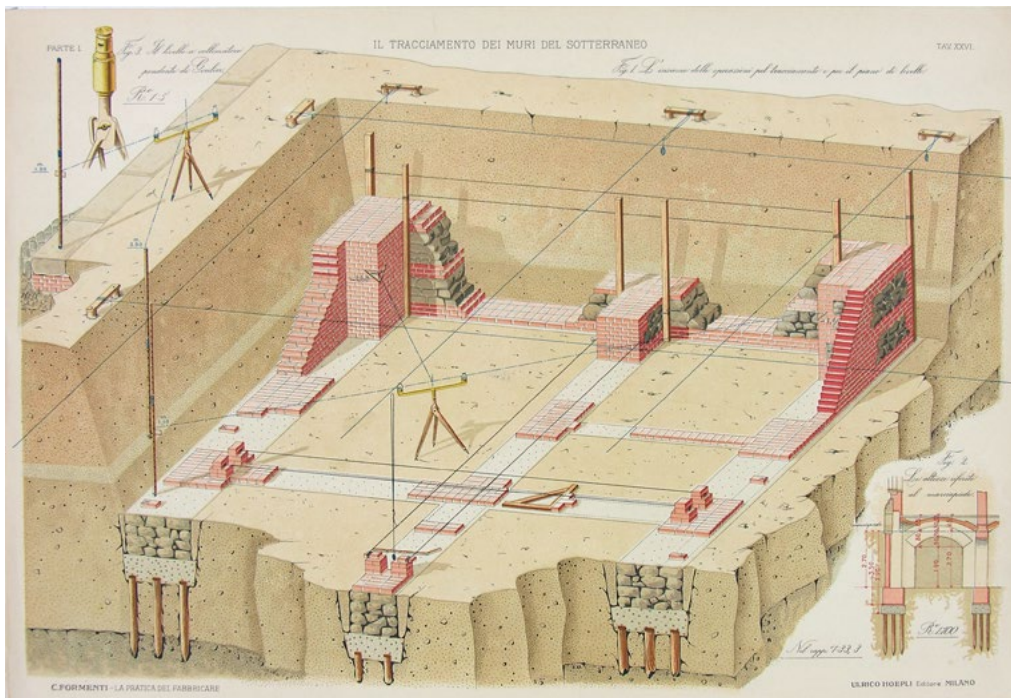
Figure 33 C. Formenti, La pratica del fabbricare / per Carlo Formenti PARTE PRIMA

Source: [71, p. TAV XXVI]

- Movable properties image

From the basement point cloud, it was observed that some furniture and some construction materials, most of which are not particularly valuable, were stored there. However, due to the occlusion, the point cloud data is incomplete. Since these items are unique and single-use

Figure 34 Part of Movable Properties in the Basement of Valentino Castle，Point cloud(left),model (right)
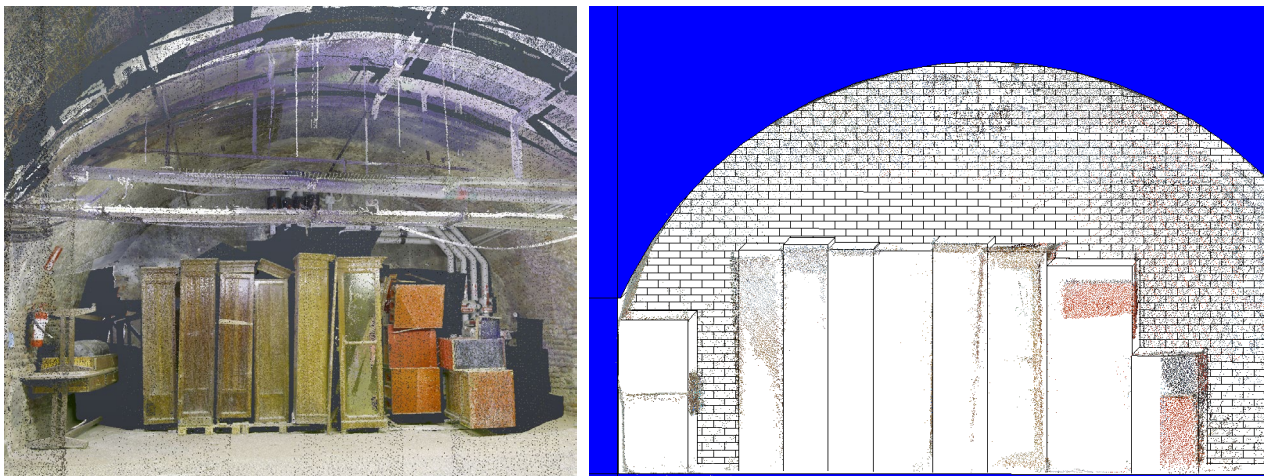
elements in Revit, they were modelled "in-place," with only the outlines of movable furniture and construction materials roughly represented for efficiency. These simplified volumes are sufficient for assessing potential flood risks and determining whether these items should be relocated to a safer area or moved upstairs to prevent damage.

- Services

Various services pipes, ducts and fittings are installed in the basement, most of which are vulnerable to floodwater. Some of these pipelines are embedded within the ground or walls, making them inaccessible. Due to lack of detailed information on these services and the inability to accurately simulated specific flood damage, on-site inspections and assessments by professionals are required. Consequently, only the visible portions of these elements, similar to movable items, were modelled with in place family, using simplified outlines to indicate potential risk areas. In the actual flood event, losses and necessary repairs should be evaluated by qualified personnel.

Figure 35 . Parts of services pipe, Point cloud(left), model (right)

Mapping and Modelling of Existing Decay in Buildings

Existing decay in a building represents one of its most vulnerable parts when facing flood risks. Therefore, this study considers mapping and modelling of existing decay. Since the nature of the damage involves irregular geometries and may further develop, the flood assessment focuses on determining whether the decayed areas are at risk from flooding. A simplified modelling approach is employed, using predefined in-place cuboids family with a thickness of 0.01 meters to represent specific damage. These cuboids describe the location and extent of the damage. The cuboid size in the model is adjusted according to the actual position and size of damage, fully covering the decay areas.

Two main types of damage were modelled. The first type includes partial damage to specific components and elements (e.g., biological erosion, spalling, discoloration/deposits, etc.). A damage catalogue was created based on standards and literature regarding building damage types, and different colours were assigned to each type of damage (figure 36)[67], [68]. Each cuboid in the project is set as a specific in-place component/Architecture/Signage category, distinguishing the corrosion model from building elements. It can be exported in IFC format or imported directly into ArcGIS in RVT format for interoperation.

Figure 36 South facade decay representation, collaborated with Xiang Li.
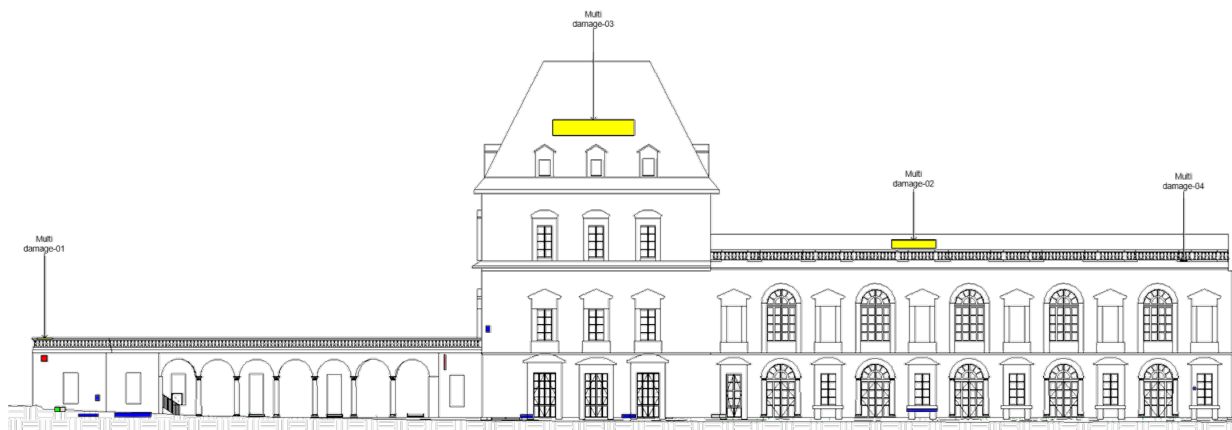
Legend:

1. Cracks and deformation – red
2. Spalling – blue
3. Biological erosion – green
4. Material loss – grey
5. Discoloration/deposits – orange
6. Human intervention – purple
7. Others – yellow

The second type of damage concerns structural damage, either to the entire or partial structure, such as deformation or collapse of walls, columns, or timber trusses. Precise structural deformations should be generated using high-accuracy GOA models with high GOG modeling methods. However, this study does not include the analysis of structural deformations or stability. Therefore, a multi-category label marked as "Other - Yellow" is used to identify

structural damage. This method only provides a general description of overall damage and is intended to signal risk in flood analysis but cannot be used for structural analysis.

Figure 37 Spalling represented using patch-type objects (in-situ components/identifications) in blue.

Model Validation

After completing the modelling, the accuracy of the model was verified using the Surface Analysis Tools in As-built, which quantified deviations between the point cloud and the model elements. The verification process focused primarily on the ground floor and basement areas, as these zones are more susceptible to floodwater. Ensuring that the model met GOA200 tolerance standards was critical for the reliability of subsequent flood assessments. Figure 38 provides a global deviation analysis for the entire basement wall and floor, with a calculation range of 200mm, confirming compliance with GOA200 standards. Similarly, Figure 38 shows the deviation analysis for the ground floor, with particular attention to the position of openings and walls, also within a 200mm calculation range, further validating adherence to GOA200 standards.

Figure 38 Model Validation
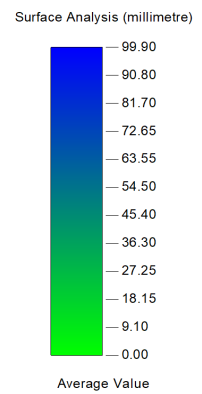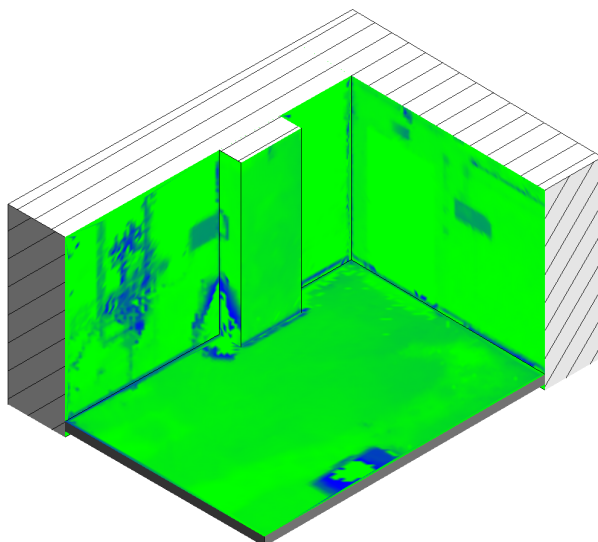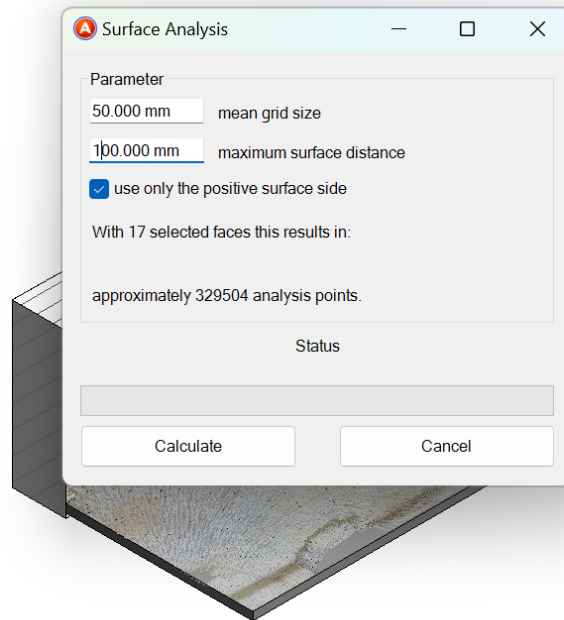
4.3 GIS Environment Modelling

4.3.1 Valentino Castle Surrounding Environment modelling at LoDs

To develop a comprehensive multi-scale 3D GIS project for flood impact assessment, a 3D geodatabase was designed and implemented within the ArcGIS environment. The geodatabase exploits rich datasets from the Geoportale Piemonte, integrating them into structured layers that support multi-scale analysis, management, and visualization of flood-related data.

The multi-scale approach employs varying Levels of Detail (LoDs) to provide both high-resolution representations of critical areas, such as Valentino Castle and its immediate surroundings, and broader, lower-resolution models of the regional hydrological context. At LoD 0, regional flood risk zones, including river networks, floodplains, and hydrological parameters such as soil permeability and rainfall intensity, are visualized to inform large-scale planning. At LoD 1, generalized 3D building representations, delineated into residential, productive, and service categories, are included, with a DTM resolution of 1 meter providing detailed topographical context. At LoD 2, detailed urban models, such as simplified representations of key structures like Valentino Castle, include sloped roofs, openings, and terrain models generated from point cloud data for district-level flood risk assessments. At LoD 3, detailed models of buildings and surrounding topography are developed for building element level flood risk assessments (Table 5).

The 3D geodatabase has several key features that enhance flood simulation and impact assessment: 1) It operates within a multi-scale environment, organising data across different levels of detail (LoDs) to enable seamless transitions between detailed and contextual views. 2) Integrated 3D models provide precise geometries for simulating flood scenarios, supporting advanced visualisation and analysis, which support flood risk management, emergency planning, and the development of resilience strategies. 3) Hydrological data integration further enriches the database by incorporating permeability, precipitation, and watercourse morphology layers, facilitating sophisticated flood simulations. 4) Time-enabled data, including temporal datasets for precipitation and flood extents, supports time-series analyses and animations of flood events. 5) By leveraging the compatibility of the 3D geodatabase with ArcGIS tools, the project ensures scalability and adaptability for future enhancements or extensions.

Table 5 LoDs of the 3D GIS Project

LoD	Scale	Description	Source
LoD 0			
Digital Terrain Model (DTM) 1:5000	1:5000	The DTM (Digital Terrain Model) covers the entire regional territory and was acquired using a uniform methodology (LiDAR) at Level 4 standards. The grid resolution (spacing) is 5 meters, with an elevation accuracy of ±0.30 meters (±0.60 meters in areas of lower precision, such as forested and densely urbanized zones).	[72]
Precipitation Data	Resolution: 800 m	The **Intense Rainfall Atlas** (Atlante piogge intense) service allows users to determine rainfall probability curves at any point within the regional territory. These curves, based on assigned return periods and durations ranging from 10 minutes to 24 hours, are essential tools for hydraulic design and probabilistic flood flow assessments. The statistical analysis utilized the entire available dataset, including historical stations from the National Hydrographic and Mareographic Service, operational from 1913 to 2002, and stations from the regional network established in 1987.	[73]
Hydrology Predominant Permeability of the Unsaturated Zone	1:100 000	This thematic layer is based on the vertical equivalent hydraulic conductivity (Kz) of the unsaturated zone as the reference parameter. The soils identified from approximately 2,000 stratigraphies of the unsaturated zone were grouped into lithological classes, each assigned a hydraulic conductivity value derived from the literature. The vertical equivalent hydraulic conductivity was calculated by dividing the thickness of the unsaturated zone by the summation of the ratios between the thickness of each individual lithological layer within the zone and its specific hydraulic conductivity. This process yielded approximately 2,000 point-specific vertical hydraulic conductivity values, which were then interpolated using a statistical method to generate the corresponding cartographic representation.	[74]
Topsoil texture and properties	1:50 000	The Atlas is an online service for consulting and disseminating soil analysis data. It provides "point-specific" information on the surface layers of agricultural soils in Piedmont (0–30 cm and 30–60 cm). Specifically, it includes the results of chemical and physical analyses conducted by the Regional Agrochemical Laboratory (LAR) since the 1980s, along with analyses from other laboratories in Piedmont (CadirLab, INIPA, IPLA, ARPA, and the University of Turin - DISAFA). This georeferenced and validated dataset was developed following a dedicated protocol drafted by LAR in collaboration with the Agricultural Chemistry section of the Faculty of Agriculture in Turin (now DISAFA).	[75]
Watercourse Morphology	1:10 000	The GEmMA dataset, GEodatabase of River Morphology, compiles all morphological information related to the watercourses of the Piedmont region. GEmMA was developed as both a working tool and a resource for calculating the Morphological Quality Index (IQM), an indicator that, together with the Hydrological Regime Alteration Index (IARI), assesses the hydromorphological status of a watercourse as required by the EU Water Framework Directive (Directive 2000/60/EC). This directive was implemented in Italy through Decree 260/2010, which sets technical criteria for characterizing water bodies. The service provides access to selected data extracted from the GEmMA dataset.	[76]
Flood-prone areas	1:100 000	The dataset represents, by way of example, areas potentially subject to flooding, differentiated based on return periods and the type of deposited material. The dataset originates from a meticulous analysis of historical archival documents and a systematic interpretative study of aerial photographs, conducted repeatedly across the Piedmont region until the 1990s. This approach enabled the identification of flooded and/or inundated areas along watercourses, with indications of the frequency of such phenomena over the past 100 years and the type of material deposited during flood events.	[77]

LoD	Scale	Description	Source
		The original thematic data was produced using the I.G.M. 1:100,000 scale framework by structuring and integrating data already collected by CNR-IRPI in Turin as part of research aimed at assessing the hazards associated with hydrological events in the Piedmont region.	
BDTRE (Banca Dati Territoriale di Riference degli Enti) 2024 （including building, transportation, vegetation and so on.）	1:10 000	The Territorial Reference Database of Entities (BDTRE) is the geo-topographic database of the Piedmont Region, structured according to national technical specifications (DPCM, November 10, 2011) and organized into Layers, Themes, and Classes. The Class serves as the reference structure, defining the representation of specific types of territorial objects. Initiated in 2007, BDTRE integrates local implementations and information from various sources available to the Piedmont Region and is continuously updated. A cartographic representation derived from BDTRE is produced at a scale of 1:10,000 (Reference Cartographic Base) with annual editions.	[78]
LoD 1			
DTM 1:1000 WMS (Web Map Service)	1:1000	The Digital Terrain Model (DTM) has a ground resolution of 1 meter and is derived from LiDAR scanning conducted from an aerial platform. This data was acquired by the Ministry of the Environment and Protection of Land and Sea as part of the Extraordinary Environmental Remote Sensing Plan. The survey covered first- and second-order river channels, as classified in the hierarchical order provided in the IGM river catalogue.	[79]
3D Buildings WMS (Web Map Service)	1:10 000	The dataset contains the delineations of individual volumetric units of regional buildings, including their average elevation. It identifies three categories of buildings: R: Residential. P: Productive. S: Services.	[80]
LoD 2			
Simplified model of Valentino Castle	1:100	Simplified Valentino Castle BIM model: A model with sloped roofs and openings.	Collaborative Modeling Based on Point Cloud Data
Terrain model of Valentino Castle's District	1:100	Generated from point cloud data, showing moderate detail.	Individual Modeling Based on Point Cloud Data
LoD3			
Detailed model of Valentino Castle	1:500	Detailed and complete Valentino Castle BIM model: A highly precise model used for flood risk assessment.	Collaborative Modeling Based on Point Cloud Data

LoD	Scale	Description	Source
Terrain model surrounding Valentino Castle	1:500	Terrain model surrounding Valentino Castle: Generated from point cloud data with high accuracy.	Individual Modeling Based on Point Cloud Data

4.3.2 HBIM-GIS Data Interoperability

In order to test different solutions and methods, this study employs both commercial software and open-source software to convert the HBIM's IFC data format into GML format, aligning with the CityGML 2.0 or 3.0 standard for detailed 3D GIS projects.

Commercial Software Approach

In ArcGIS Pro, as is common, geopositioning is achieved using the coordinates and angle of the project base point, along with a corresponding Esri PRJ file, rather than relying on the survey point. Prior to importing the BIM data into ArcGIS Pro, it is essential to assign the real-world coordinates (x=396553.556967, y=4789811.813018, z=229.352981) to the project base point as identified in Chapter 3 in Revit software. Subsequently, the BIM data will be accurately positioned in ArcGIS Pro using the Esri PRJ file with the projected coordinate system WGS 1984 UTM 32N.

In this thesis Esri ArcGIS Pro 3.3 was used in the workflow. ArcGIS Pro 3.3 directly supports 2018-2023 Autodesk Revit (RVT) files 2018-2023 as ArcGIS BIM file workspaces.

The geometry and parameter elements in BIM files are used in ArcGIS Pro as a read-only GIS data source of point, polygon, polyline, and multipatch feature classes. The BIM file workspace, along with its datasets and feature classes, is valid data source for feature layer in maps and scenes and functions as read-only inputs for geoprocessing tools.

In ArcGIS, the BIM file workspace for RVT provides a geodatabase structure and organisation to a BIM file. The datasets of feature classes in BIM file workspace named after common industry construction disciplines ——architectural, structural, electrical, mechanical, piping, and infrastructure. These disciplines are used conventionally in BIM software to organise the category of elements. The element categories in BIM file defines the feature classes which are organised within the discipline datasets according to the same construction discipline conventions. ArcGIS Pro generates a feature class for each of the construction categories defined in an RVT file or IFC file. In Autodesk Revit software, all elements used to model structures are organised into predefined categories. The variations of the element in Revit, known as families and family type, represent as attribute field.
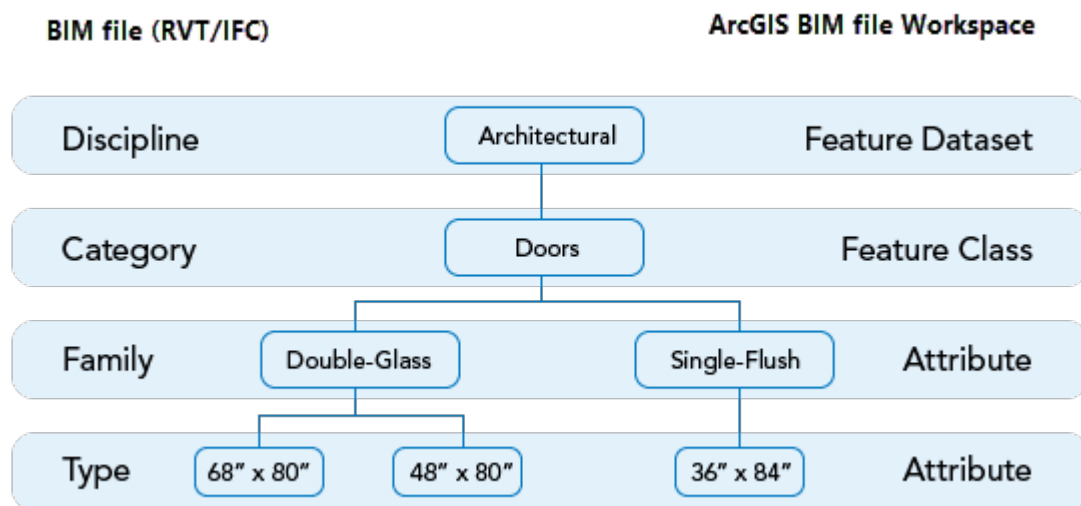
Figure 39 BIM files as a BIM file workspace

(source: https://pro.arcgis.com/en/pro-app/latest/help/data/revit/what-is-bim-data-.htm)

In ArcGIS Pro, geodatabase is a system of record for geospatial data. BIM data can be converted into a geodatabase by BIM File to Geodatabase geoprocessing tool. This tool converts read-only BIM data to an editable geodatabase version of the data. Once the BIM data is stored in a geodatabase, their attributes and geometry can be maintained and updated like any other dataset.

Open-source Software Approach

To address the conversion from IFC to CityGML, FME 2024.0, developed by Safe Software, was employed. FME is also Data Interoperability extension in ArcGIS Pro, allowing data to be converted from one format to another. Although the CityGML 3.0 Conceptual Model Standard has been released, the CityGML 3.0 GML Encoding Standard is not published. So, FME can currently export only CityGML 2.0 or earlier versions.

IFC is more structured than CityGML in data hierarchical structure and has lots of intermediate classes which are not required in CityGML. To remove the unnecessary intermediate classes, the workflow in Figure 40 was adopted. The reader reads all the IFC features and populates a lookup table of feature and parent IDs as variables, and a lookup table of parent types. The generated Parent/child lookup table stores as global variables to support following steps. It also

links IFC features with their parent IDs and grandparent IDs and makes it possible to subsequently establish the correct parent/child relationships in CityGML.
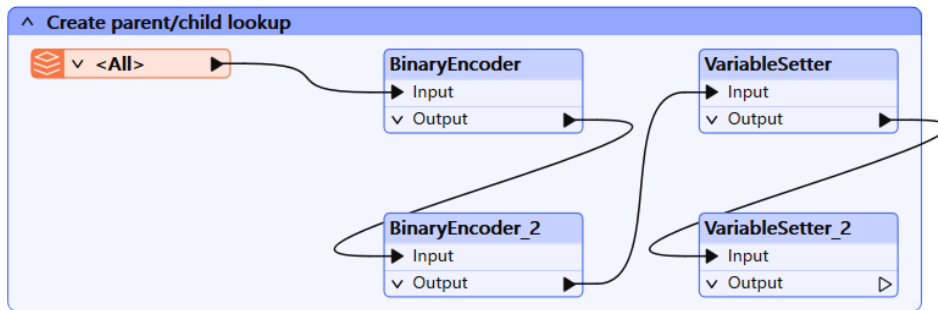
Figure 40 Create Parent/Child Lookup.

Then, all geometry is removed by "GeometryRemover" transformer and "AttributeRenamer" transformer set the ifc_unique_id to the gml_id. The second step aims to remove geometric data and map IFC id to CityGML id (Figure 41).
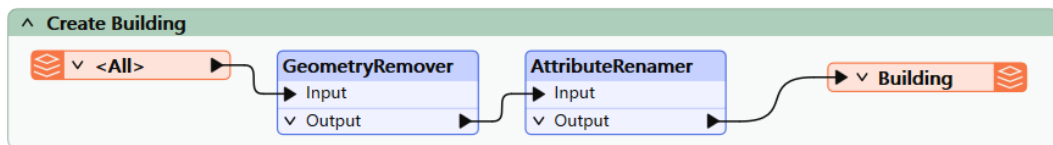
Figure 41 Remove Geometry from the Building and Id mapping.

Afterward, Each IFC (including "IfcBuildingElementProxy," "IfcWindow," "IfcDoor," "IfcStair," "IfcSite," "IfcRoof," "IfcSlab," "IfcWallStandardCase," and "IfcWall.") geometric data to be converted employed following workflow (Figure 42). There are three custom transformers used in this workflow:
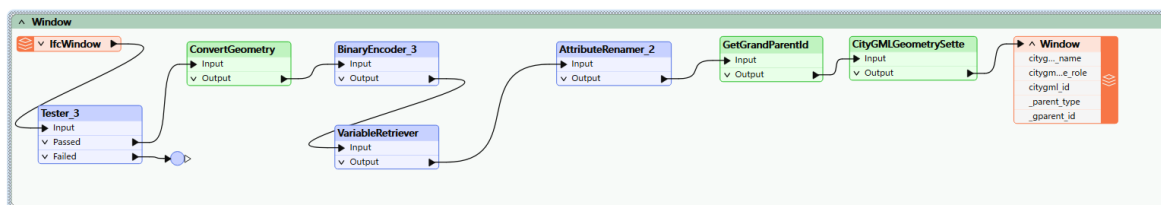
Figure 42 Workflow for Converting "IfcWindow" to CityGML

ConvertGeometry

The IFC geometry composed by solid while CityGML geometry by MultiSurface. Geometry conversion is the most important step in the process of IFC to CityGML. This custom transformer is applied to convert complex IFC solid geometry to MultiSurface. The "GeometryPartExtractor" extracts the solid geometry from the property sets. "GeometryCoercer" convert them "composite_surface" and "Deaggregator" to flatten them on several levels. Then the geometry is re-aggregate into MultiSurfaces through Aggregator transformer with the Mode "set to Geometry - Assemble One Level". Eventually "GeometryRefiner" refines the geometries (Figure 43).
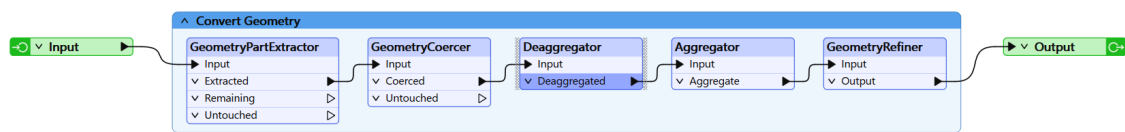
Figure 43 ConvertGeometry custom transformer

GetGrandParentID

Almost all parent links of IFC features stay at the intermediate level (for example, linking to a Building Story, not the building itself). This transformer creates a correspondence between IFC and CityGML by obtaining the grandparent node ID. (Linkto the building). The "BinaryEncoder" transformer processes the attributes to be encoded and creates a User Parameter to store the encoding results. Then, a "VariableRetriever" transformer is added to extract and set a special variable _gparent_id. Finally, this _gparent_id is decoded and then a new User Parameter is generated through the "BinaryDecoder" transformer to store the decoded result of the target attribute (Figure 44).
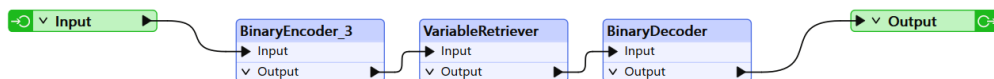
Figure 44 GetGrandParentID custom transformer

CityGMLGeometrySetter

This custom transformer is used for setting "citygml_lod_name" and "citygml_feature_role" to the transformed geometric data following a strict naming convention. "AttributeCreator" is used to create attribute and "CityGMLGeometrySetter," which can automatically set LoD name and feature role, avoiding errors in manual input (Figure 45) [81], [82].
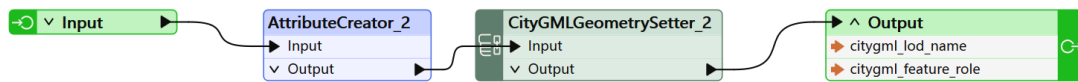
Figure 45 CityGMLGeometrySetter Transformer.

In this study, when initially converting IFC to CityGML using the aforementioned methods, data loss or failures occurred due to the complex geometries contained in historical building models. Simple geometries, such as IfcWindow, IfcDoor, and IfcProxy, were successfully exported to the CityGML format. However, these .gml files could be displayed correctly in the FZK Viewer and QGIS 2D view, but they failed to display in the QGIS 3D viewer. Complex geometries, such as IfcWall and IfcRoof, failed to export because of the inability to convert the geometries into multi-surfaces. These complex geometries may require simplification before conversion, but the simplification process often fails.

Another solution is available on GitHub [83]. However, this solution does not convert the complex geometries (figure 46), resulting in a file that is visually correct in the FZK viewer (figure 47) but cannot be imported into QGIS. Using FME Quick Translator yielded the same result.
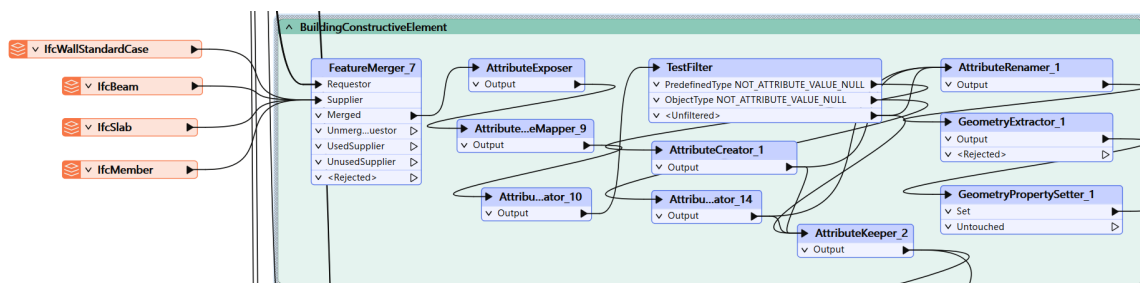
Figure 46 FME workspace on GitHub; does not convert complex geometries.

Therefore, while the open-source approach is theoretically feasible. converting simple models might succeed, but errors frequently occur with complex heritage building models. These

conversions also require high-performance computers. Additionally, Although the converted files are much lighter, they are still very heavy for QGIS, which leads to long loading processes or failures in representing 3D views. Further research is needed to improve conversion efficiency, success rate and open platform support for 3D data.
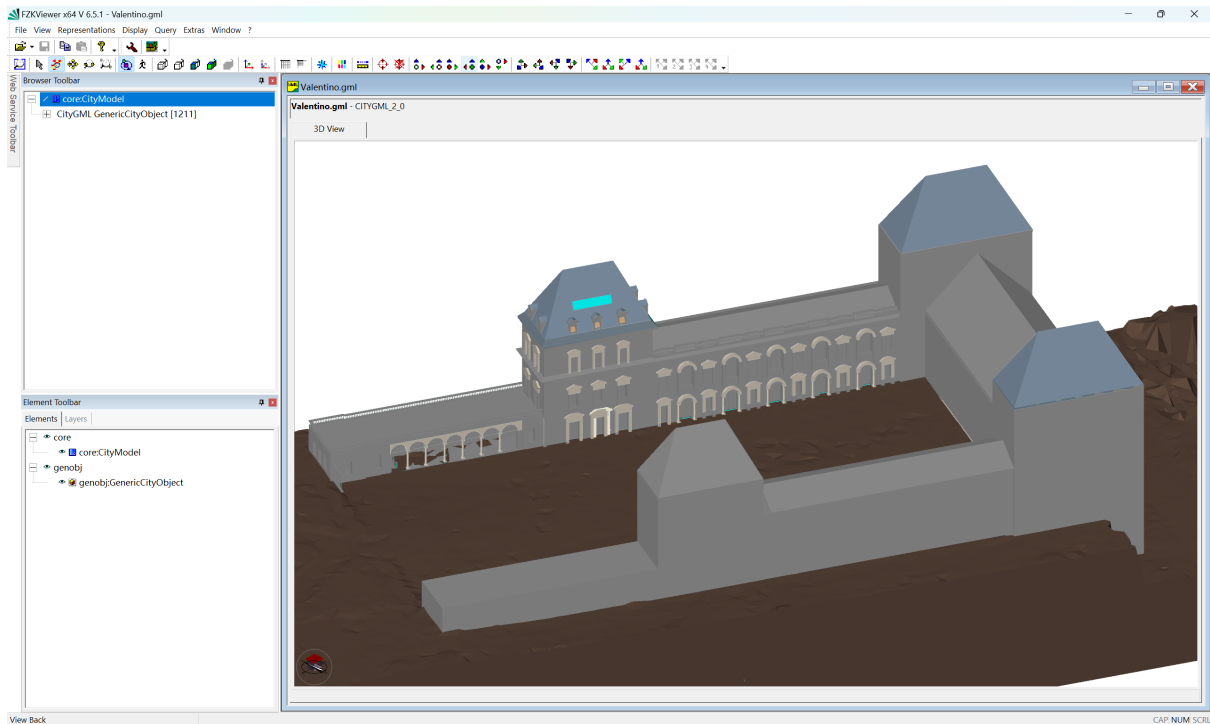
Figure 47 Output CityGML file viewed in FZK Viewer

Chapter 5 Integrated HBIM-GIS for Flood Impact Analysis

Flood types can be broadly classified into three main categories: riverine floods (also known as fluvial floods), coastal floods, stormwater (or urban) flood and groundwater floods. In this thesis, we mainly discuss two types of floods: riverine floods and urban floods. Urban floods occur in densely populated areas where most areas covered by impervious surface like concrete and asphalt and the drainage systems are often inadequate to handle intense, short-duration rainfall events. These floods are typically characterised by rapid water accumulation on streets, parking lots, and other urban surfaces, leading to significant disruptions in daily activities and substantial economic losses. Urban floods can lead to traffic congestion, infrastructure and building damage, and health risks due to contaminated water. Riverine floods occur when river overflow their banks due to excessive rainfall, snowmelt, or dam failure. These floods can inundate vast areas, extending far from the river itself. Riverine floods typically develop over a longer period compared to urban floods and can persist for days or even weeks. The impacts include widespread damage to agriculture, infrastructure and communities, often requiring significant recovery efforts. These two types of floods are usually predictable to some extent, allowing for the implementation of early warning systems, evacuation measures, and comprehensive flood management plans[6, pp. 3–4].

5.1 The Hydrology and Geology Background of Turin

The Po River basin, Italy's largest, includes significant stretches near Turin. Originating from Monviso, the Po River flows north to Chivasso, east to Casale Monferrato, south to Valenza, and east again, passing through the Turin hills and Monferrato region. In Turin, major watercourses such as the Dora Riparia and Stura di Lanzo join the Po River, influencing local hydrology and flood risks. These rivers contribute significantly to the area's hydrological dynamics, necessitating numerous hydrological interventions due to large alluvial deposits and potential flood impacts.[83, pp. 10–34]

The majority of the plain in the municipality of Turin consists of "fluvio-glacial gravelly and cobbly alluvium," characterized by the presence of "ferretto," a clay-rich soil that causes surface water stagnation, potentially leading to plant asphyxiation. The remaining plain areas consist of recent gravelly alluvium and sandy-silty alluvium, associated with the Po, Dora, Stura di Lanzo, and Sangone rivers. Conversely, the Turin hills are composed of various

lithotypes, with a more impermeable nature, containing silt and clay or rocks that allow water infiltration through fissure. These classifications, as shown in Figure 48, provide a simplified understanding of the different soil behaviours within the region, which is essential for creating detailed cartography for hydrological studies and urban planning in Turin.

Figure 48 Topsoil Texture map of the city of Turin.
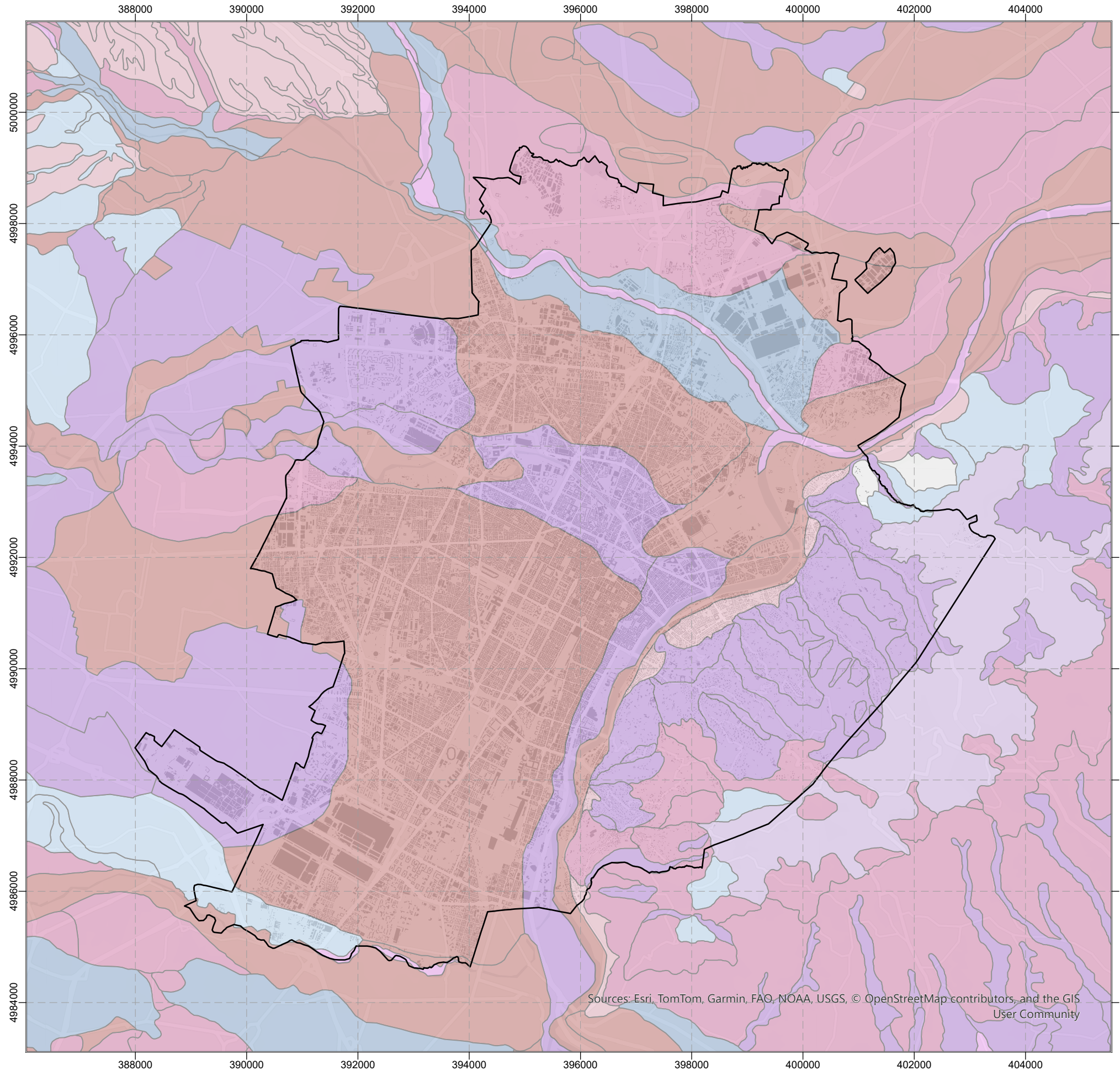
Description

The dataset presents the geometries of the Cartographic Units, defined according to pedogenetic criteria and functional soil properties, describing them in terms of the geography and the relative distribution of the various Soil Typological Units that characterize them.

The left map identifies the topsoil texture within the Turin municipal area.The majority of the plain in the municipality of Turin consists of "fluvio-glacial gravelly and cobbly alluvium," characterized by the presence of "ferretto," a clay-rich soil that causes surface water stagnation, potentially leading to plant asphyxiation. The remaining plain areas consist of recent gravelly alluvium and sandy-silty alluvium, associated with the Po, Dora, Stura di Lanzo, and Sangone rivers. Conversely, the Turin hills are composed of various lithotypes, with a more impermeable nature, containing silt and clay or rocks that allow water infiltration through fissure.

Scale: 1:50,000.

Source: Arpa Piemonte

Legend

- Buildings
- Municipality of Turin
- Argilloso
- Argilloso limoso
- Franco
- Franco argilloso
- Franco limoso
- Franco limoso argilloso
- Franco sabbioso
- Franco sabbioso argilloso
- Sabbioso
- Sabbioso franco

Sources: Esri, TomTom, Garmin, FAO, NOAA, USGS, © OpenStreetMap contributors, and the GIS User Community

N

0 0.75 1.5 3 4.5 6 Kilometers

5.2 Flood Simulation in Arc-GIS

Flood Simulation in Arc-GIS allows to simulate how water flows and accumulates in a scene layer (simulation layer) using shallow water equations within a defined area. The process begins with capturing the elevation value of the area of interest within the simulation layer, generating an elevation surface raster at the specified analysis cell size. Subsequently, water is added to each cell, typically through simulated rainfall, and its movement over the surface is calculated using shallow water equations.

5.2.1 Data Download and Organisation

The primary data sources are Arpa (Agenzia Regionale per la Protezione Ambientale del Piemonte) and Geoportale Piemonte. These organisations provide various geological data about the Piemonte region. These datasets are crucial for understanding the region's environmental characteristics and supporting various analytical and simulation processes. They constitute the LoD0 and LoD1 of the geodatabase outlined in Chapter 4.3.1. LoD 0 includes fundamental geospatial data such as the Digital Terrain Model (DTM) at a scale of 1:5000, precipitation data with an 800 m resolution, hydrology predominant permeability of the unsaturated zone at a scale of 1:100,000, topsoil texture and properties at a scale of 1:50,000, watercourse morphology at a scale of 1:10,000, flood-prone areas at a scale of 1:100,000, and the BDTRE (Banca Dati Territoriale di Riferimento degli Enti) 2024, which encompasses buildings, transportation, and vegetation at a scale of 1:10,000. LoD 1 includes more detailed datasets—a high-resolution Digital Terrain Model (DTM) at a scale of 1:1000 and 3D building models at a scale of 1:10,000, both accessible via WMS (Web Map Service).

To configure the flood scenarios in ArcGIS Pro, the following parameters should be considered:

Area of Interest:

The Valentino Castle and surrounding area, as depicted in Figure 49, have been selected as the area of interest for this study. Most of the selected area has similar topsoil texture and falls within the same drainage basin. Considering the cell size is directly proportional to the size of the area of interest and the requirement for high accuracy in the analysis results, the area of interest has been deliberately kept relatively small. This approach ensures the precision and reliability of analytical outcomes.

The Digital Terrain Model (DTM) around the Valentino Castle was generated as specified in Chapter 4.2. The remaining part of the area of interest, including the DTM at a scale of 1:5000 and the 3D building model, is sourced from Geoportale Piemonte.
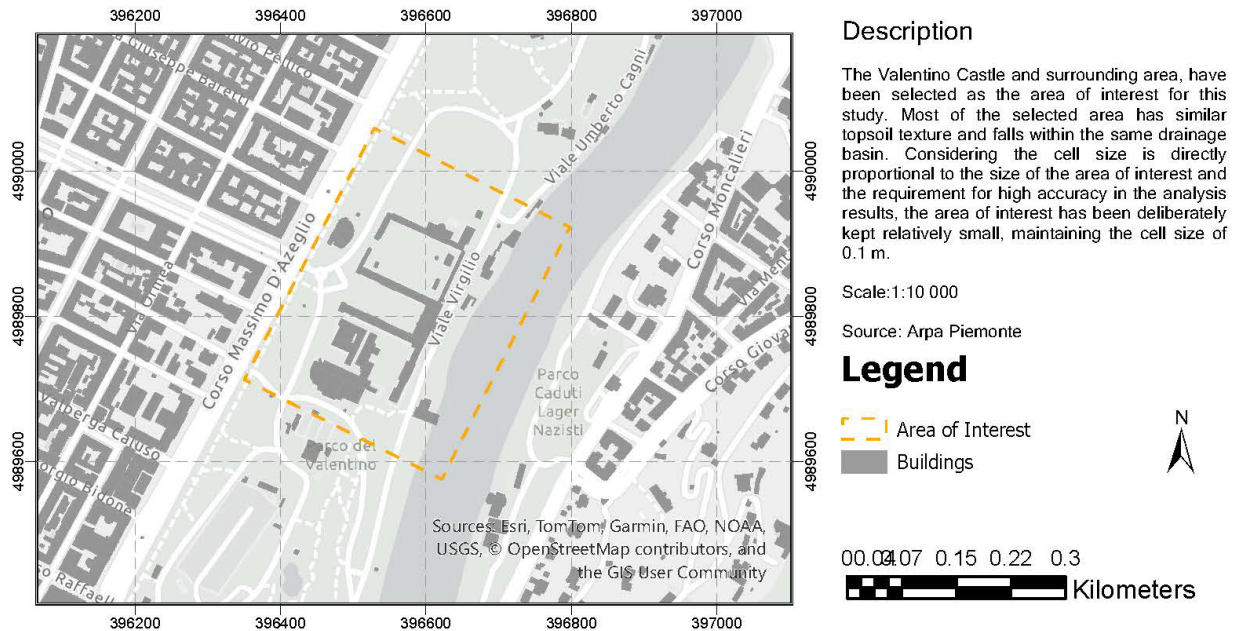
Figure 49 The Area of Interest

1) Rainfall rate through time:

Arpa Piemonte provides Atlante piogge intense in Piemonte(atlas of intense rainfall in Piemonte) [73] which offers rainfall probability lines for any point within the regional territory for duration ranging from 10 minutes to 24 hours. These lines are an essential tool for hydraulic design and in the probabilistic assessment of flood discharges.

This service is based on available data, including historical records from the National Hydrographic and Mareographic Service (Servizio Idrografico e Mareografico Nazionale), which operated from 1913 to 2002, and data from the regional network established in 1987. By applying ordinary Kriging to a square mesh interpolation grid, maps were created representing synthetic series of annual maximum precipitation for each point on the grid. The determination of the coefficients of the rainfall probability curve was carried out by considering the averages of the maximum precipitation values. Once the rainfall probability curve parameters are known, Gumbel and GEV probabilistic models are applied to determine the rainfall probability lines, which define, for various durations, the maximum precipitation corresponding to a given return period [84].

87

In this thesis, the intense rainfall data of Valentino Castle and the surrounding area is downloaded in GeoJSON format and then imported into ArcGIS to manipulate (Figure 50).
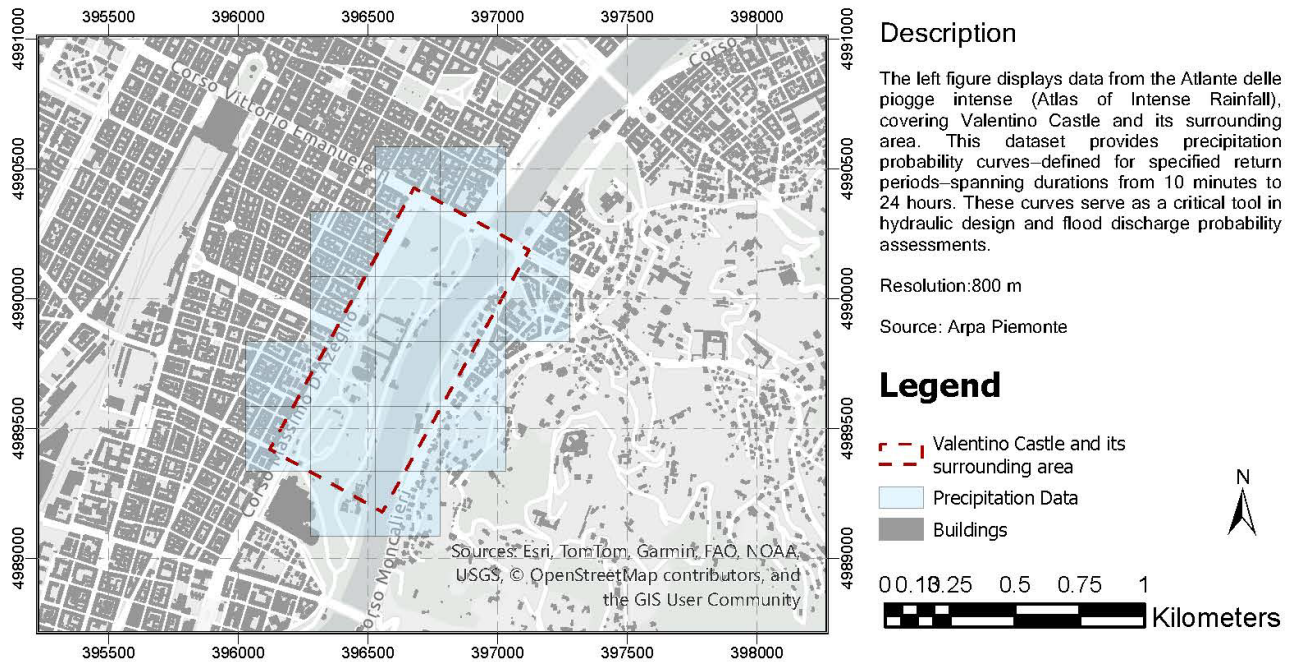
Figure 50 Atlas of Intense Rainfall

2) Cell size:

Due to the high accuracy requirements for the analysis results, the cell size is set to 0.1 meters. This resolution strikes a balance between the accuracy of the BIM model and computational capabilities of the software and hardware.

3) Ground infiltration rates （Drainage Data）

Arpa Piemonte provides an atlas of topsoil texture and infiltration rates for the Piemonte region. However, the resolution of these data is insufficient for the current simulation process. According to the *Idrogeologia - Permeabilità prevalente della zona non satura 1:100.000*(https://www.geoportale.piemonte.it/geonetwork/srv/ita/catalog.search#/metadata/r_piemon:47b602ce-56fb-4a7e-a7ee-d6df1bc203c0) the infiltration rate in the area of interest ranges from 10^{-5} to 10^{-3} m/s. And the topsoil texture is characterised as sandy loam and mix of loam and silty loam. Because there is no laboratory-specific infiltration rate data for this area, the ArcGIS predefined infiltration rates for loam and sandy loam are utilised for the simulation scenario respectively, which are aligned with mentioned range.

Furthermore, data pertaining to drainage systems for this area could not be found on the official geological data websites.

4) Water source point:

It is allowed to introduce multiple water source point to modelling the arrival of water from upstream regions of the area of interest. However, in ArcGIS water source is added to a cell size square as a high column of water at a specified flow rate. Several factors are not considered in this simulation, such as, the initial velocity of the river flow. Consequently, this method dose not accurately represent the real-world scenario of riverine flood.

5) Water flow barriers and channels:

Not included in the selected area of interest.

6) The starting water level:

The initial water level is integrated into the DTM (Digital Terrain Model) used in this study. Therefore, no additional data is required.

7) Vegetation:

Although vegetation is an important parameter, it is not yet included in the ArcGIS simulation configuration. Therefore, the retention of rainwater by plants is not taken into account, and this study has not considered the vegetation in the flood simulation.

8) Evaporation:

Evaporation was not considered in the simulation process. because evaporation per unit area in the urban environment is approximately 0.5% of accumulated rainfall for a 3-day flood event[85].

5.2.2 Storm Water Simulation

Different flood scenarios are simulated in this study. For storm water, the return period (T) of 10 years ,50 years and 200 years are simulated which represent high, medium and low risk respectively. Except the rainfall rate and infiltration rate, other parameters stay the same over whole simulation process.The original data from *Atlante piogge intense in Piemonte* (https://webgis.arpa.piemonte.it/agportal/apps/webappviewer/index.html?id=378e0fcb7ddd45 65ba836c07dd1c4c9b) or different return period, the precipitation and rainfall rate changed over time as table 6:

	Return Period		
Start Time -End time	T=10	T=50	T=200
0-10min	29.74	40.17	49.53
10min-20min	35.49	47.95	59.11
20min-30min	39.21	52.96	65.30
30min-60min	46.30	62.54	77.11
60min-180min	60.09	81.17	100.08

Table 6 Precipitation (mm) over Time
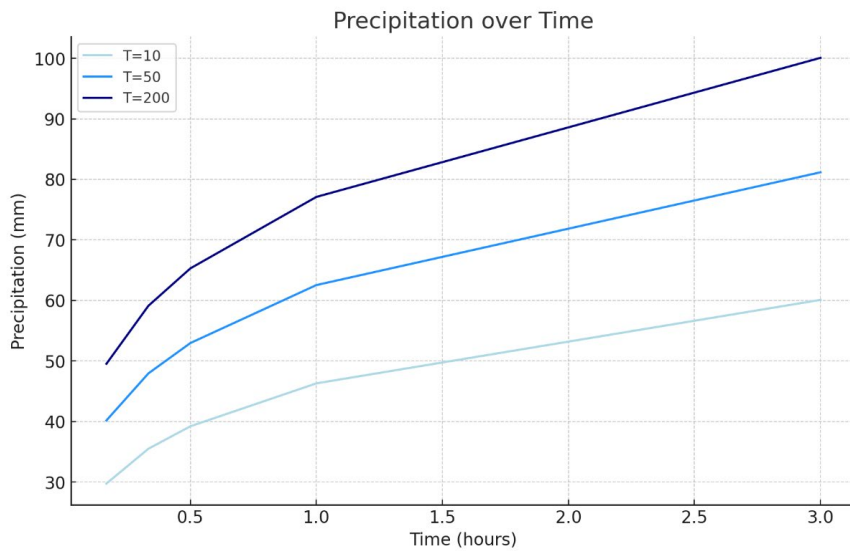
Figure 51 Precipitation (mm) over Time

	Return Period		
Start Time -End time	T=10	T=50	T=200
0-10min	178.41	241.01	297.15
10min-20min	34.54	46.66	57.54
20min-30min	22.28	30.10	37.11
30min-60min	21.27	28.73	35.43
60min-180min	6.90	9.32	11.49

Table 7 Rainfall Rate (mm/h) over Time
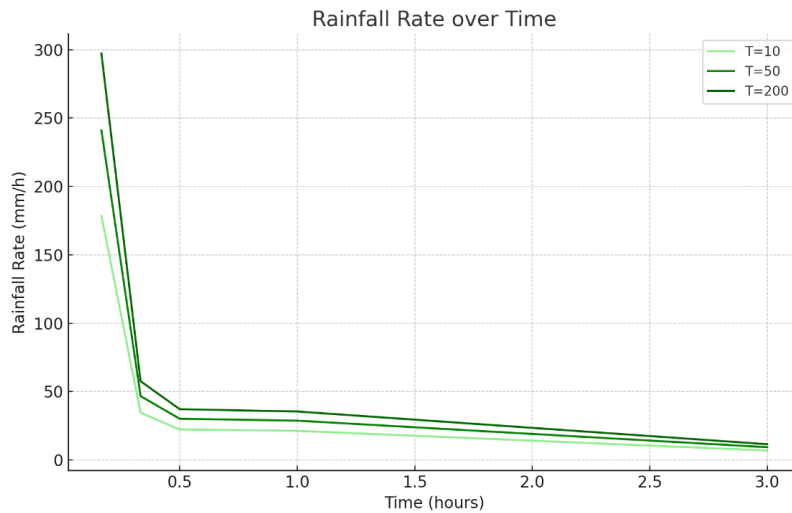
Figure 52 Rainfall Rate (mm/h) over Time

ArcGIS simulations—whether using built-in functions or Python scripts—capture only the height values of the building's upper surfaces, failing to account for recesses and projections. This results in missing values for ground areas below features such as colonnades and cornices due to occlusion (Figure 53). For these areas, smooth blocks were used to replace buildings with decorations during the flood simulation process. When analysing the results, the simplified model is replaced with the complete model that includes decorations.
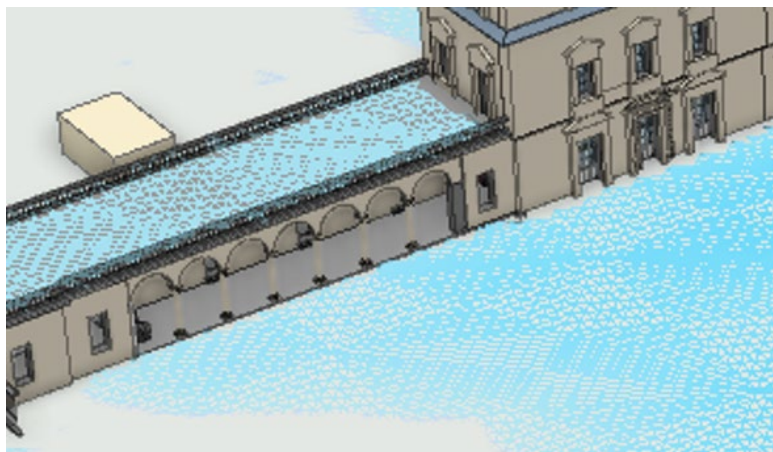
Figure 53 Limitations of ArcGIS Simulation for Building Recesses and Projections

Results—3D Visualisation

Figure 54 A 3D view of the ground surface water depth at the tenth minute under wet surface conditions, given a 200-year storm return period.
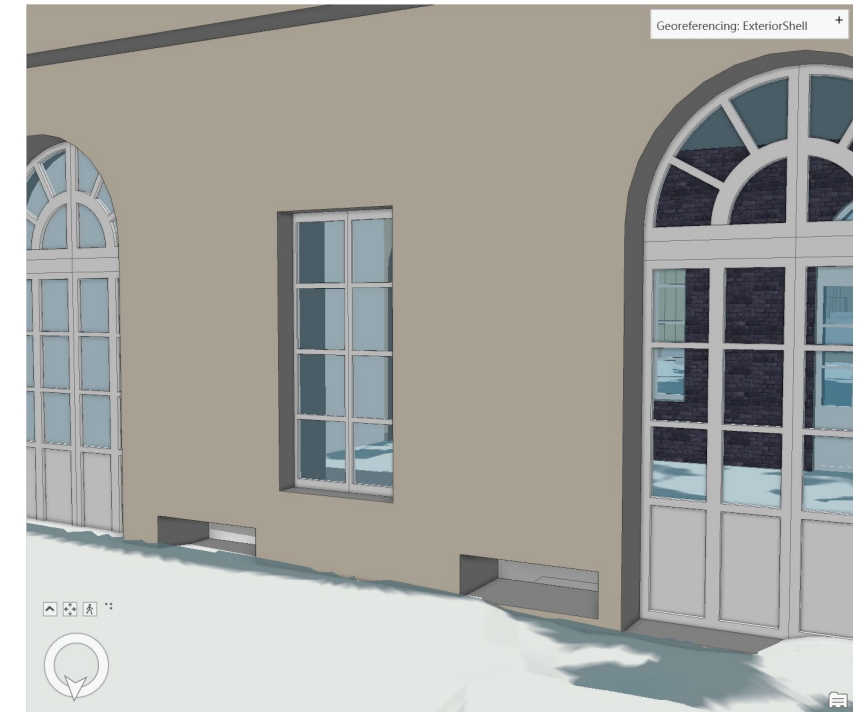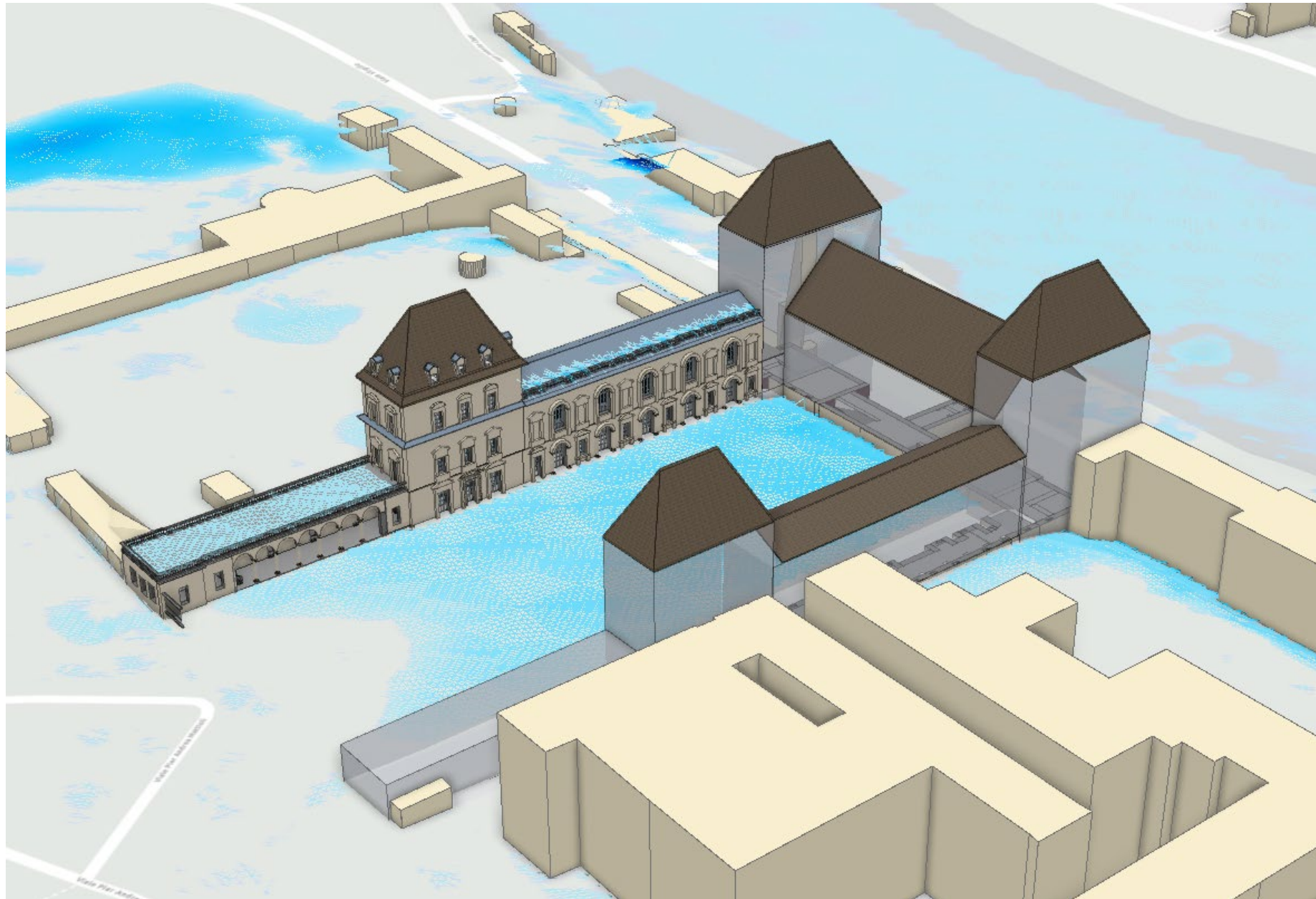
The left image (figure 54) shows 3D visualization results of a simulated intense rainfall event with a 200-year return period, ten minutes after precipitation began. It can be observed that there is significant surface water accumulation. As shown in the right image (figure 54), the light and ventilation windows linked to the basement, due to their low position, are likely to cause rainwater infiltration into the basement due to water pooling in the area, potentially resulting in damage.

The left image shows the 3D visualization results of a simulated 200-year return period storm at the 10th minute after the onset of the rainfall event. It can be observed that there is significant surface water accumulation. As shown in the image, the light and ventilation windows connected to the basement, due to their low position, are likely to cause rainwater infiltration into the basement due to water pooling in the area, potentially resulting in damage.

This simulation can produce a series of outputs, such as the water depth, water absolute height, and water velocity at ten-minute intervals for storm events with return periods of 10, 50, and 200 years, along with corresponding animations. The extracted data can be used for element level flood risk assessment, enabling the identification of specific building elements impacted by flooding.

5.2.3 Riverine Flood Simulation

The most impactful flood in Turin in recent years occurred from October 13-16, 2000. This flood was classified as a 200-year flood but only affected areas surrounding the Valentino Castle, as illustrated in the accompanying figure 3. The floodwaters did not reach the castle itself.
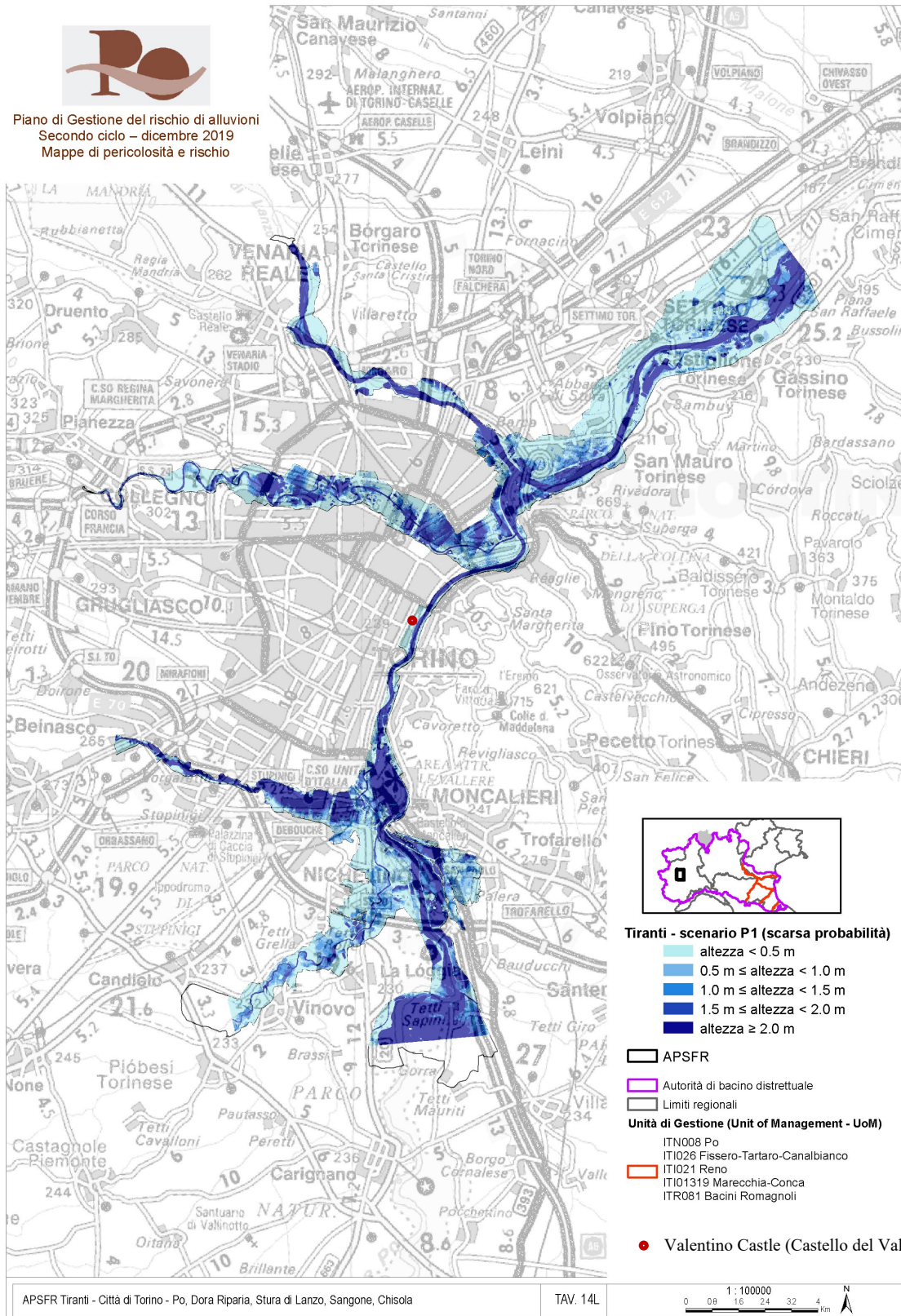
Figure 55 Low Probability Flood Depth Map

In a low-probability flood scenario, the flood depth around the location of Valentino Castle is below 0.5 meters. (Figure 56) However, for an accurate analysis of potential flood damage to specific elements of the historic building, this depth range information is insufficient. Therefore, it is assumed that the castle's basement (the lowest point of the building) experiences a flood depth of 0.5 meters. This assumption allows for the evaluation of the maximum potential damage Valentino Castle might face under extreme flood conditions.

Additionally, floods can lead to a rise in groundwater levels, which may impact Valentino Castle's basement. Although floodwater might not be visible indoors due to the basement floor structure acting as a barrier, the groundwater can still infiltrate and deteriorate the building's elements through capillary action. Such damage requires long-term monitoring of the building following flood events or groundwater level warnings to assess and evaluate the extent of impact.

5.3 Discussions

Traditional Flood damage assessment (FDA) methods primarily estimate economic loss using various data sources and formulas. These methods vary depending on the scale of assessment, such as at the building, community, or urban levels, each requiring distinct data inputs [86], [87]. While one study has addressed flood damage assessment at the building component or element level; however, its primary focus remains on formula development and index calculation [88]. Despite these advancements, quantifying the monetary and cultural value of heritage buildings and their assets poses significant challenges. Furthermore, conventional FDA approaches lack the capacity to guide the development of tailored emergency flood response plans for heritage structures.

Flood impact assessment is critical for various institutions, including water management agencies, spatial planning authorities, flood risk management decision-makers, and insurance companies. With growing demand, there is an increasing expectation to simulate flood damage and risk with high spatial and temporal resolution across different scales. Building element level flood risk assessments and visualisation are particularly important for built heritage which is situated in floodplains. Assessing the impact of flooding at the building element level and systematically recording the results in a database (e.g., an attribute table) can provide valuable insights for future risk management and mitigation strategies.

However, these simulations are complex, involving extensive datasets and numerous computational processes, and they require high-performance computers. Therefore, stable and reliable software is essential for ensuring efficient execution.

The flood simulation function in ArcGIS is primarily designed for large-scale applications, such as urban and regional flood assessments. Consequently, there are several limitations when applying it to simulations at an individual cultural heritage site. Vegetation is a critical parameter that has not yet been incorporated into the ArcGIS flood simulation configuration. River dynamics, such as the water flow velocity, cannot be properly integrated into the model within the native ArcGIS flood simulation framework. Therefore, further development and enhancement of the flood simulation capabilities in ArcGIS are required to meet the high-precision demands of flood risk assessments for cultural heritage sites.

In addition, due to the lack of detailed data on permeability, infiltration rate, and saturated hydraulic conductivity for different ground covers, such as asphalt and vegetation, the average permeability values of the overall topsoil of the area of interest were used in the simulation, which potentially leads to inaccurate results.

In the proposed methodology, GIS is primarily a tool for data query and management rather than flood simulation software. It mainly provides a platform for data sharing, supports collaborative decision-making, and enables 3D visualization. There are many 2D-based simulation methods for flood simulation using GIS. These methods are widely used, including the Green-Ampt method and Soil Conservation Service (SCS)-Curve Number (CN) method [85], [89]. They are more conventional and well-established urban flood simulation methods that comprehensively consider the influence of vegetation and ground cover of different materials. Future studies can analyse and compare the results obtained from 2D-based methods with those generated by ArcGIS's built-in simulation capabilities. Given the highly specialized nature of flood simulation, it is advisable to collaborate with domain experts and use more specialized software and methods to generate high-precision and reliable simulation results that are compatible with the GIS environment. This would be an effective way to improve the accuracy and reliability of flood assessments.

Conclusion

In the methodology proposed in this study, Building Information Modelling (BIM) is used to create comprehensive digital representations of the physical and functional characteristics of buildings, enabling precise simulations of flood impacts at the building element level. Geographic Information Systems (GIS) manage and analyze geospatial data, facilitating the integration of the BIM data and geospatial data into the flood simulation and flood risk assessment process. BIM serves as a data repository, addressing building entities, geometrical and topological relationships, and attributes, while GIS manages the geospatial relationships between buildings and surrounding features. Together, BIM and GIS facilitate the evaluation of specific flood risks to buildings and enable the development of tailored flood mitigation recommendations by leveraging high-resolution data for both built heritage and geospatial data. The HBIM-GIS framework also forms a geodatabase for flood risk assessment, which is scalable and adaptable for future enhancements or extensions. It promotes comprehensive flood risk management.

One effective way to communicate the potential impacts of flooding on historic buildings is to illustrate its specific effects on individual building elements. 3D visualizations of flood scenarios effectively illustrate the extent and severity of potential damage, offering a clear representation of flood risk. These realistic visualizations improve communication, enabling stakeholders and community members to understand the risks better and make informed decisions, thus contributing to heritage conservation. However, the accuracy and reliability of this study depend on the availability and precision of geospatial data, point cloud data, and related resources. To obtain more precise and reliable results, access to more detailed and accurate data is required. However, obtaining such high-quality data requires significant financial and human resource costs.

Assessing flood risk at the element level requires multidisciplinary collaboration and expertise. Historic buildings often contain complex non-standard geometries, so model quality and efficiency are highly dependent on the skills and experience of the operator. Changes in modeling methods can affect data interoperability, thereby affecting subsequent analysis. Effective HBIM modelling for a specific problem requires a thorough understanding of the problem context and developing an appropriate strategy. Further research could focus on

optimizing methods and standards for simplified modeling of historic buildings and how to promote interoperability during the modeling phase.

Due to resource and technical constraints, this study employs relatively simple flood simulation methods available in ArcGIS. Compared to advanced flood modelling techniques, such as those using specialised software like HEC-RAS which accounts for detailed hydrodynamic factors. The results produced by ArcGIS provide limited accuracy and reliability for assessing flood impacts on heritage buildings. Given that this aspect requires expertise from other specialised fields, interdisciplinary collaboration in future research would greatly enhance the accuracy and reliability of the analysis.

This study explores the interoperability between BIM and GIS, focusing on two main approaches: application-level integration using commercial software and data-level integration between widely adopted formats---IFC and CityGML. Specifically, the conversion of IFC data into CityGML for use in GIS environments was evaluated. Commercial software proved to be more stable and convenient, particularly for managing large-scale models; however, its limited openness and reliance on proprietary solutions present challenges. Despite extensive research on BIM-GIS integration, persistent issues—such as the loss of geometric and informative data—continue to hinder seamless interoperability.

Furthermore, for heritage buildings, it is challenging to quantify the exact value of each component. However, under known damage conditions, the costs associated with restoring certain architectural structures or elements can be estimated. The methods discussed in this study enable the simulation of specific flood scenarios, allowing for the assessment of potential damage at the building element level. This facilitates a more accurate estimation of restoration costs. Consequently, the approach presented in this paper could be applied to insurance assessments for more accurate risk valuation and budget planning for restoration work.

Overall, the method proposed in this study is theoretically feasible and has certain practical significance. However, due to the current hardware and technical limitations, there are still many barriers to applying this method in specific cultural heritage flood risk assessment and conservation cases. The subsequent research steps can concentrate on refining details within the proposed framework, enhancing workflow efficiency, and increasing the accuracy and reliability of results.

Acknowledgement

First of all, I would like to express my sincere gratitude to Professor Lorenzo Teppati Lose', Professor Elisabetta Colucci and Professor Fulvio Rinaudo for their guidance and help throughout my research. For me, this research field is full of challenges, and I encountered many difficulties in the process. The three professors always patiently answered my questions and provided many constructive suggestions, which benefited me a lot. I am especially grateful to Professor Lorenzo Teppati Lose' and Professor Elisabetta Colucci for their timely assistance and understanding, which helped me a lot.

Secondly, I would like to express my special thanks to my family. They have given me unlimited support, tolerance and care in the process of pursuing my academic goals. At the same time, I would also like to thank my friends who accompanied me through this academic research stage. Their company and encouragement made me full of motivation.

Lastly, although this research still has many imperfections, it represents a new and exciting challenge for me. During the countless moments when I felt like giving up, it was persistence that enabled me to complete this project and gain invaluable experience.

References

[1]   F. Dottori *et al.*, 'Increased human and economic losses from river flooding with anthropogenic warming', *Nature climate change*, vol. 8, no. 9, pp. 781–786, 2018, doi: 10.1038/s41558-018-0257-z.

[2]   K. Boudreau, M. Robinson, and Z. Farooqi, 'IPCC Sixth Assessment Report: Climate Change 2021: The Physical Science Basis Summary For Policymakers', *Canadian Journal of Emergency Management*, vol. 2, no. 1, 2022, doi: 10.25071/6sw6za31.

[3]   'SNPA, Il clima in Italia nel 2023, Report ambientali SNPA, n. 42/2024'. Accessed: Jan. 12, 2025. [Online]. Available: https://www.snpambiente.it/wp-content/uploads/2024/07/Rapporto-SNPA-clima-2023.pdf

[4]   'Citta Clima Bilancio finale 2024', legambiente. Accessed: Jan. 12, 2025. [Online]. Available: https://www.legambiente.it/wp-content/uploads/2021/11/Citta-Clima-Bilancio-finale-2024.pdf

[5]   G. Nanni, A. Minutolo, and E. Rapiti, 'Rapporto Città Clima 2023 speciale alluvioni', legambiente, 2023.

[6]   D. Pickles, 'Flooding and Historic Buildings', Archaeology Data Service, 2015. doi: 10.5284/1110937.

[7]   'Rapporto Spiagge 2024 Gli impatti di erosione ed eventi meteo estremi nelle aree costiere italiane.', legambiente. Accessed: Jan. 12, 2025. [Online]. Available: https://www.legambiente.it/wp-content/uploads/2021/11/Report_Spiagge_2024.pdf

[8]   T. Tingsanchali, 'Urban flood disaster management', *Procedia engineering*, vol. 32, pp. 25–37, 2012, doi: 10.1016/j.proeng.2012.01.1233.

[9]   S. A. H. B. S. Muzamil *et al.*, 'Proposed Framework for the Flood Disaster Management Cycle in Malaysia', *Sustainability*, vol. 14, no. 7, pp. 4088-, 2022, doi: 10.3390/su14074088.

[10]   K. Dinicola, 'The "100-Year Flood"', U.S. Geological Survey, 229–96, 1997. doi: 10.3133/fs22996.

[11]   W. Kron, 'Flood Risk = Hazard • Values • Vulnerability', *Water International*, vol. 30, no. 1, pp. 58–68, Mar. 2005, doi: 10.1080/02508060508691837.

[12]   E. E. Koks, B. Jongman, T. G. Husby, and W. J. W. Botzen, 'Combining hazard, exposure and social vulnerability to provide lessons for flood risk management', *Environmental Science & Policy*, vol. 47, pp. 42–52, Mar. 2015, doi: 10.1016/j.envsci.2014.10.013.

[13]   Spano D., Mereu V., Bacciu V., Barbato G., Buonocore M., Casartelli V., Ellena M., Lamesso E., Ledda A., Marras S., Mercogliano P., Monteleone L., Mysiak J., Padulano R., Raffa M., Ruiu M.G.G., Serra V., Villani V, 'Analisi Del Rischio i cambiamenti climatici in sei città italiane -Torino', 2021. [Online]. Available: https://www.cmcc.it/it/report-torino

[14]   'Consumo di suolo,dinamiche territoriali e servizi ecosistemici edizione 2023', SNAP, 2023. [Online]. Available: file:///C:/Users/supei/Zotero/storage/J7JSRNX6/consumo-di-suolo-dinamiche-territoriali-e-servizi-ecosistemici-edizione-2023.html

[15]   *Aggiornamento e revisione del Piano di Gestione del Rischio di Alluvione redatto ai sensi dell'art. 7 del D.Lgs. 49/2010 attuativo della Dir. 2007/60/CE – II ciclo di gestione Allegato 2.1 Schede monografiche APSFR Distrettuali Città di Torino Distretto del fiume Po.*

[16]   *Aggiornamento e revisione del Piano di Gestione del Rischio di Alluvione redatto ai sensi dell'art. 7 del D.Lgs. 49/2010 attuativo della Dir. 2007/60/CE – II ciclo di gestione*

Allegato 2.2 Approfondimenti nelle APSFR arginate Relazione di approfondimento sui corsi d'acqua arginati Distretto del fiume Po.

[17]   *Aggiornamento e revisione del Piano di Gestione del rischio di alluvione redatto ai sensi dell'art. 7 del D.lgs. 49/2010 attuativo della Dir. 2007/60/CE – II ciclo di gestione Area a potenziale rischio significativo di alluvione APSFR Regionali Relazione Regione Piemonte Distretto del fiume Po dicembre 2021*.

[18]   M. Murphy, E. McGovern, and S. Pavia, 'Historic building information modelling (HBIM)', *Structural Survey*, vol. 27, no. 4, pp. 311–327, Jan. 2009, doi: 10.1108/02630800910985108.

[19]   C. Dore and M. Murphy, 'Integration of Historic Building Information Modeling (HBIM) and 3D GIS for recording and managing cultural heritage sites', IEEE, 2012, pp. 369–376. doi: 10.1109/VSMM.2012.6365947.

[20]   C. D. Tomlin, *Geographic information systems and cartographic modeling*. Englewood Cliffs: Prentice-Hall, 1990.

[21]   P. Carbajales-Dale *et al.*, 'Using GIS to improve public health emergency response in rural areas during the COVID-19 crisis: A case study of South Carolina, US', *Transactions in GIS*, vol. 27, no. 4, pp. 975–995, 2023, doi: 10.1111/tgis.13069.

[22]   Y. Rui, D. Shen, S. Khalid, Z. Yang, and J. Wang, 'GIS-based emergency response system for sudden water pollution accidents', *Physics and chemistry of the earth. Parts A/B/C*, vol. 79–82, pp. 115–121, 2015, doi: 10.1016/j.pce.2015.03.001.

[23]   P. Longley, *Geographic Information Science & Systems*, Fourth edition. New York: John Wiley & Sons, 2015.

[24]   G. Sammartano, M. Avena, E. Fillia, and A. Spanò, 'Integrated HBIM-GIS Models for Multi-Scale Seismic Vulnerability Assessment of Historical Buildings', *Remote sensing (Basel, Switzerland)*, vol. 15, no. 3, p. 833, 2023, doi: 10.3390/rs15030833.

[25]   F. Matrone, E. Colucci, E. Iacono, and G. M. Ventura, 'The HBIM-GIS main10ance platform to enhance the maintenance and conservation of historical built heritage', 2023.

[26]   G. Vacca, E. Quaquero, D. Pili, and M. Brandolini, 'Gis-hbim integration for the management of historical buildings', *International archives of the photogrammetry, remote sensing and spatial information sciences.*, vol. XLII–2, pp. 1129–1135, 2018.

[27]   A. Aien, A. Rajabifard, M. Kalantari, and D. Shojaei, 'Integrating Legal and Physical Dimensions of Urban Environments', *ISPRS International Journal of Geo-Information*, vol. 4, no. 3, Art. no. 3, Sep. 2015, doi: 10.3390/ijgi4031442.

[28]   X. Liu, X. Wang, G. Wright, J. Cheng, X. Li, and R. Liu, 'A State-of-the-Art Review on the Integration of Building Information Modeling (BIM) and Geographic Information System (GIS)', *ISPRS international journal of geo-information*, vol. 6, no. 2, pp. 53-, 2017, doi: 10.3390/ijgi6020053.

[29]   D. Janisio-Pawłowska and W. Pawłowski, 'Implementation of BIM Data in CityGML—Research and Perspectives for Creating a QGIS Plugin for Spatial Analysis: Experience from Poland', *Sustainability*, vol. 16, no. 2, Art. no. 2, Jan. 2024, doi: 10.3390/su16020642.

[30]   Y. Deng, J. C. P. Cheng, and C. Anumba, 'Mapping between BIM and 3D GIS in different levels of detail using schema mediation and instance comparison', *Automation in Construction*, vol. 67, pp. 1–21, Jul. 2016, doi: 10.1016/j.autcon.2016.03.006.

[31]   A. Borrmann, J. Beetz, C. Koch, T. Liebich, and S. Muhic, 'Industry Foundation Classes: A Standardized Data Model for the Vendor-Neutral Exchange of Digital Building Models', in *Building Information Modeling*, A. Borrmann, M. König, C. Koch, and J. Beetz, Eds., Cham: Springer International Publishing, 2018, pp. 81–126. doi: 10.1007/978-3-319-92862-3_5.

[32]   ‘IFC 4.3.2 Documentation’. Accessed: Jan. 15, 2025. [Online]. Available: https://ifc43-docs.standards.buildingsmart.org/

[33]   Albert, J.; Bachmann, M.; Hellmeier, A., ‘Zielgruppen und Anwendungen für Digitale Stadtmodelle und Digitale Geländemodelle.’, *Erhebung im Rahmen der SIG 3D der GDI NRW*, pp. 1–5, 2003.

[34]   Gröger, G., Kolbe, T. H., Nagel, C., & Häfele, K. H., *OGC City Geography Markup Language (CityGML) En-coding Standard. Version 2.0*, 2012.

[35]   ‘OGC City Geography Markup Language (CityGML) 3.0 Conceptual Model Users Guide’. Accessed: Jan. 15, 2025. [Online]. Available: https://docs.ogc.org/guides/20-066.html

[36]   R. de Laat and L. van Berlo, ‘Integration of BIM and GIS: The Development of the CityGML GeoBIM Extension’, in *Advances in 3D Geo-Information Sciences*, Springer, Berlin, Heidelberg, 2011, pp. 211–225. doi: 10.1007/978-3-642-12670-3_13.

[37]   Y. Tan, Y. Liang, and J. Zhu, ‘CityGML in the Integration of BIM and the GIS: Challenges and Opportunities’, *Buildings*, vol. 13, no. 7, Art. no. 7, Jul. 2023, doi: 10.3390/buildings13071758.

[38]   S. Amirebrahimi, A. Rajabifard, P. Mendis, and T. Ngo, ‘A BIM-GIS integration method in support of the assessment and 3D visualisation of flood damage to a building’, *Journal of spatial science*, vol. 61, no. 2, pp. 317–350, 2016, doi: 10.1080/14498596.2016.1189365.

[39]   S. Amirebrahimi, A. Rajabifard, P. Mendis, and T. Ngo, ‘framework for a microscale flood damage assessment and visualization for a building using BIM–GIS integration’, *International journal of digital earth*, vol. 9, no. 4, pp. 363–386, 2016, doi: 10.1080/17538947.2015.1034201.

[40]   K. Kalogeropoulos, K. Tsanakas, N. Stathopoulos, D. E. Tsesmelis, and A. Tsatsaris, ‘Cultural Heritage in the Light of Flood Hazard: The Case of the "Ancient" Olympia, Greece’, *Hydrology*, vol. 10, no. 3, p. 61, 2023, doi: 10.3390/hydrology10030061.

[41]   X. Meng *et al.*, ‘A Simple GIS-Based Model for Urban Rainstorm Inundation Simulation’, *Sustainability (Basel, Switzerland)*, vol. 11, no. 10, p. 2830, 2019, doi: 10.3390/su11102830.

[42]   B. M. Feilden and J. Jokilehto, *Management guidelines for world cultural heritage sites*, 2. ed. Rome: ICCROM, 1998.

[43]   ‘UNESCO - Text of the Convention for the Safeguarding of the Intangible Cultural Heritage’. Accessed: Jul. 01, 2024. [Online]. Available: https://ich.unesco.org/en/convention

[44]   M. Bernardi, F. Cognasso, M. Bernardi, M. Bernardi, and F. Cognasso, ‘Il Castello del Valentino / a cura di Marziano Bernardi ; hanno collaborato al testo Francesco Cognasso ... [et al.]’, in *Il Castello del Valentino*, Torino: SIP, 1949.

[45]   *LEVEL OF DEVELOPMENT (LOD) SPECIFICATION*, 2023. Accessed: Jul. 14, 2024. [Online]. Available: https://bimforum.org/wp-content/uploads/2023/10/LOD-Spec-2023-Part-I-2024-02-27.pdf

[46]   *UNI11337 lEdilizia e infrastrutture Gestione digitale dei processi informativi delle costruzioni (BIM)*, 2017. Accessed: Jul. 14, 2024. [Online]. Available: https://www.bimidea.it/uni11337/

[47]   *UNI EN ISO 19650-1:2018; Building Information Modelling (BIM)—Gestione Informativa Mediante Il Building Information Modelling*, Milan, Italy., 2018.

[48]   *UNI EN 17412-1:2021; Building Information Modelling—Livello Di Fabbisogno Informativo*, Milan, Italy., 2021.

[49]   R. Brumana, F. Banfi, L. Cantini, M. Previtali, and S. Della Torre, ‘HBIM LEVEL OF DETAIL-GEOMETRY-ACCURACY AND SURVEY ANALYSIS FOR

ARCHITECTURAL PRESERVATION', Copernicus GmbH, 2019, pp. 293–299. doi: 10.5194/isprs-archives-XLII-2-W11-293-2019.

[50]   R. Brumana *et al.*, 'Generative HBIM modelling to embody complexity (LOD, LOG, LOA, LOI): surveying, preservation, site intervention—the Basilica di Collemaggio (L'Aquila)', *Applied geomatics*, vol. 10, no. 4, pp. 545–567, 2018, doi: 10.1007/s12518-018-0233-3.

[51]   R. Brumana, C. Stanga, and F. Banfi, 'Models and scales for quality control: toward the definition of specifications (GOA-LOG) for the generation and re-use of HBIM object libraries in a Common Data Environment', *Applied Geomatics*, vol. 14, Mar. 2021, doi: 10.1007/s12518-020-00351-2.

[52]   M. A. Gomarasca, *Basics of Geomatics*. Springer Science & Business Media, 2009.

[53]   Historic England, *Geospatial Survey Specifications for Cultural Heritage*, York.Historic England., 2024.

[54]   Historic England, *Photogrammetric Applications for Cultural Heritage. Guidance for Good Practice.*, Swindon. Historic England., 2017. Accessed: Jan. 22, 2025. [Online]. Available: https://historicengland.org.uk/images-books/publications/photogrammetric-applications-for-cultural-heritage/heag066-photogrammetric-applications-cultural-heritage/

[55]   Historic England, *Using Airborne Lidar in Archaeological Survey: The Light Fantastic.*, Swindon. Historic England., 2018. Accessed: Jan. 26, 2025. [Online]. Available: https://historicengland.org.uk/images-books/publications/using-airborne-lidar-in-archaeological-survey/heag179-using-airborne-lidar-in-archaeological-survey/

[56]   G. Patrucco, F. Rinaudo, and A. Spreafico, 'MULTI-SOURCE APPROACHES FOR COMPLEX ARCHITECTURE DOCUMENTATION: THE "PALAZZO DUCALE" IN GUBBIO (PERUGIA, ITALY)', 2019.

[57]   A. Conti, L. Fiorini, R. Massaro, C. Santoni, and G. Tucci, 'HBIM for the preservation of a historic infrastructure: the Carlo III bridge of the Carolino Aqueduct', *Applied geomatics*, vol. 14, no. Suppl 1, pp. 41–51, 2022, doi: 10.1007/s12518-020-00335-2.

[58]   D. Costantino, M. Pepe, and A. G. Restuccia, 'Scan-to-HBIM for conservation and preservation of Cultural Heritage building: the case study of San Nicola in Montedoro church (Italy)', *Applied geomatics*, 2021, doi: 10.1007/s12518-021-00359-2.

[59]   B. Tanduo, L. Teppati Losè, and F. Chiabrando, 'DOCUMENTATION OF COMPLEX ENVIRONMENTS IN CULTURAL HERITAGE SITES. A SLAM-BASED SURVEY IN THE CASTELLO DEL VALENTINO BASEMENT', Copernicus GmbH, 2023, pp. 489–496. doi: 10.5194/isprs-archives-XLVIII-1-W1-2023-489-2023.

[60]   P. Tang, D. Huber, B. Akinci, R. Lipman, and A. Lytle, 'Automatic reconstruction of as-built building information models from laser-scanned point clouds: A review of related techniques', *Automation in construction*, vol. 19, no. 7, pp. 829–843, 2010, doi: 10.1016/j.autcon.2010.06.007.

[61]   Q. Wang, J. Guo, and M.-K. Kim, 'An Application Oriented Scan-to-BIM Framework', *Remote sensing (Basel, Switzerland)*, vol. 11, no. 3, p. 365, 2019, doi: 10.3390/rs11030365.

[62]   F. Matrone and F. Remondino, 'Comparing Machine and Deep Learning Methods for Large 3D Heritage Semantic Segmentation', 2020.

[63]   D. Treccani, J. Balado, A. Fernández, A. Adami, L. Dı́az-Vilari, 'A Deep Learning Approach for the Recognition of Urban Ground Pavements in Historical Sites', 2022, Accessed: Jul. 16, 2024. [Online]. Available: https://pico.polito.it/discovery/fulldisplay?docid=cdi_doaj_primary_oai_doaj_org_article_a93df78429db4d2baca2233a11109910&context=PC&vid=39PTO_INST:VU&lang=it&

search_scope=MyInst_and_CI&adaptor=Primo%20Central&tab=Everything&query=any
,contains,A%20Deep%20Learning%20Approach%20for%20the%20Recognition%20of%
20Urban%20Ground%20Pavements%20in%20Historical%20Sites&offset=0

[64]   *UNI 8290:1981*. Accessed: Oct. 24, 2024. [Online]. Available:
https://www.unirc.it/documentazione/materiale_didattico/597_2007_45_1983.pdf

[65]   J. M. Coughlan and A. L. Yuille, 'Manhattan World: compass direction from a single
image by Bayesian inference', in *Proceedings of the Seventh IEEE International
Conference on Computer Vision*, Kerkyra, Greece: IEEE, 1999, pp. 941–947 vol.2. doi:
10.1109/ICCV.1999.790349.

[66]   M. Previtali and F. Banfi, 'Towards the Definition of Workflows for Automation in
HBIM Generation', Cham: Springer International Publishing, 2018, pp. 52–63. doi:
10.1007/978-3-030-01762-0_5.

[67]   A. Weyer *et al.*, *EwaGlos - European illustrated glossary of conservation terms for
wall paintings and architectural surfaces*, vol. 17. Petersberg, Germany: Michael Imhof
Verlag, 2015. Accessed: Oct. 25, 2024. [Online]. Available:
https://openarchive.icomos.org/id/eprint/1706/

[68]   *ICOMOS-ISCS: Illustrated glossary on stone deterioration patterns = ICOMOS-
ISCS: Glossaire illustré sur les formes d'altération de la pierre*, vol. XV. Paris:
ICOMOS, 2008. Accessed: Oct. 25, 2024. [Online]. Available:
http://www.international.icomos.org/publications/monuments_and_sites/15/pdf/Monume
nts_and_Sites_15_ISCS_Glossary_Stone.pdf

[69]   G. A. Breymann, *Allgemeine Bau-Constructions-Lehre, mit besonderer Beziehung auf
das Hochbauwesen. Ein Leitfaden zu Vorlesungen und zum Selbstunterrichte, von G.A.
Breymann ..: v. 1*, vol. 1. Germany: Hoffmann-54, 1854. Accessed: Jul. 24, 2024.
[Online]. Available: https://hdl.handle.net/2027/nyp.33433066384920

[70]   G. Musso, *Particolari di costruzioni murali e finimenti di fabbricati / Musso e
Copperi*. Torino: Paravia, 1885.

[71]   C. Formenti, *La pratica del fabbricare : Parte prima - Il rustico delle
fabbriche.Seconda edizione ampliata, LXVIII tavole.* Milano: Hoepli, 1893.

[72]   'RIPRESA AEREA ICE 2009-2011 - DTM 5'. Accessed: Jan. 14, 2025. [Online].
Available:
https://www.geoportale.piemonte.it/geonetwork/srv/chi/catalog.search#/metadata/r_piem
on:224de2ac-023e-441c-9ae0-ea493b217a8e

[73]   'Atlante piogge intense in Piemonte'. Accessed: Jan. 14, 2025. [Online]. Available:
https://webgis.arpa.piemonte.it/agportal/apps/webappviewer/index.html?id=378e0fcb7dd
d4565ba836c07dd1c4c9b

[74]   'Idrogeologia - Permeabilità prevalente della zona non satura 1:100.000'. Accessed:
Jan. 14, 2025. [Online]. Available:
https://www.geoportale.piemonte.it/geonetwork/srv/ita/catalog.search#/metadata/r_piemo
n:47b602ce-56fb-4a7e-a7ee-d6df1bc203c0

[75]   'Carta dei Suoli della Regione Piemonte'. Accessed: Jan. 14, 2025. [Online].
Available:
https://www.geoportale.piemonte.it/geonetwork/srv/ita/catalog.search#/metadata/r_piemo
n:37c6413b-b07f-4f4c-9344-f2e43ea52bbd

[76]   'GEmMA -GEodatabase Morfologia corsi d'Acqua in Piemonte'. Accessed: Jan. 14,
2025. [Online]. Available:
https://webgis.arpa.piemonte.it/gpserver_arpa/catalog/search/resource/details.page?uuid=
arlpa_to:01-05-01-D_2019-02-15_14:45

[77] 'BDGeo100 - Aree inondabili'. Accessed: Jan. 14, 2025. [Online]. Available: https://webgis.arpa.piemonte.it/gpserver_arpa/catalog/search/resource/details.page?uuid= arlpa_to:07.03.01_ai-D_2013-10-08:14:38

[78] 'BDTRE - Base Dati Territoriale di Riferimento degli Enti'. Accessed: Jan. 14, 2025. [Online]. Available: https://www.geoportale.piemonte.it/geonetwork/srv/chi/catalog.search#/metadata/r_piem on:903f1ad3-6821-4d87-b500-0c8028fd303b

[79] 'DTM LiDAR con risoluzione a terra 1 metro - Regione Piemonte'. Accessed: Jan. 14, 2025. [Online]. Available: http://www.pcn.minambiente.it/geoportal/catalog/search/resource/details.page?uuid=m_a mte%3A299FN3%3Aa64cc56f-5352-4597-94a2-2ae9b3518842

[80] 'Arpa Piemonte - Edifici 3D 2017'. Accessed: Jan. 14, 2025. [Online]. Available: https://www.geoportale.piemonte.it/geonetwork/srv/eng/catalog.search#/metadata/arlpa_t o:EDIF_2017-12-21-11:00

[81] E. Colucci, V. de Ruvo, A. Lingua, F. Matrone, and G. Rizzo, 'HBIM-GIS integration: From IFC to cityGML standard for damaged cultural heritage in a multiscale 3D GIS', *Applied sciences*, vol. 10, no. 4, p. 1356, 2020, doi: 10.3390/app10041356.

[82] 'BIM to GIS (Intermediate) | IFC LOD 300 to LOD 4 CityGML', FME Support Center. Accessed: Nov. 25, 2024. [Online]. Available: https://support.safe.com/hc/en-us/articles/25407718003341-BIM-to-GIS-Intermediate-IFC-LOD-300-to-LOD-4-CityGML

[83] *Aggiornamento e revisione del Piano di Gestione del Rischio di Alluvione redatto ai sensi dell'art. 7 del D.Lgs. 49/2010 attuativo della Dir. 2007/60/CE – II ciclo di gestione RELAZIONE METODOLOGICA Distretto del fiume Po Rev.*

[84] 'GUIDA ALL'UTILIZZO DELL' ATLANTE DELLE PIOGGE INTENSE'. Accessed: Feb. 07, 2025. [Online]. Available: https://webgis.arpa.piemonte.it/w-metadoc/aria_meteocli/precipitazioni_intense.pdf

[85] J. Chen, A. A. Hill, and L. D. Urbano, 'A GIS-based model for urban flood inundation', *Journal of hydrology (Amsterdam)*, vol. 373, no. 1, pp. 184–192, 2009, doi: 10.1016/j.jhydrol.2009.04.021.

[86] O. D. Aribisala, S.-G. Yum, M. D. Adhikari, and M.-S. Song, 'Flood Damage Assessment: A Review of Microscale Methodologies for Residential Buildings', *Sustainability (Basel, Switzerland)*, vol. 14, no. 21, p. 13817, 2022, doi: 10.3390/su142113817.

[87] M. Neubert, T. Naumann, J. Hennersdorf, and J. Nikolowski, 'The Geographic Information System-based flood damage simulation model HOWAD', *Journal of flood risk management*, vol. 9, no. 1, pp. 36–49, 2016, doi: 10.1111/jfr3.12109.

[88] R. Figueiredo, X. Romão, and E. Paupério, 'Component-based flood vulnerability modelling for cultural heritage buildings', *International journal of disaster risk reduction*, vol. 61, p. 102323, 2021, doi: 10.1016/j.ijdrr.2021.102323.

[89] S. Abedin and H. Stephen, 'GIS Framework for Spatiotemporal Mapping of Urban Flooding', *Geosciences (Basel)*, vol. 9, no. 2, p. 77, 2019, doi: 10.3390/geosciences9020077.

Figures

Table